PHARMACOKINETIC SCALING OF ANTICANCER DRUGS IN DOGS

By

SATYANARAYANA ACHANTA

Bachelor of Veterinary Science and Animal Husbandry
Acharya N.G. Ranga Agricultural University
Hyderabad, Andhra Pradesh, India
2005

Submitted to the Faculty of the
Graduate College of the
Oklahoma State University
in partial fulfillment of
the requirements for
the Degree of
DOCTOR OF PHILOSOPHY
July, 2012

PHARMACOKINETIC SCALING OF ANTICANCER

DRUGS IN DOGS

Dissertation Approved:

Dr. Lara K. Maxwell

Dissertation Adviser

Dr. David W.A. Bourne

Dr. Jerry W. Ritchey

Dr. Jarrad R. Wagner

Outside Committee Member

Dr. Sheryl A. Tucker

Dean of the Graduate College

TABLE OF CONTENTS

LIST OF TABLES

Table Page

CHAPTER III

CHAPTER IV

CHAPTER V

LIST OF FIGURES

Figure Page

CHAPTER II

CHAPTER III

CHAPTER I

INTRODUCTION

Accurate dosing of anticancer drugs from the initiation of treatment is of paramount importance to the outcome of cancer therapy. Inappropriate dosing of anticancer drugs leads to therapeutic failure, toxicity, and drug resistance. Anticancer drugs have a narrow therapeutic index, that is the safety margin between therapeutically effective dose and toxic dose is very narrow. Also, wide inter-individual variability was reported in therapeutic responses to anticancer drug therapy. Currently, the doses of anticancer drugs are calculated based on the body surface area (BSA) of the patient. The formulae for the determination of BSA were developed based on the studies in fewer subjects leading to inaccuracies both in the BSA determination and eventually in the dose calculation. Also, several studies have proven that the assumptions of BSA dosing methodology do not hold good for patients of different body sizes and for all drugs. Several alternative dosing equations were proposed but none of them could normalize the drug exposure of anticancer agents in disparate canine patients. Dogs have wide range of body weights ranging from 2.5 pound Chihuahua to 160 pound Saint Bernard for which, BSA dosing failed to normalize drug exposure for these widely variable patients.

The objective of this study was to develop novel dosing equation for the calculation of doses of anticancer drugs considering different anatomical and physiological parameters and drug kinetics which play an important role in deciding the dosage of anticancer drugs. Unlike other therapeutic drugs, the efficacy of anticancer drugs depends on the drug exposure and not on the peak concentration of the drug. For most of the drugs, liver and kidney are two primary organs of metabolism and excretion. Excretion of drugs occurs primarily by glomerular filtration and biliary secretion. Clearance of drugs is one of the important pharmacokinetic parameters which will influence the dose of a drug and is highly variable among patients leading to over-dosing or under dosing of anticancer drugs. For a given drug, if clearance is known, then dose can be accurately calculated for a desired drug exposure using the equation, Dose = (desired drug exposure) x (clearance).

We hypothesized that the concomitant consideration of the effects of patient signalment such as, body weight, gender, and ontogeny on organ weights, physiological parameters, and anticancer drug handling will accurately predict the clearance of model anticancer drugs. In order to test our hypothesis, two model anticancer drugs were chosen: vinblastine and cisplatin. Vinblastine is a vinca alkaloid which is metabolized in the liver and excreted in bile/feces and to some extent in urine. Cisplatin [*cis*-Diamminedicholoroplatinum II, *cis* $PtCl_2(NH_3)_2$] is a platinum containing alkylating agent. Cisplatin is metabolized in kidneys and excreted through urine. Vinblastine and cisplatin will serve as model anticancer drugs for other anticancer drugs having similar route of metabolism and excretion.

The central hypothesis was tested by following specific aims:

1. Determine the influence of individual factors, such as body weight, gender, and ontogeny on cardiac, hepatic and renal mass.

2. Determine the influence of body weight on renal and hepatic physiological parameters.

3. Establish the relations between body size and intrinsic clearance of vinca alkaloids.

4. Establish the relations between body size and total body clearance of selected model anticancer drugs.

5. Establish correlations between *in vitro* and *in vivo* clearance of selected anticancer drugs.

6. Create an improved mathematic model for calculating doses of model anticancer drugs and compare the newly developed dosing equations to the current BSA dosing method.

Our hypothesis and specific aims to test hypothesis in question were innovative in approach. Our approach integrates separate fields of anatomy, physiology, pharmacology, and oncology to come up with novel dosing equations which would normalize drug exposure in disparate canine patients. Attempts were made to develop novel dosing equations that would optimize the drug exposure between disparate canine patients. We are also anticipating to extrapolate results from this study to other anticancer drugs that are similarly metabolized and excreted from the body. The long term goal of our lab is to extrapolate the resulting equations to human beings as human oncologists also face similar problems in optimizing doses of anticancer drugs.

In this dissertation, the studies were categorized based on manuscript format. A manuscript on 'Allometric Scaling of Renal Clearance of Cisplatin in Dogs' was summarized in chapter III. In chapter IV, 'Allometry of Hepatic Metabolism of Vinblastine in Dogs' was presented. In chapter V, analytical method development manuscript, 'Simultaneous

Quantification of Vinblastine and Desacetylvinblastine Concentrations in Canine Plasma and Urine Samples using LC-APCI-MS/MS' was presented.

CHAPTER II

REVIEW OF LITERATURE

1. Anticancer drugs:

Cancer is one of the major causes of death both in human and animals. Chemotherapy alone or in combination with other therapies is an important approach for cancer treatment. German bacteriologist, Paul Erlich is considered to be the father of chemotherapy who received Nobel Prize in 1908 for his studies on effects of chemicals on tissues and treatment of syphilis. Anticancer drugs are characterized by narrow therapeutic index (Hempel and Boos, 2007). Narrow therapeutic index means the safety margin between therapeutically effective dose and toxic dose is very narrow. Development of drug resistance is another issue in chemotherapy. Therefore, in order to achieve optimal therapeutic efficacy, most of the cytotoxic drugs are administered at the maximum tolerated dose (MTD) (Hempel and Boos, 2007). Also, individuals have a highly variable capacity to metabolize and eliminate drugs, which comes from a combination of physiological variables, genetic (intrinsic) characteristics, and individual's phenotype. Unlike many therapeutic drugs, the efficacy of anticancer agents correlates with the drug exposure (Moore and Erlichman, 1987; van den Bongard et al., 2000). Mathematically, drug exposure is calculated as area under plasma concentration versus time curve (AUC)(Calvert et al., 1989; Hempel and Boos, 2007). The systemic drug exposure after standard doses of cytotoxic drugs varies 4 – 10 folds between patients (Evans and Relling, 1989; Masson and Zamboni, 1997). There are several reasons for variation in systemic drug exposure in patients and were summarized in Figure 1 (Mathijssen et al., 2007). In addition, many anticancer drugs have unique and peculiar pharmacokinetic and pharmacodynamic profiles. This results in variable therapeutic outcome with the same dose in similar patients.

The major classes of commonly used anticancer drugs: (Hess, 1977)

Antimicrotubule agents: These agents are cell cycle specific and induce metaphase arrest. They act by destroying the mitotic spindle of the cell and preventing further cell division. Also, disrupts

other tubulin dependent events, such as intracellular transport, organelle movement, and membrane trafficking E.g., vinca alkaloids, such as vinblastine, vincristine, vinflunine, vindesine and vinorelbine; taxanes, such as paclitaxel and docetaxel.

Antimetabolites: These agents interfere with the biosynthesis of nucleic acids by substituting for normal metabolites and inhibiting normal enzymatic reactions. E.g., 5-fluorouracil, methotrexate

Alkylating agents: These agents act by crosslinking cellular DNA, thus arresting its ability to act as a template for RNA synthesis. These are not cell cycle specific. E.g., cyclophosphomide, lomustine, cisplatin, carboplatin, and oxaliplatin.

Topoisomerase inhibitors: These agents act by inhibition of topoisomerase II and causing DNA strand breaks. E.g., doxorubicin, epirubicin, daunorubicin, etoposide, and teniposide.

Enzyme therapy: These agents act by depletion of asparagines, on which leukemic cells depend. E.g., asparginase

Hormone receptor therapy: these agents are thought to act by interfering with cell membrane receptors that stimulate growth. E.g., tamoxifen, leuprolide acetate, and megestrol acetate

Tyrosine kinase inhibitors: These agents act by inhibition of c-kit. E.g., toceranib phosphate, imatinib, mastinib, erlotinin, and gefitinib.

Cell cycle:

Normal cells have four basic properties, such as ability to proliferate, capacity for self-renewal, ability to differentiate, and sensitivity to regulatory mechanisms. On the other hand, tumor cells have ability to proliferate and capacity for self-renewal without control. Cytotoxic agents work on the more proliferating cells. Some of the cytotoxic agents are cell cycle specific and knowledge of the cell cycle or the proliferative state of the cell populations is important to understand the

cytotoxic effects of cancer chemotherapy. Figure 2 is an illustration of different phases of cell cycle (Hess, 1977; Alberts et al., 2002). The cell cycle is divided into following stages: G_0 = resting phase; G_1 = protein synthesis; RNA transcription; S = DNA synthesis; G_2 = protein synthesis; RNA transcription; M = Mitosis; and G_1+S+G_2 = Interphase. The goal of the treatment is to kill tumor cells without hurting normal cells. Cells in S-phase are particularly susceptible to cytotoxic treatment affecting the formation of nucleotides and inhibition of DNA repair. Rapidly growing tumors are more susceptible to treatment compared to resting tumor cells. The favorable prognosis of a tumor with chemotherapy is inversely proportional to the tumor population.

Adverse drug reactions and dose limiting toxicities of cytotoxic drugs:

Anticancer drugs are characterized by narrow therapeutic index. That is, the safety margin between therapeutic effective dose and toxic dose is very narrow. For an example, the minimum lethal dose of cisplatin in dogs is 2.5 mg/kg (≈80 mg/m^2) (Schaeppi et al., 1973) while the therapeutic dose is 60 – 70 mg/ m^2 (Knapp et al., 1988). Understanding about potential toxicities associated with chemotherapy is important in determining the maximum tolerated doses (Chatelut et al., 2003). Dose dependent toxicity is seen with several anticancer drugs. On the other hand, if doses are administered below maximum tolerated doses, then drug resistance will develop (Powis, 1983). Gametes, gastrointestinal epithelium, hair follicles, bone marrow progenitor cells are highly dividing normal cells in the body. Chemotherapeutic drugs are most effective on highly dividing tumor cells. Therefore, cytotoxic drugs also act on normal highly dividing cells along with neoplastic cells. The common toxicities associated with chemotherapy are bone marrow depression, lymphocytopenia, gastrointestine tract (GIT) disturbances, diarrhea, alopecia, hyperuricaemia, nausea, and vomiting. Among these toxicities, bone marrow depression, alopecia, and gastrointestinal disturbance are the most common side effects of chemotherapy, commonly known with an acronym, B-A-G. Also the organ systems in which metabolism and excretion of chemotherapeutics occur are also highly susceptible to chemotherapy toxicity

(Erdlenbruch et al., 2001; Barabas et al., 2008). Most of these adverse drug toxicities and dose limiting toxicities are dependent on the mechanism of action of each chemotherapeutic agent.

Dosing strategies:

Chemotherapy is most effective when initiated as soon as possible after diagnosis of a tumor. The proportion of cells killed by chemotherapy is greater when tumor cells are less in number. Also, the regrowth of tumor population is more when the number of tumor cells are fewer (Foote, 1998). With the toxicity of chemotherapy, usually planned doses are reduced or delayed but this change in dosing regimen will have great impact on the therapeutic outcome. Figure 3 shows the effect of dose intensity of chemotherapy on tumor cell kill and regrowth between cycles (Norton, 1997; Foote, 1998). Gompertzian model of tumor growth suggests that tumor growth is highest when the size of tumor is small. Also, between treatment cycles, regrowth of tumor cells will be more. The best approach would be to dose at the maximum tolerated doses at the shortest possible dosing intervals while monitoring the toxicity.

Drug resistance:

Development of drug resistance to anticancer agents is another big issue in addition to their narrow therapeutic indices. The mechanisms of drug resistance are (figure 4): development of alternative metabolic pathways and repair mechanisms; destruction of drug by the cell; changes in the permeability of the cell membrane or altered p-glycoprotein pumps; tumor cells entering the resting phase of the cell cycle; and deletion of cellular drug activation mechanisms (Gottesman, 2002; Rabik and Dolan, 2007). Unfortunately, normal cells do not develop drug resistance on par with tumor cells. Synergistic effects of combinations of cytotoxic agents were exploited to decrease resistance and increase therapeutic efficiency (O'Connor, 2007).

2. Dosing of Anticancer Drugs:

Current dosing methodology for anticancer drugs:

The doses of anticancer drugs are calculated based on the body surface area (BSA)(Ratain, 1998). Appropriate doses of drugs are calculated based on pharmacokinetic parameters, but these parameters differ highly for anticancer agents between patients. In an attempt to normalize doses of anticancer drugs between different body sizes, BSA based dosing was suggested based on studies with 6-mercaptopurine, actinomycin-D, and triethylenethiophosphoramide in different animal species and humans (Pinkel, 1958). The dose normalized to body surface area appeared to be more uniform across different animal species and humans. In clinical medicine, body surface area based dosing approach was used for the determination of amount of parenteral fluids and electrolytes administration. The daily normal water requirement of the young infant (100 mL/kg) and adult (50 mL/kg) were both met by administration of 2 liters of water per square meter of body surface (Baker et al., 1957). The rationale for Pinkel's approach was based on earlier studies in which metabolic rate appeared to be directly proportional to body surface area and vary allometrically with body weight (DuBois and DuBois, 1916). Later, correlations were found between body surface area and different physiological parameters, such as renal function (glomerular filtration rate), cardiac output, and hepatic blood flow (Coppoletta and Wolbach, 1933; Kanamori et al., 2002). These findings suggested that BSA might have value in calculating the doses of anticancer agents.(Fukuoka et al., 2004)

BSA based dosing and limitations:

Although BSA based dosing is intuitively logical and simple to understand, there were several studies that reported toxicities and questioned its ability to explain the disposition of several anticancer drugs (Mathijssen et al., 2007) Jones et al., 1984; Page et al., 1988; Arrington

et al., 1994). It was found that BSA based dosing did not reduce the variability of drug exposure (AUC, area under plasma concentration versus time curve) among disparate patients. The assumptions that were made for BSA dosing methodology were also proven to be inaccurate, such as glomerular filtration rate (GFR) (Dooley and Poole, 2000), hepatobiliary excretion system and liver function (Arrington et al., 1994; Gurney, 1996). Bone marrow toxicity is one of the common side effects of chemotherapy. It was shown that the number of hematopoietic stem cells is proportional to body weight but not BSA (Vriesendorp, 1985). Unless the metabolism or excretion of drug is increased in small animals, their bone marrow stem cells would be exposed to larger concentrations of drug for a longer period when dosed by BSA - based dosing (Vriesendorp, 1985; Arrington et al., 1994). A number of studies examining pharmacokinetic parameters have also questioned the application of BSA as a means of individualizing chemotherapeutic doses (Grochow et al., 1990; Gurney, 1996; Gurney et al., 1998; Dooley and Poole, 2000; Felici et al., 2002). In one investigational study to see the suitability of BSA dosing approach in 33 anticancer agents, BSA dosing reduced interpatient variability only for five drugs, namely docosahexaenoic acid-paclitaxel, 5-fluorouracil/eniluracil, paclitaxel, temozolomide, and troxacitabine (Baker et al., 2002). Docetaxel is the only drug for which BSA is the good predictor of drug clearance. (Felix et al., 2001;Bruno et al., 1998). Furthermore, the drugs for which clearance was associated with BSA, the relative reduction in variability of clearance was between 15% and 35%. This means, only one third of the total variability could be explained by BSA (Baker et al., 2002; Miller, 2002). Blood volume, total body water (TBW) and extracellular water (ECW) are better correlated with the BSA than body weight (Baker et al., 1957). Accordingly, BSA based dose calculations would seem rationale for the drugs which are distributed in the central compartment and having low volume of distribution (Baker et al., 1957; Friis-Hansen, 1961; Felici et al., 2002).

BSA is estimated based on nomograms or computer programs that contain Du Bois and Du Bois formula. Several questions have also arisen on the equations to calculate body surface area in both humans and animals. The widely used Dubois and Dubois equation was developed based on studies in nine individuals (DuBois D and EF, 1916; Du Bois and Du Bois, 1989). Several alternative equations and methods were proposed to measure BSA in both humans and animals but none of them were free of disputes (Haycock et al., 1978; Sawyer and Ratain, 2001; Wang and Hihara, 2004; Verbraecken et al., 2006). There is also a confusion regarding which body weight (ideal, lean or actual body weight) should be used for the calculation of BSA (Dooley and Poole, 2000). In other words, BSA calculations do not consider the question whether a kilogram of fat is equivalent to a kilogram of muscle or of lower-extremity edema (Egorin, 2003).

The equation to calculate BSA in humans: BSA (m^2) = $W^{0.425}$ x $H^{0.725}$ x 0.007184 where W = weight in kilograms, H = height in centimeters (DuBois and DuBois, 1916). The following equation is widely used to determine the BSA in dogs: BSA (m^2) = 10.1 x (body weight in $grams^{2/3}$) x 10^{-4}. There are approximately 400 breeds of dogs worldwide out of which, 156 were recognized by American Kennel Club (http://www.akc.org/breeds/complete_breed_list.cfm). As there are several breeds of dogs and body weights of dog breeds range from 2 pounds to 200 pounds, different values of mass co-efficient and mass exponents were suggested (Cowgill and Drabkin, 1927; Price and Frazier, 1998). A single value of mass co-efficient will not be sufficient for a wide range of body weights in dogs. Further, different values were suggested for cats, rats, and guinea pigs which have relatively uniform body conformation (Price and Frazier, 1998). Canine breeds differ markedly in their conformation and it would be more obvious to have different values of mass co-efficient. Similarly, different values were suggested for mass exponents (Cowgill and Drabkin, 1927; Price and Frazier, 1998). It might be that even if BSA is

determined accurately, it may not correlate with the factors that influence the drug exposure in dogs.

There is a continuous need from both veterinary and human oncologists for a better alternative to current BSA based dosing. Different alternative dosing methodologies were suggested (Gurney, 1996; Canal et al., 1998) to overcome the limitations in BSA based dosing, such as body weight (Page et al., 1988; Arrington et al., 1994), flat fixed dosing (Hempel and Boos, 2007; Mathijssen et al., 2007), fixed dosing for BSA clusters (Loos et al., 2006), therapeutic drug monitoring, toxicity adjusted dosing, and etc. However, these alternative dosing methodologies worked only for one or few drugs but the toxicity adjusted dosing is more popular. As there is a wide variability in therapeutic outcome with chemotherapy, toxicity adjusted dosing could be useful to attain optimal therapeutic efficacy (Rassnick et al., 2008; Welle et al., 2008). In humans, dosing based on renal functional marker was successfully implemented for carboplatin, a sister analogue of cisplatin (Calvert et al., 1989). As there is no widely accepted alternative dosing methodology, currently BSA based dosing is being used for initial dose calculation of several drugs.

Allometry: Allometry is the study of relationship between body size and structural or functional capacities of organs(Jurgens and Prothero, 1991). The word, 'allometry' was coined by Huxley and Tessier in 1936. Allometry is opposite to isometry, which means 'by the same measure' whereas allometry means 'by a different measure'. Geometrically similar objects are often called isometric. In isometric relationship, the proportion remains the same whereas in allometric relationship, the proportions are altered in a regular manner. In other words, this change in a specific parameter correlates with differences in size of the organism (Mahmood, 2007). Several anatomical (BSA, liver weight, kidney weight, and other organs), physiological (basal metabolic rate, glomerular filtration rate, renal blood flow, and cardiac output), and pharmacokinetic parameters (clearance, volume of distribution, and elimination half life) depend on body weight

with allometric relationship. Figure 5 illustrates the allometric relationship. As the volume of the cube increases, surface area also increases but not in direct proportion. Surface area becomes disproportionately smaller in relation to the volume of larger cubes. If the surface area of a cube is plotted against the volume on logarithmic coordinates, the slope will be 0.67. If the surface area per unit volume of the cube is plotted (dashed line) against volume of cube, then the slope of the regression line will be -0.33 (figure 6).

$S = k \times V^{0.67}$

$S/V = k V^{0.67}/V$

$= k V^{0.67 - 1.0}$

$S/V = k V^{-0.33}$

As a consequence, smaller bodies have, relative to their volumes, larger surface areas than larger bodies of the same shape (figure 5). Based on these observations for geometrically similar objects, it was considered that intraspecific (allometric scaling within a species) exponent is 0.67 (Hoppeler and Weibel, 2005). On the other hand, based on interspecies scaling of basal metabolic rate in mammals and birds, it was assumed that 0.75 is the exponent of interspecies allometric scaling (Schmidt-Nielsen, 1984; Hoppeler and Weibel, 2005). Three – fourth allometric exponent of interspecies scaling is widely accepted based on the structure and design of vascular system (West et al., 1997). However, over the last century, several studies questioned these exponents of intraspecies and interspecies scaling (Ritschel et al., 1992; White and Seymour, 2003; Hoppeler and Weibel, 2005; White and Seymour, 2005).

3. Scaling of organ weights in dogs

Intraspecies allometric scaling is the study of allometric relationship between structural and functional capacities of organs in relation with the body weight within a species. Study of

allometric relationship between organ weights and body weights is important in estimating the organ weights in species like dogs, in which there is a wide variation in body weights. There are several utilities of organ weight estimations, such as estimation of organ volume or size for surgery and organ transplantation(Gregory et al., 1987), incorporation of allometric equations in population based pharmacokinetic and physiological based pharmacokinetic (PBPK) software programs, and to differentiate between normal and pathological lesions in autopsy . Most of the previous studies of organ scaling were limited to either few numbers of subjects or uniform subjects (Jackson and Cappiello, 1964; Deavers et al., 1972; Steward et al., 1975; Lutzen et al., 1976; Steel et al., 1976; Schoning et al., 1995). In dogs, there is an approximate 100 fold difference in their weights. The existing studies would not be helpful to estimate the organ weights with good accuracy. Also, most of the studies are based on fixed proportion of body weights rather than allometric relationships (Jackson and Cappiello, 1964; Nemec and Vortel, 1981). Heart, liver, and kidney are three important organs which play direct or indirect role in the metabolism and excretion of many therapeutic drugs. Human and veterinary pathologists estimate heart, liver, and kidney weights as 0.75%, 3.5%, and 0.4% (juvenile) and 1.13% (adult) of body weights, respectively(Steward et al., 1975). However, these fixed proportions of body weights may not give good estimates of organ weights in dogs because of their wide variation in body conformation within the species. Fixed proportion of body weights approach gives mean value of proportion of an organ weight to body weight. Allometric equations give good estimate of organ weights as a function of all significant factors in the multiple linear regressions.

4. Renal physiological parameters

Kidneys are one of the most complex organs in the body which play a gamut of biological roles. The main role is maintenance of homeostasis of body fluids by filtering and secreting metabolites and minerals from the blood and excreting them, along with water, as urine. This is achieved by glomerular filtration, tubular reabsorption and tubular secretion. Renal blood

flow accounts for 20-25% of the cardiac output. In a 15 kg dog about 200 ml of fluid enters renal tubules per min (60 L/day). The animal produces only about 600 ml of urine per day, indicating most of the glomerular filtrate is reabsorbed rather than excreted. The other important functions of kidneys are blood filtering, excretion of waste products, homeostasis, acid-base balance, and maintenance of blood pressure and plasma volume, and hormone secretion.

Glomerular filtration rate:

Glomerular Filtration Rate (GFR) is defined as the volume of plasma that can be completely cleared of a particular substance by the kidneys in a unit of time. The main factors that influence GFR are molecular size, protein binding, glomerular integrity, resistance of afferent and efferent arterioles, and total number of functional nephrons. The basis of urine formation is the ultrafiltration of plasma in the glomerulus. A measure of the magnitude of this filtration therefore is generally accepted to be the best overall index of renal function. Accurate GFR determination may facilitate prognostic decisions in patients with established renal disease. GFR estimation is useful in therapeutic drug monitoring of several drugs with narrow therapeutic index. GFR is useful in old and critically ill patients to make drug dosage adjustments. Glomerular filtration rate in the dog may be influenced by several nonrenal factors such as protein intake, hydration status, sodium balance, gender, age, and breed, as well as day-to-day and circadian variations for the individual dog (Finco et al., 1981; Izzat and Rosborough, 1989; Levey, 1989; Gleadhill et al., 1995; Koopman et al., 1996). Thus, the range of reference values in healthy dogs is wide.

Different methods which are commonly used to measure GFR are: inulin clearance (Earle and Berliner, 1946), blood urea nitrogen (BUN) , creatinine (Jung et al., 1987; Lawson et al., 2002; Braun et al., 2003), radioactive isotopes (^{125}I-iothalamate (Boschi and Marchesini, 1981; Odlind et al., 1985; Perrone et al., 1990; Agarwal, 1998),^{99m}Tc-diethylenethiaminepenta-acetic acid (^{99m}Tc-DPTA) (Moe and Heiene, 1995) and Cr-ethylenediaminetetra-acetic acid (^{51}Cr-

EDTA) (Rehling et al., 1984; Effersoe et al., 1990)), radiographic contrast media (Frennby and Sterner, 2002), and cystatin C (Tenstad et al., 1996; Laterza et al., 2002).

Glomerular filtration rate (GFR) cannot be measured directly but rather is estimated using the clearance of a filtration marker. The GFR is equal to the renal clearance (CL_{renal}) of a filtration marker if the marker is not protein bound, does not enter red blood cells, and is only excreted through the kidney solely by filtration, with neither tubular secretion nor reabsorption. In addition, the substance must not be toxic and must not in itself alter GFR. For such a substance, CL_{plasma} equals CL_{renal}. Renal clearance of surrogate marker of GFR is calculated by using the classical formula, $CL_{renal} = (U \times C_u) / C_{p,}$ which was introduced by (Rehberg, 1926) where U = urine flow in mL/min, C_u = marker concentration in urine in mg/mL, and C_p = marker concentration in plasma in mg/mL. This approach is accurate provided urine collection is complete. In practice, it is often difficult to make sure that the bladder is empty after urine collection, and incomplete bladder emptying will lead to underestimation of GFR (Finco, 2005). Risk of infection due to catheterization is also a complicating factor.

Estimation of renal clearance by the classical formula from blood and urine data has been the most common approach, but the use of CL_{plasma} methods is becoming more common these days to shorten the time of assay and to avoid tedious urine collection process. Plasma clearance is calculated by using either $CL_{plasma} = D/AUC$, where D = dose of marker and AUC = area under the plasma concentration versus time curve or ratio of infusion rate of inulin to plasma steady state concentration of inulin, $GFR\ (mL/\text{min}) = \frac{Infusion\ rate\ of\ inulin\ (mg/\text{min})}{C_{p(ss)}(mg/\text{mL})}$ (Fischer P.A et al., 2000)

Inulin clearance:

Inulin is a fructose polysaccharide which is mainly obtained from tubers of Dahlia and Chicory, and dozens of other tubers, roots and artichokes of plants (figure 7). Inulin is non-toxic,

completely freely filtered by glomerular filtration, neither absorbed nor secreted by renal tubules (Earle and Berliner, 1946; Richards and Hoe, 1967; Perrone et al., 1990; Prescott et al., 1991). Therefore, renal clearance of inulin using continuous infusion is generally considered to be the gold standard for the measurement of GFR (Earle and Berliner, 1946; Brochner-Mortensen, 1985). If a new marker is introduced, it is common to compare the results to CL_{renal} of inulin for validation of the new method (Brenner et al., 1976). Inulin must be administered intravenously since it is hydrolyzed to fructose in the gastrointestinal tract and is erratically and poorly absorbed from subcutaneous or intramuscular routes of administration. The classical method of measuring urinary clearance includes intravenous administration of a priming dose followed by a constant infusion of inulin (Smith et al., 1938). Under these conditions, plasma and urine inulin concentrations reach a constant level, which is equal in arterial and venous blood. After an equilibration period of approximately 60 - 80 minutes, several blood and urine samples are collected ranging from 10 - 20 minute intervals. Then, GFR is calculated by using the standard formula: $CL_{renal} = (U \times C_u) / C_p$ where U = urine flow in mL/min, C_u = marker concentration in urine in mg/mL, and C_p = marker concentration in plasma in mg/mL. The need for timed urine collection is obviously cumbersome and pretends to be a great limitation for routine measurement of GFR in the classical urinary clearance of inulin method. In the recent years, plasma clearance of inulin has been introduced in the veterinary medicine as a promising alternative for estimating GFR in a clinical setting (Fettman et al., 1985; Rogers et al., 1991; Brown et al., 1996; Miyamoto, 1998). For the measurement of plasma inulin clearance, inulin is given either as a constant intravenous infusion alone or followed by infusion of a bolus dose. When plasma or serum levels of inulin reach steady state during an intravenous infusion of the compound, the rate of excretion is equal to the rate of infusion. From this assumption, GFR (mL/min) = Rate of infusion (mg/min) / $C_{p(ss)}$ (mg/mL) [where $C_{p(ss)}$ is the plasma steady state concentration of inulin] (Shnurr et al., 1980; Fischer P.A et al., 2000). It has been shown that the plasma clearance of inulin values are overestimated than urinary clearance values (Hellerstein et al., 1993; Van Acker et al., 1995).

The reason for overestimation of GFR values is due to failure to obtain constant inulin plasma concentrations during intravenous infusion. The error would be pronounced if the shorter infusion times were chosen (Rahn et al., 1999).

Most of the analytical methods used for the quantification of inulin are based on the acid hydrolysis. Several substances such as resorcinol, anthrone, diphenylamine and indole-3-acetic acid, have been used and the color formed from the reaction with fructose was measured photometrically. The colorimetric assays are often inaccurate, mainly due to interference from plasma hexoses and potentially dangerous owing to the use of concentrated corrosive reagents (Heyrovsky, 1956; Fjeldbo and Stamey, 1968). Other methods involving the use of enzymatic procedures after acid hydrolysis are time consuming. Analysis of inulin in plasma and urine samples after acid hydrolysis by reversed phase HPLC gave good results (Dall'Amico et al., 1995; Pastore et al., 2001).

The limitations of inulin clearance as a surrogate marker of GFR are: Inulin has a relatively high molecular weight and it takes quite a long time to attain equilibration (Hellerstein et al., 1993). Furthermore, there is no commercially available sterile inulin preparation which can be used readily. Each lab or clinic has to prepare and standardize to their conditions. Anaphylactic reactions have reported with the administration of inulin (Bacchetta et al., 2008a; Bacchetta et al., 2008b). Because of lack of alternative methods which could measure GFR with maximum accuracy, inulin clearance is still considered as gold standard for the measurement of GFR.

Effective Renal Plasma Flow (ERPF):

Renal plasma flow is estimated from the clearance of a compound that is almost completely extracted from the renal blood. Since no compound is totally extracted in a single pass through the kidney, the measurement of renal plasma flow realistically falls slightly below the actual renal plasma flow, and thus is known as effective renal plasma flow (ERPF). Para amino hippuric acid (PAH) (N-(4-aminobenzoyl)-glycine) (figure 8) is an organic anion that is

freely filtered by the glomerulus and extensively secreted into the proximal convoluted tubule by active transport and very poorly reabsorbed into the tubules. The secretion of PAH is so effective that 90% or more of the PAH in renal arterial plasma may be removed in a single passage through the kidney. In practice, the concentration of PAH in renal venous plasma is ignored and the concentration of PAH in peripheral venous plasma is taken as an estimate of the renal arterial plasma PAH concentration. As PAH is removed from the blood exclusively by the kidney and is nearly completely cleared from the renal plasma in one passage through the kidney, the renal clearance of PAH is approximately equal o the total effective renal plasma flow (Shnurr et al., 1980; Mann and Kinter, 1993). ERPF is determined following administration of bolus dose and intravenous administration of PAH for approximately 180 minutes or until steady state is achieved. Plasma samples are collected during the steady state and concentrations of PAH are determined to calculate ERPF and ERBF using the following equations (Mann and Kinter, 1993; Fischer P.A et al., 2000):

$$ERPF\ (mL/\text{min}) = \frac{Infusion\ rate\ of\ PAH\ (mg/\text{min})}{ER \cdot C_{p(ss)}\ (mg/\text{mL})}$$

$$ERBF\ (mL/\text{min}) = \frac{Infusion\ rate\ of\ PAH\ (mg/\text{min})}{(ER)C_{p(ss)}(1 - Hct/100)}$$

The clearance of PAH depends on the rate of delivery of PAH to the kidney. This transport mechanism is ATP dependent and saturable. Delivery of PAH into the proximal tubule in excess of the maximal rate of PAH (T_m, or transport maximum) results in incomplete extraction and spillage of PAH into the renal venous plasma. This results in underestimation of renal blood flow and will approach the values of GFR (Mann and Kinter, 1993). Earlier analytical methods to measure PAH by colorimetric reaction was often difficult and frequently inaccurate in the presence of glucose and other drugs (Boschi and Marchesini, 1981). Recent

advancement in chromatography techniques have lead to development of good analytical methods using HPLC (Baccard N et al., 1999 ; Brenna et al., 1998)

Other methods for measurement of ERPF: electromagnetic, ultrasonic and Doppler flow probes placed directly on the renal artery; magnetic resonance imaging; using radioactive tracers, such as ^{131}I orthoiodohippurate (OIH), ^{99m}Tc-mercaptoacetyl-triglycine (MAG3) (Itoh, 2001).

5. Vinblastine

Vinblastine (vincaleucoblastine, VLB) is a vinca alkaloid isolated from periwinkle plant, *Catharanthus roseus* (family: Apocyanaceae). Vinca alkaloids consist of indole nucleus (catharanthine) and dihydroindole nucleus (vindoline portion) (figure 9). Vinblastine was the first vinca alkaloid isolated. Its clinical use was first discovered when leucopenia was noticed after consumption of leaves of periwinkle plant in tea. This led to hypothesis that vinblastine might be useful to treat white blood cell cancers, such as lymphoma. In order to increase the therapeutic utility and decrease the potential for toxic side effects, semi-synthetic vinca alkaloids, such as vinflunine, vindesine sulfate, and vinorelbine (VRB) were developed (Damen et al., 2010). Although all of these vinca alkaloids share common features in their structure and affinity for microtubules, there is variability in their therapeutic efficiency, therapeutic indications, and toxicities (Damen et al., 2009).

Vinca alkaloids bind to beta - tubulin and inhibit the assembly of microtubules during M phase of cell cycle (figure 2). Microtubules are highly dynamic cytoskeleton fibers that are composed of tubulin subunits (Pasquier and Kavallaris, 2008). For the separation of chromosomes during anaphase of mitosis, microtubules - an important component of the mitotic spindle, and kinetochore are necessary. This binding of tubulin results in arrest of mitosis (Schneider-Affeld et al., 1977; Hashizume et al., 1988; Jordan and Wilson, 2004; Gan and Kavallaris, 2008; Kavallaris et al., 2008; Cheng et al., 2009).

Development of resistance to microtubule targeted drugs have several possible mechanisms including changes in microtubule dynamics as a result of altered expression of tubulin isotypes, tubulin mutations, and altered expression or binding of microtubule regulatory proteins (Jordan and Wilson, 2004).

Vinblastine is effective against soft tissue tumors, such as lymphomas, carcinomas, splenic tumors, and mast cell tumors as a single agent or in combination with other anticancer drugs. Vinblastine is administered intravenously. Oral absorption of vinblastine is erratic and incomplete (Golden and Langston, 1988; Camps-Palau et al., 2007; Vickery et al., 2008).

Reversible myelosuppression and peripheral neuropathy (Park et al., 2008) are the principle side effects of vinblastine chemotherapy. In vinblastine treated patients, dose related granulocytopenia with a nadir at 4 to 9 days after treatment and recovery in 2 to 3 weeks is commonly seen. Gastrointestinal signs, malaise, weakness, and alopecia may be seen. Because of the pattern of myelosuppression associated with vinblastine, dosing regimens include biweekly administrations preceded by WBC counts (Bailey et al., 2008).

Vinblastine is primarily metabolized by cytochrome P450 enzymes in the liver and eliminated in feces (Creasey et al., 1975; Chabner et al., 1977). Urinary excretion of vinblastine is minimal compared to biliary route (Creasey et al., 1975; de Lannoy et al., 1994). Vinblastine is metabolized to desacetylvinblastine (figure 10) which is presumed to be pharmacologically active.

Different analytical methods were developed using reversed phase high performance liquid chromatography(De Smet et al., 1987; van Tellingen et al., 1991; Volkov and Grodnitskaya, 1994), radioimmunoassay, liquid chromatography – tandem mass spectrometry (LC/MS/MS) (Ramirez et al., 1997; Zhou et al., 2005; Damen et al., 2008) to quantify vinblastine and its metabolite, desacetylvinblastine in different matrices in different species.

6. Cisplatin

Cisplatin (*cis*-diamminedichloroplatinum (II) (CDDP); *cis*-$PtCl_2(NH_3)_2$is a platinum containing alkylating agent indicated for the treatment of solid tumors (figure 11). The cytotoxic effects of platinum were discovered while studying the effects of electrical current on bacterial growth (Rosenberg et al., 1965) . The mechanism of action of cisplatin is by establishing cross links within and between purine bases. Intrastand cross linking between Guanine – Guanine association was shown to be more common than other linking (Bellon et al., 1991). Cisplatin is indicated for the treatment of several solid tumors in both humans and dogs including but not limited to ovarian, testicular, transitional cell tumor, germ cell tumors, osteosarcomas, neuroblastomas, medulloblastomas (Pinkerton et al., 1986; Peng et al., 1997; Greene et al., 2007; Fouladi et al., 2008). Cisplatin is a powerful emetic and requires antiemetic therapy prior to administration of cisplatin. Ondansetron has shown to be a potent antiemetic in cisplatin administration. Nephrotoxicity is the dose limiting toxicity of cisplatin (Daugaard et al., 1987a; Daugaard et al., 1987b; Erdlenbruch et al., 2001; Barabas et al., 2008; Townsend et al., 2009). Therefore, saline diuresis prior to and after cisplatin administration is necessary to reduce possible nephrotoxicity. Cisplatin is contraindicated in cats as it causes fatal pulmonary edema. Cisplatin is given intravenously and some studies have shown efficacy with intralesional injection with sesame oil or epinephrine gel. Many mechanisms of cisplatin resistance have been proposed including changes in cellular uptake and efflux of the drug, increased detoxification of the drug, inhibition of apoptosis and increased DNA repair (Rabik and Dolan, 2007).

Carboplatin is sister analogue of cisplatin with reduced nephrotoxicity and non-emetic. Carboplatin can be used in cats unlike cisplatin. Carboplatin replaced cisplatin in veterinary medicine. However, cisplatin is still considered for treating several solid tumors because of its efficacy against several tumors both in humans and dogs (Fouladi et al., 2008). Carboplatin is more expensive than cisplatin. Unlike cisplatin, the clearance of carboplatin correlates with the

glomerular filtration rate in humans (Calvert et al., 1989; de Jongh et al., 2001). In humans, creatinine clearance was used as a surrogate marker of glomerular filtration rate (GFR) and an equation was developed retrospectively to calculate the doses of carboplatin more accurately as a function of creatinine clearance.

Dose (mg) = target AUC (mg.min/mL) x (GFR [mL/min] + 25)

Where the target AUC is 5 – 7 mg.min/mL for previously untreated patients receiving single agent carboplatin; or 4 – 6 mg.min/mL for previously treated patients receiving single agent carboplatin or previously untreated patients receiving carboplatin plus cyclophosphomide (Calvert et al., 1989).

7. **Mast cell tumors**

Mast cells are normal components of different tissues throughout the body. They are round cells roughly one to three times the size of neutrophils. In the dog, skin, lung, gut and liver contain the highest number of mast cells. Mast cells derive from CD34 progenitor cells in bone marrow (Kirshenbaum et al., 1991; Rottem et al., 1991). Unlike other bone marrow differentiated cells, mast cells leave bone marrow as immature cells and mature only after localizing in the connective or mucosal tissues (Hatanaka et al., 1979; Kitamura et al., 1979a; Kitamura et al., 1979b; Hayashi et al., 1985; Kitamura et al., 1985). Hayashi C, 1985.

Important characteristic feature of mature mast cells is the presence of cytoplasmic granules which contain many biologically active substances, such as histamine, heparin chemotactic factors, and cytokines and metabolites of arachidonic acid (Misdorp, 2004). Mast cells also release proteolytic enzymes, including collagenase, which may cause collagen lysis; lipid mediators, such as prostaglandins, leukotrienes, and platelet activating factors; and cytokines (London and Seguin, 2003). Degranulation occurs under the influence of rapid calcium ion influx and thus the biologically active substances are released. This confers mast cells an important role

in immunological, inflammatory and immediate type allergic reactions (Galli et al., 1999; Wedemeyer et al., 2000). Occasionally, both normal as well as neoplastic mast cells show a characteristic color change when stained with toluidine blue or Giemsa stain. This metachromasia is caused by hexasaccharides, the fundamental unit of heparin (London and Seguin, 2003; Misdorp, 2004).

Mast cell tumors are most common skin tumors in dogs (London and Seguin, 2003; Thamm et al., 2006). In dogs, mast cell tumors develop most frequently in skin, but they can also grow in the intestine, liver, spleen and elsewhere (Smith et al., 2002). Dog breeds, such as Boxer, Boston terrier, English Bulldog, Labrador retriever, Golden retriever, Cocker spaniel, Schnauzer, Shar pei, and Pug are at higher risk for mast cell tumors (Patnaik et al., 1984; Rothwell et al., 1987). However, all breeds are susceptible and both sexes are equally affected. No gender predilection was reported. The mean age for presentation of mast cell tumor is eight years, although young puppies have also shown manifestations of this disease. The risk increases with increasing age (Welle et al., 2008).

Mast cell tumors are classified based on histological appearance for staging prognosis. World Health Organization classification (Dobson and Scase, 2007) and Patnaik grading (Patnaik et al., 1984) of mast cell tumors were widely used. However, recent multicenter research work had replaced previous grading system with 2-tier histological grading – low grade and high grade (Kiupel et al.). Cutaneous MCTs are typically solitary lesions, but their clinical appearance can be variable, and some dogs can develop more than one apparently unrelated MCT. MCT should be considered in the differential diagnosis of any skin tumor. Low-grade, well-differentiated MCTs usually present as a solitary, slowly growing dermal nodule. More aggressive MCTs may present as large, ill-defined soft tissue masses, and some may be surrounded by satellite nodules as the tumor spreads to surrounding lymph nodes. The clinical behavior of MCTs is also variable,

ranging from benign to highly malignant. Because of this variable clinical behavior and the potential for associated paraneoplastic syndromes, these tumors become difficult to manage.

The exact etiology of the MCTs is unknown but genetic predisposition and other multiple factors are well documented by several researchers (London and Seguin, 2003; Dobson and Scase, 2007; Welle et al., 2008). Recently, a stem cell factor receptor - KIT, has been implicated in the etiology of canine MCTs (London et al., 1996). C-Kit is activated by ligand-dependent tyrosine kinase activity. Activated KIT binds and phosphorylates intracellular substrate proteins, initiating a signaling cascade that culminates in a wide array of biologic activities including proliferation, migration, maturation, and survival of hematopoietic stem cells, MCs, melanocytes, and germ cell lineages (Welle et al., 2008) . In addition to genetic mutations, some authors have suggested that chronic inflammation may play a role in MCT development (Govier, 2003).

Based on the earlier Patnaik grading system (Patnaik et al., 1984), surgery with wide margins is the mainstay of treatment for mast cell tumors for low grade, well differentiated mast cell tumors. Surgery and radiation therapy are indicated for the treatment of grade II tumors. Chemotherapy is reserved for grade III tumors and incompletely excised grade II tumors (Govier, 2003; London and Seguin, 2003; Dobson and Scase, 2007). However, based on 2-tier histological grading of cutaneous mast cell tumors in dogs (Kiupel et al.), surgery with wide margins or surgery coupled with radiation therapy would be indicated whereas chemotherapy is generally reserved for high grade mast cell tumors and for incompletely excised low grade mast cell tumors. Vinblastine and prednisone combination is chemotherapy of choice to treat mast cell tumors. Toceranib phosphate (Palladia®), a tyrosine kinase inhibitor was approved by FDA with the indications to treat mast cell tumors in dogs. However, treatment of mast cell tumors with vinblastine is still considered as standard of care of mast cell tumors in dogs (Robat et al., ; Rassnick et al., 2008).

8. *In vitro* studies

Intrinsic clearance:

Intrinsic clearance (CL_{int}) is the ability of an organ to remove drug from the blood. The best described techniques to predict *in vivo* pharmacokinetic parameters in humans are from the *in vivo* laboratory animal data using allometric scaling. However, there were some physiological differences between humans and animals leading to under or over prediction of human PK parameters. Also, increased expenses, issues with animal rights, and time frame for the development of drugs in the pharmaceutical research lead to increased interest in the use of *in vitro* studies to predict *in vivo* pharmacokinetic parameters (Houston, 1994; Obach, 1999c; Obach, 1999b; Obach, 2001; Venkatakrishnan et al., 2001; Venkatakrishnan et al., 2003). Retrospective analyses of new chemical entities (NCEs) which have entered into clinical development shows that approximately 40% of the drugs were discontinued because of unacceptable pharmacokinetic parameters (Prentis et al., 1988). *In vitro* methods became popular in the recent years in choosing the potential drug candidate possessing acceptable pharmacokinetic parameters, such as optimal clearance to reduce dose, half-life permitting once a day oral dose. Commonly predicted *in vivo* pharmacokinetic parameters from *in vitro* data include but are not limited to clearance, volume of distribution, elimination half-life, and bioavailability.The Common assumptions for *in vitro* metabolism studies are (Obach, 2011):

1. Liver is the only organ responsible for metabolism
2. Cytochrome P450 enzymes are the only enzyme system responsible for metabolism and clearance
3. Metabolic clearance is the primary route of clearance ($CL_{metabolic} = CL_{renal} + CL_{biliary} + CL_{other}$)

4. During acquisition of liver tissues and processing to obtain microsomes, cytochrome P450 enzymes remain fully intact
5. The artificial conditions used to support *in vitro* metabolism (e.g. Buffers, NADPH) do not hamper the rate of metabolism.
6. The substrate concentration used *in vitro* is reflective of that which occurs in the liver *in vivo* and is sub-saturating
7. The substrate is completely unbound in the incubation mixture
8. Hepatic transport does not alter clearance

Commonly used matrices for *in vitro* drug metabolism studies are microsomes, hepatocytes, liver cytosol fractions, liver S9 fractions, liver slices, and heterologously expressed cytochrome P450 enzymes.

Microsomes are commonly used *in vitro* systems to study drug metabolism. Microsomes are vesicle like structures formed from the endoplasmic reticulum when eukaryotic cells are subjected to differential centrifugation(Schneider, 1948). Microsomes are rich in phase I enzymes including cytochrome P450 enzymes and phase II enzymes, such as UGTs. Microsomes are easy to prepare and store at – 80 ^{0}C without losing potency. For monoxygenase activity of cytochrome P450 enyzmes, NADPH – regenerating system (contains NADP, glucose-6-phosphate, and glucose-6-phosphate dehydrogenase) is required to initiate enzyme reaction (Hariparsad et al., 2006). Pooled liver microsomes are available commercially for different species. There are some limitations of microsomes in the drug metabolism studies. Firstly, acidic drugs tend to bind less to microsomal proteins whereas basic drugs tend to bind more to microsomes. This will have impact in *in vitro / in vivo* correlations. Secondly, substrates and their metabolites will have ready access to enzymes unlike in the real *in vivo* situation. Thirdly, the concentrations of substrates used in the *in vitro* systems may not reflect the concentrations of drugs in the *in vivo* system. And lastly, several soluble enzyme systems are not present leading to some metabolites not being formed.

In classical Michaelis – Menten kinetics, a series of drug concentrations will be incubated in the *in vitro* systems and rate of product or metabolite will be monitored. Theoretical maximum rate of reaction, V_{max} and Michaelis constant, K_m will be determined by plotting substrate concentration on x-axis and rate of product formation on y - axis. K_m is the value of substrate concentration at which rate of reaction is half of theoretical maximum rate of reaction. For new chemical entities (NCEs), and for some drugs, product or metabolite may not be identified or standards for metabolites may not be available. In such cases, alternative approaches, such as substrate depletion approach (Jones and Houston, 2004; Nath and Atkins, 2006) and *in vitro* half life method (Obach, 1999a) are useful to predict V_{max} and K_m. Regardless of approaches to determine the values of V_{max} and K_m, the equations to calculate intrinsic clearance of drugs are same. Several studies have shown methods based on rate of product formation and substrate depletion approach are comparable (Stringer et al., 2009).

In vitro intrinsic clearance of a drug is calculated as a ratio of theoretical maximum rate of reaction (V_{max}) to Michaelis constant (K_m).

$$In\ vitro\ CL_{int} = \frac{V_{max}}{K_m}$$

The calculated *in vitro* intrinsic clearance must be scaled up to clearance of drug at the animal level using certain scaling factors to obtain *in vivo* intrinsic clearance (Proctor et al., 2004; Smith et al., 2008). The *in vivo* intrinsic clearance must be combined with other factors, such as fraction of unbound drug and hepatic blood flow with some assumptions to determine hepatic clearance (Venkatakrishnan et al., 2003).

$$In\ vivo\ CL_{int} = In\ vitro\ CL_{int} \cdot \frac{55\ mg\ microsomal\ protein}{g\ of\ liver} \cdot \frac{g\ of\ liver}{kg\ of\ body\ weight}$$

There are three commonly used predictive models to predict hepatic clearance, such as well-stirred model, parallel tube model, and dispersion model (Pang and Rowland, 1977; Roberts and Rowland, 1986; Ito and Houston, 2004).

Well-stirred model:

$$CL_{hepatic} = \frac{Q_h \bullet f_u \bullet CL_{\text{int}}}{Q_h + f_u \bullet CL_{\text{int}}}$$

Parallel tube model:

$$CL_{hepatic} = Q_h \left[1 - \exp\left(\frac{f_u \bullet CL_{\text{int}}}{Q_h} \right) \right]$$

Dispersion model:

$$CL_{hepatic} = Q_h \left[1 - \frac{4a}{(1+a)^2 \exp\left[\frac{a-1}{2Dn} \right] - (1-a)^2 \exp\left[-\frac{a+1}{2Dn} \right]} \right]$$

Where Q_h = hepatic blood flow, CL_{int} = *in vivo* intrinsic clearance, $a = \sqrt{1 + 4Rn \cdot Dn}$, Rn = efficiency number = $\frac{f_u \cdot CL_{int}}{Q_h}$, and D_n = dispersion number.

Of these three models, Well-Stirred model is the simplest with minimal assumptions. However, its accuracy was found to be least in several studies. Well-stirred model assumes that liver is a single well-stirred compartment and the concentration of unbound drug within the liver is in equilibration with unbound drug in the emergent blood (Pang and Rowland, 1977). Parallel tube model assumes that liver is composed of series of similar parallel tubes with same concentration of enzymes in each cross section. There are other assumptions for all three models, such as intimate mixing of blood between hepatic portal blood and the hepatic arterial blood, only unbound drug crosses the membrane, no barrier between enzymes in the hepatocytes and drug in

the blood, the rate of drug elimination is a function of unbound drug. Dispersion model is considered to predict hepatic clearance better than other two models. However, the complexity of the dispersion model is a limitation and not used frequently.

9. *In vitro / in vivo* correlations

Several studies have shown the utility of *in vitro / in vivo* correlations in predicting the pharmacokinetic parameters. Integrating in vitro metabolism data with limited in vivo studies improves the predictive ability of the allometric scaling of pharmacokinetic parameters (Lave et al., 1999; NARITOMI et al., 2001; Houston and Galetin, 2003; Venkatakrishnan et al., 2003; Poulin et al., 2011). The ability of *in vitro* methods to predict *in vivo* pharmacokinetic parameters is tested by different ways, such as simple percent accuracy, correlation analyses, and statistical methods (average fold error, mean square error, and root mean square error) (Sheiner and Beal, 1981; Ito and Houston, 2004). Average fold error (*afe*) is the geometric mean of the ratio of predicted and actual values and gives a measure of bias. If the predicted value is equal to actual value, then the average fold error would be equal to one. The *afe* would be equal to 2 if the predicted value is within 100% above or 50% below the observed value (Sheiner and Beal, 1981). Root mean squared prediction error (*rmse*) calculates the variance of the predictions from the sum of the squares to the prediction errors. Root mean squared prediction error represents precision of the assay.

$$afe = 10^{\left|\frac{1}{n}\Sigma\frac{predicted}{observed}\right|}$$

$$mse = \frac{1}{n}\sum(predicted - observed)^2$$

$$rmse = \sqrt{mse}$$

References

Body surface area for adjustment of drug dose. *Drug Ther Bull* **48:**33-36.

Agarwal R (1998) Chromatographic estimation of iothalamate and p-aminohippuric acid to measure glomerular filtration rate and effective renal plasma flow in humans. *J Chromatogr B Biomed Sci Appl* **705:**3-9.

Alberts B, Johnson A, Lewis J, Raff M, Robers K and Walter P (2002) The cell cycle and programmed cell death. *Molecular biology of the cell***:**983-985.

Arrington KA, Legendre AM, Tabeling GS and Frazier DL (1994) Comparison of body surface area-based and weight-based dosage protocols for doxorubicin administration in dogs. *Am J Vet Res* **55:**1587-1592.

Baccard N, Hoizey G, Frances C, Lamiable D, Trenque T and H. M (1999) Simultaneous determination of inulin and p-aminohippuric acid (PAH) in human plasma and urine by high-performance liquid chromatography. *Analyst* **124:**833-836.

Bacchetta J, Cochat P, Villard F, Astier M, Vial T, Dubourg L, Hadj-Aissa A and Kassai B (2008a) Hypersensitivity to inulin: a rare and mostly benign event. *Am J Kidney Dis* **52:**632-633.

Bacchetta J, Villard F, Vial T, Dubourg L, Bouvier R, Kassai B and Cochat P (2008b) 'Renal hypersensitivity' to inulin and IgA nephropathy. *Pediatr Nephrol* **23:**1883-1885.

Bailey DB, Rassnick KM, Kristal O, Chretin JD and Balkman CE (2008) Phase I dose escalation of single-agent vinblastine in dogs. *J Vet Intern Med* **22:**1397-1402.

Baker RJ, Kozoll DD and Meyer KA (1957) The use of surface area as a basis for establishing normal blood volume. *Surg Gynecol Obstet* **104:**183-189.

Baker SD, Verweij J, Rowinsky EK, Donehower RC, Schellens JH, Grochow LB and Sparreboom A (2002) Role of body surface area in dosing of investigational anticancer agents in adults, 1991-2001. *J Natl Cancer Inst* **94:**1883-1888.

Barabas K, Milner R, Lurie D and Adin C (2008) Cisplatin: a review of toxicities and therapeutic applications. *Vet Comp Oncol* **6:**1-18.

Bellon SF, Coleman JH and Lippard SJ (1991) DNA unwinding produced by site-specific intrastrand cross-links of the antitumor drug cis-diamminedichloroplatinum(II). *Biochemistry* **30:**8026-8035.

Boschi S and Marchesini B (1981) High-performance liquid chromatographic method for the simultaneous determination of iothalamate and o-iodohippurate. *J Chromatogr* **224:**139-143.

Braun JP, Lefebvre HP and Watson AD (2003) Creatinine in the dog: a review. *Vet Clin Pathol* **32:**162-179.

Brenna S, Grigoras O, Drukker AG and Jean-Pierre. (1998) Pitfalls in measuring inulin and para-amino-hippuric acid clearances. *Pediatric Nephrology* **12:**489-491.

Brenner BM, Deen WM and Robertson CR (1976) Determinants of glomerular filtration rate. *Annu Rev Physiol* **38:**11-19.

Brochner-Mortensen J (1985) Current status on assessment and measurement of glomerular filtration rate. *Clin Physiol* **5:**1-17.

Brown SA, Finco DR, Boudinot FD, Wright J, Taver SL and Cooper T (1996) Evaluation of a single injection method, using iohexol, for estimating glomerular filtration rate in cats and dogs. *Am J Vet Res* **57:**105-110.

Calvert AH, Newell DR, Gumbrell LA, O'Reilly S, Burnell M, Boxall FE, Siddik ZH, Judson IR, Gore ME and Wiltshaw E (1989) Carboplatin dosage: prospective evaluation of a simple formula based on renal function. *J Clin Oncol* **7:**1748-1756.

Camps-Palau MA, Leibman NF, Elmslie R, Lana SE, Plaza S, McKnight JA, Risbon R and Bergman PJ (2007) Treatment of canine mast cell tumours with vinblastine, cyclophosphamide and prednisone: 35 cases (1997-2004). *Vet Comp Oncol* **5:**156-167.

Canal P, Chatelut E and Guichard S (1998) Practical treatment guide for dose individualisation in cancer chemotherapy. *Drugs* **56:**1019-1041.

Chabner BA, Myers CE and Oliverio VT (1977) Clinical pharmacology of anticancer drugs. *Semin Oncol* **4:**165-191.

Chatelut E, Delord JP and Canal P (2003) Toxicity patterns of cytotoxic drugs. *Invest New Drugs* **21:**141-148.

Cheng T, Si D and Liu C (2009) Rapid and sensitive LC-MS method for pharmacokinetic study of vinorelbine in rats. *Biomed Chromatogr* **23:**909-911.

Coppoletta JM and Wolbach SB (1933) Body Length and Organ Weights of Infants and Children: A Study of the Body Length and Normal Weights of the More Important Vital Organs of the Body between Birth and Twelve Years of Age. *Am J Pathol* **9:**55-70.

Cowgill GR and Drabkin DL (1927) Determination of a formula for the surface area of the dog together with a consideration of formulae available for other species. *Am J PHysiol* **81:**36-61.

Creasey WA, Scott AI, Wei CC, Kutcher J, Schwartz A and Marsh JC (1975) Pharmacological studies with vinblastine in the dog. *Cancer Res* **35:**1116-1120.

Dall'Amico R, Montini G, Pisanello L, Piovesan G, Bottaro S, Cracco AT, Zacchello G and Zacchello F (1995) Determination of inulin in plasma and urine by reversed-phase high-performance liquid chromatography. *J Chromatogr B Biomed Appl* **672:**155-159.

Damen CW, Lagas JS, Rosing H, Schellens JH and Beijnen JH (2009) The bioanalysis of vinorelbine and 4-O-deacetylvinorelbine in human and mouse plasma using high-performance liquid chromatography coupled with heated electrospray ionization tandem mass-spectrometry. *Biomed Chromatogr* **23:**1316-1325.

Damen CW, Rosing H, Schellens JH and Beijnen JH (2010) High-performance liquid chromatography coupled with mass spectrometry for the quantitative analysis of vinca-

alkaloids in biological matrices: a concise survey from the literature. *Biomed Chromatogr* **24:**83-90.

Damen CW, Rosing H, Tibben MM, van Maanen MJ, Lagas JS, Schinkel AH, Schellens JH and Beijnen JH (2008) A sensitive assay for the quantitative analysis of vinorelbine in mouse and human EDTA plasma by high-performance liquid chromatography coupled with electrospray tandem mass spectrometry. *J Chromatogr B Analyt Technol Biomed Life Sci* **868:**102-109.

Daugaard G, Abildgaard U, Holstein-Rathlou NH, Amtorp O and Leyssac PP (1987a) Effect of cisplatin on renal haemodynamics and tubular function in the dog kidney. *Int J Androl* **10:**347-351.

Daugaard G, Abildgaard U, Larsen S, Holstein-Rathlou NH, Amtorp O, Olesen HP and Leyssac PP (1987b) Functional and histopathological changes in dog kidneys after administration of cisplatin. *Ren Physiol* **10:**54-64.

de Jongh FE, Verweij J, Loos WJ, de Wit R, de Jonge MJ, Planting AS, Nooter K, Stoter G and Sparreboom A (2001) Body-surface area-based dosing does not increase accuracy of predicting cisplatin exposure. *J Clin Oncol* **19:**3733-3739.

de Lannoy IA, Mandin RS and Silverman M (1994) Renal secretion of vinblastine, vincristine and colchicine in vivo. *J Pharmacol Exp Ther* **268:**388-395.

De Smet M, Van Belle SJ, Seneca V, Storme GA and Massart DL (1987) Determination of vinblastine in MO4 mouse fibrosarcoma cells by high-performance liquid chromatography. *J Chromatogr* **416:**375-381.

Deavers S, Huggins RA and Smith EL (1972) Absolute and relative organ weights of the growing beagle. *Growth* **36:**195-208.

Dobson JM and Scase TJ (2007) Advances in the diagnosis and management of cutaneous mast cell tumours in dogs. *J Small Anim Pract* **48:**424-431.

Dooley MJ and Poole SG (2000) Poor correlation between body surface area and glomerular filtration rate. *Cancer Chemother Pharmacol* **46:**523-526.

Du Bois D and Du Bois EF (1989) A formula to estimate the approximate surface area if height and weight be known. 1916. *Nutrition* **5:**303-311; discussion 312-303.

DuBois D and EF D (1916) A formula to estimate the approximate surface area if height and weight be known. *Arch Intern Med* **17:**863-871.

DuBois D and DuBois EF (1916) A formula to estimate the approximate surface area if height and weight be known. *Arch Intern Med* **17:**863-871.

Earle DP, Jr. and Berliner RW (1946) A simplified clinical procedure for measurement of glomerular filtration rate and renal plasma flow. *Proc Soc Exp Biol Med* **62:**262-264.

Effersoe H, Rosenkilde P, Groth S, Jensen LI and Golman K (1990) Measurement of renal function with iohexol. A comparison of iohexol, 99mTc-DTPA, and 51Cr-EDTA clearance. *Invest Radiol* **25:**778-782.

Egorin MJ (2003) Horseshoes, hand grenades, and body-surface area-based dosing: aiming for a target. *J Clin Oncol* **21:**182-183.

Erdlenbruch B, Pekrum A, Roth C, Grunewald RW, Kern W and Lakomek M (2001) Cisplatin nephrotoxicity in children after continuous 72-h and 3x1-h infusions. *Pediatr Nephrol* **16:**586-593.

Evans WE and Relling MV (1989) Clinical pharmacokinetics-pharmacodynamics of anticancer drugs. *Clin Pharmacokinet* **16:**327-336.

Felici A, Verweij J and Sparreboom A (2002) Dosing strategies for anticancer drugs: the good, the bad and body-surface area. *Eur J Cancer* **38:**1677-1684.

Fettman MJ, Allen TA, Wilke WL, Radin MJ and Eubank MC (1985) Single-injection method for evaluation of renal function with 14C-inulin and 3H-tetraethylammonium bromide in dogs and cats. *Am J Vet Res* **46:**482-485.

Finco DR (2005) Measurement of glomerular filtration rate via urinary clearance of inulin and plasma clearance of technetium Tc 99m pentetate and exogenous creatinine in dogs. *Am J Vet Res* **66:**1046-1055.

Finco DR, Coulter DB and Barsanti JA (1981) Simple, accurate method for clinical estimation of glomerular filtration rate in the dog. *Am J Vet Res* **42:**1874-1877.

Fischer P.A, Claudia B. Bogoliuk, Agusti'n J. Ramirez, Ramiro A Sa'nchez and Masnatta LD (2000) A new procedure for evaluation of renal function without urine collection in rat *Kidney International* **58:**1336-1341.

Fjeldbo W and Stamey TA (1968) Adapted method for determination of inulin in serum and urine with an AutoAnalyzer. *J Lab Clin Med* **72:**353-358.

Foote M (1998) The Importance of Planned Dose of Chemotherapy on Time: Do We Need to Change Our Clinical Practice? *Oncologist* **3:**365-368.

Fouladi M, Chintagumpala M, Ashley D, Kellie S, Gururangan S, Hassall T, Gronewold L, Stewart CF, Wallace D, Broniscer A, Hale GA, Kasow KA, Merchant TE, Morris B, Krasin M, Kun LE, Boyett JM and Gajjar A (2008) Amifostine protects against cisplatin-induced ototoxicity in children with average-risk medulloblastoma. *J Clin Oncol* **26:**3749-3755.

Frennby B and Sterner G (2002) Contrast media as markers of GFR. *Eur Radiol* **12:**475-484.

Friis-Hansen B (1961) Body water compartments in children: changes during growth and related changes in body composition. *Pediatrics* **28:**169-181.

Galli SJ, Maurer M and Lantz CS (1999) Mast cells as sentinels of innate immunity. *Curr Opin Immunol* **11:**53-59.

Gan PP and Kavallaris M (2008) Tubulin-targeted drug action: functional significance of class ii and class IVb beta-tubulin in vinca alkaloid sensitivity. *Cancer Res* **68:**9817-9824.

Gleadhill A, Peters AM and Michell AR (1995) A simple method for measuring glomerular filtration rate in dogs. *Res Vet Sci* **59:**118-123.

Golden DL and Langston VC (1988) Uses of vincristine and vinblastine in dogs and cats. *J Am Vet Med Assoc* **193:**1114-1117.

Gottesman MM (2002) Mechanisms of cancer drug resistance. *Annu Rev Med* **53:**615-627.

Govier SM (2003) Principles of treatment for mast cell tumors. *Clin Tech Small Anim Pract* **18:**103-106.

Greene SN, Lucroy MD, Greenberg CB, Bonney PL and Knapp DW (2007) Evaluation of cisplatin administered with piroxicam in dogs with transitional cell carcinoma of the urinary bladder. *J Am Vet Med Assoc* **231:**1056-1060.

Gregory CR, Gourley IM, Taylor NJ, Broaddus TW, Olds RB and Patz JD (1987) Preliminary results of clinical renal allograft transplantation in the dog and cat. *J Vet Intern Med* **1:**53-60.

Grochow LB, Baraldi C and Noe D (1990) Is dose normalization to weight or body surface area useful in adults? *J Natl Cancer Inst* **82:**323-325.

Gurney H (1996) Dose calculation of anticancer drugs : a review of the current practice and introduction of an alternative. *Journal of clinica oncology* **14:**2590-2611.

Gurney HP, Ackland S, Gebski V and Farrell G (1998) Factors affecting epirubicin pharmacokinetics and toxicity: evidence against using body-surface area for dose calculation. *J Clin Oncol* **16:**2299-2304.

Hariparsad N, Sane RS, Strom SC and Desai PB (2006) In vitro methods in human drug biotransformation research: implications for cancer chemotherapy. *Toxicol In Vitro* **20:**135-153.

Hashizume T, Akiba S, Sato T, Fujii T, Watanabe S and Sasaki J (1988) Vinblastine inhibits platelet aggregation by a microtubule-independent mechanism, probably by its perturbing action on the plasma membrane. *Thromb Res* **50:**181-190.

Hatanaka K, Kitamura Y and Nishimune Y (1979) Local development of mast cells from bone marrow-derived precursors in the skin of mice. *Blood* **53:**142-147.

Hayashi C, Sonoda T, Nakano T, Nakayama H and Kitamura Y (1985) Mast-cell precursors in the skin of mouse embryos and their deficiency in embryos of Sl/Sld genotype. *Dev Biol* **109:**234-241.

Haycock GB, Schwartz GJ and Wisotsky DH (1978) Geometric method for measuring body surface area: a height-weight formula validated in infants, children, and adults. *J Pediatr* **93:**62-66.

Hellerstein S, Berenbom M, Alon U and Warady BA (1993) The renal clearance and infusion clearance of inulin are similar, but not identical. *Kidney Int* **44:**1058-1061.

Hempel G and Boos J (2007) Flat-fixed dosing versus body surface area based dosing of anticancer drugs: there is a difference. *Oncologist* **12:**924-926.

Hess PW (1977) Principles of cancer chemotherapy. *Vet Clin North Am* **7:**21-33.

Heyrovsky A (1956) A new method for the determination of inulin in plasma and urine. *Clin Chim Acta* **1:**470-474.

Hoppeler H and Weibel ER (2005) Scaling functions to body size: theories and facts. *J Exp Biol* **208:**1573-1574.

Houston JB (1994) Relevance of in vitro kinetic parameters to in vivo metabolism of xenobiotics. *Toxicol In Vitro* **8:**507-512.

Houston JB and Galetin A (2003) Progress towards prediction of human pharmacokinetic parameters from in vitro technologies. *Drug Metab Rev* **35:**393-415.

Ito K and Houston JB (2004) Comparison of the use of liver models for predicting drug clearance using in vitro kinetic data from hepatic microsomes and isolated hepatocytes. *Pharm Res* **21:**785-792.

Itoh K (2001) 99mTc-MAG3: review of pharmacokinetics, clinical application to renal diseases and quantification of renal function. *Ann Nucl Med* **15:**179-190.

Izzat NN and Rosborough JP (1989) Renal function in conscious dogs: potential effect of gender on measurement. *Res Exp Med (Berl)* **189:**371-379.

Jackson B and Cappiello VP (1964) Ranges of Normal Organ Weights of Dogs. *Toxicol Appl Pharmacol* **6:**664-668.

Jones HM and Houston JB (2004) Substrate depletion approach for determining in vitro metabolic clearance: time dependencies in hepatocyte and microsomal incubations. *Drug Metab Dispos* **32:**973-982.

Jordan MA and Wilson L (2004) Microtubules as a target for anticancer drugs. *Nat Rev Cancer* **4:**253-265.

Jung K, Wesslau C, Priem F, Schreiber G and Zubek A (1987) Specific creatinine determination in laboratory animals using the new enzymatic test kit "Creatinine-PAP". *J Clin Chem Clin Biochem* **25:**357-361.

Jurgens KD and Prothero J (1991) Lifetime energy budgets in mammals and birds. *Comp Biochem Physiol A Comp Physiol* **100:**703-709.

Kanamori M, Takahashi H and Echizen H (2002) Developmental changes in the liver weight- and body weight-normalized clearance of theophylline, phenytoin and cyclosporine in children. *Int J Clin Pharmacol Ther* **40:**485-492.

Kavallaris M, Annereau JP and Barret JM (2008) Potential mechanisms of resistance to microtubule inhibitors. *Semin Oncol* **35:**S22-27.

Kirshenbaum AS, Kessler SW, Goff JP and Metcalfe DD (1991) Demonstration of the origin of human mast cells from CD34+ bone marrow progenitor cells. *J Immunol* **146:**1410-1415.

Kitamura Y, Hatanaka K, Murakami M and Shibata H (1979a) Presence of mast cell precursors in peripheral blood of mice demonstrated by parabiosis. *Blood* **53:**1085-1088.

Kitamura Y, Shimada M, Go S, Matsuda H, Hatanaka K and Seki M (1979b) Distribution of mast-cell precursors in hematopoeitic and lymphopoietic tissues of mice. *J Exp Med* **150:**482-490.

Kitamura Y, Sonoda T, Nakano T, Hayashi C and Asai H (1985) Differentiation processes of connective tissue mast cells in living mice. *Int Arch Allergy Appl Immunol* **77:**144-150.

Kiupel M, Webster JD, Bailey KL, Best S, DeLay J, Detrisac CJ, Fitzgerald SD, Gamble D, Ginn PE, Goldschmidt MH, Hendrick MJ, Howerth EW, Janovitz EB, Langohr I, Lenz SD, Lipscomb TP, Miller MA, Misdorp W, Moroff S, Mullaney TP, Neyens I, O'Toole D, Ramos-Vara J, Scase TJ, Schulman FY, Sledge D, Smedley RC, Smith K, P WS, Southorn E, Stedman NL, Steficek BA, Stromberg PC, Valli VE, Weisbrode SE, Yager J, Heller J and Miller R Proposal of a 2-tier histologic grading system for canine cutaneous mast cell tumors to more accurately predict biological behavior. *Vet Pathol* **48:**147-155.

Knapp DW, Richardson RC, Bonney PL and Hahn K (1988) Cisplatin therapy in 41 dogs with malignant tumors. *J Vet Intern Med* **2:**41-46.

Koopman MG, Koomen GC, van Acker BA and Arisz L (1996) Circadian rhythm in glomerular transport of macromolecules through large pores and shunt pathway. *Kidney Int* **49:**1242-1249.

Laterza OF, Price CP and Scott MG (2002) Cystatin C: an improved estimator of glomerular filtration rate? *Clin Chem* **48:**699-707.

Lave T, Coassolo P and Reigner B (1999) Prediction of hepatic metabolism clearance based on interspecies allometric scaling techniques and In-vitro-in vivo correlations. *Clinical pharmacokinetics* **36:**211-231.

Lawson N, Lang T, Broughton A, Prinsloo P, Turner C and Marenah C (2002) Creatinine assays: time for action? *Ann Clin Biochem* **39:**599-602.

Levey AS (1989) Use of glomerular filtration rate measurements to assess the progression of renal disease. *Semin Nephrol* **9:**370-379.

London CA, Kisseberth WC, Galli SJ, Geissler EN and Helfand SC (1996) Expression of stem cell factor receptor (c-kit) by the malignant mast cells from spontaneous canine mast cell tumours. *J Comp Pathol* **115:**399-414.

London CA and Seguin B (2003) Mast cell tumors in the dog. *Vet Clin North Am Small Anim Pract* **33:**473-489, v.

Loos WJ, de Jongh FE, Sparreboom A, de Wit R, van Boven-van Zomeren DM, Stoter G, Nooter K and Verweij J (2006) Evaluation of an alternate dosing strategy for cisplatin in patients with extreme body surface area values. *J Clin Oncol* **24:**1499-1506.

Lutzen L, Trieb G and Pappritz G (1976) Allometric analysis of organ weights: II. Beagle dogs. *Toxicol Appl Pharmacol* **35:**543-551.

Mahmood I (2007) Application of allometric principles for the prediction of pharmacokinetics in human and veterinary drug development. *Adv Drug Deliv Rev* **59:**1177-1192.

Mann WA and Kinter LB (1993) Characterization of the renal handling of p-aminohippurate (PAH) in the beagle dog (Canis familiaris). *Gen Pharmacol* **24:**367-372.

Masson E and Zamboni WC (1997) Pharmacokinetic optimisation of cancer chemotherapy. Effect on outcomes. *Clin Pharmacokinet* **32:**324-343.

Mathijssen RH, de Jong FA, Loos WJ, van der Bol JM, Verweij J and Sparreboom A (2007) Flat-fixed dosing versus body surface area based dosing of anticancer drugs in adults: does it make a difference? *Oncologist* **12:**913-923.

Miller AA (2002) Body surface area in dosing anticancer agents: scratch the surface! *J Natl Cancer Inst* **94:**1822-1823.

Misdorp W (2004) Mast cells and canine mast cell tumours. A review. *Vet Q* **26:**156-169.

Miyamoto K (1998) Evaluation of single-injection method of inulin and creatinine as a renal function test in normal cats. *J Vet Med Sci* **60:**327-332.

Moe L and Heiene R (1995) Estimation of glomerular filtration rate in dogs with 99M-Tc-DTPA and iohexol. *Research in Veterinary Science* **58:**138-143.

Moore MJ and Erlichman C (1987) Therapeutic drug monitoring in oncology. Problems and potential in antineoplastic therapy. *Clin Pharmacokinet* **13:**205-227.

NARITOMI Y, TERASHITA S, SUMIHISA KIMURA, AKIRA SUZUKI, AKIRA KAGAYAMA and SUGIYAMA Y (2001) PREDICTION OF HUMAN HEPATIC CLEARANCE FROM IN VIVO ANIMAL EXPERIMENTS AND IN VITRO

METABOLIC STUDIES WITH LIVER MICROSOMES FROM ANIMALS AND HUMANS *DRUG METABOLISM AND DISPOSITION* **29:**1316-1324.

Nath A and Atkins WM (2006) A theoretical validation of the substrate depletion approach to determining kinetic parameters. *Drug Metab Dispos* **34:**1433-1435.

Nemec J and Vortel V (1981) Absolute and relative organ weights of the beagle dog. *Z Versuchstierkd* **23:**333-336.

Norton L (1997) Evolving concepts in the systemic drug therapy of breast cancer. *Semin Oncol* **24:**S10-13-S10-10.

O'Connor R (2007) The pharmacology of cancer resistance. *Anticancer Res* **27:**1267-1272.

Obach RS (1999a) Prediction of human clearance of twenty-nine drugs from hepatic microsomal intrinsic clearance data: An examination of in vitro half-life approach and nonspecific binding to microsomes. *Drug Metab Dispos* **27:**1350-1359.

Obach RS (1999b) Prediction of human clearance of twenty - nine drugs from hepatic microsomal intrinsic celarance data: An examination of in vitro half-life approach and nonspecific binding of microsomes *Drug metabolism and disposition* **27:**1350-1359.

Obach RS (1999c) Prediction of human clearance of twenty nine drugs from hepatic microsomal intrinsic celarance data: An examination of in vitro half-life approach and nonspecific binding of microsomes *Drug Metabolism and Disposition* **27:**1350-1359.

Obach RS (2001) The prediction of human clearance from hepatic microsomal metabolism data. *Curr Opin Drug Discov Devel* **4:**36-44.

Obach RS (2011) Predicting clearance in humans from in vitro data. *Curr Top Med Chem* **11:**334-339.

Odlind B, Hallgren R, Sohtell M and Lindstrom B (1985) Is 125I iothalamate an ideal marker for glomerular filtration? *Kidney Int* **27:**9-16.

Page RL, Macy DW, Thrall DE, Dewhirst MW, Allen SL, Heidner GL, Sim DA, McGee ML and Gillette EL (1988) Unexpected toxicity associated with use of body surface area for dosing melphalan in the dog. *Cancer Res* **48:**288-290.

Pang KS and Rowland M (1977) Hepatic clearance of drugs. I. Theoretical considerations of a "well-stirred" model and a "parallel tube" model. Influence of hepatic blood flow, plasma and blood cell binding, and the hepatocellular enzymatic activity on hepatic drug clearance. *J Pharmacokinet Biopharm* **5:**625-653.

Park SB, Krishnan AV, Lin CS, Goldstein D, Friedlander M and Kiernan MC (2008) Mechanisms underlying chemotherapy-induced neurotoxicity and the potential for neuroprotective strategies. *Curr Med Chem* **15:**3081-3094.

Pasquier E and Kavallaris M (2008) Microtubules: a dynamic target in cancer therapy. *IUBMB Life* **60:**165-170.

Pastore A, Bernardini S, Dello Strologo L, Rizzoni G, Cortese C and Federici G (2001) Simultaneous determination of inulin and p-aminohippuric acid in plasma and urine by reversed-phase high-performance liquid chromatography. *J Chromatogr B Biomed Sci Appl* **751:**187-191.

Patnaik AK, Ehler WJ and MacEwen EG (1984) Canine cutaneous mast cell tumor: morphologic grading and survival time in 83 dogs. *Vet Pathol* **21:**469-474.

Peng B, English MW, Boddy AV, Price L, Wyllie R, Pearson AD, Tilby MJ and Newell DR (1997) Cisplatin pharmacokinetics in children with cancer. *Eur J Cancer* **33:**1823-1828.

Perrone RD, Steinman TI, Beck GJ, Skibinski CI, Royal HD, Lawlor M and Hunsicker LG (1990) Utility of radioisotopic filtration markers in chronic renal insufficiency: simultaneous comparison of 125I-iothalamate, 169Yb-DTPA, 99mTc-DTPA, and inulin. The Modification of Diet in Renal Disease Study. *Am J Kidney Dis* **16:**224-235.

Pinkel D (1958) The Use of Body Surface Area as a Criterion of Drug Dosage in Cancer Chemotherapy. *Cancer Research* **18:**853-856.

Pinkerton CR, Pritchard J and Spitz L (1986) High complete response rate in children with advanced germ cell tumors using cisplatin-containing combination chemotherapy. *J Clin Oncol* **4:**194-199.

Poulin P, Kenny JR, Hop CE and Haddad S (2011) In vitro-in vivo extrapolation of clearance: modeling hepatic metabolic clearance of highly bound drugs and comparative assessment with existing calculation methods. *J Pharm Sci* **101:**838-851.

Powis G (1983) Dose-dependent metabolism, therapeutic effect, and toxicity of anticancer drugs in man. *Drug Metab Rev* **14:**1145-1163.

Prentis RA, Lis Y and Walker SR (1988) Pharmaceutical innovation by the seven UK-owned pharmaceutical companies (1964-1985). *Br J Clin Pharmacol* **25:**387-396.

Prescott LF, McAuslane JAN and Freestone S (1991) The concentration-dependent disposition and kinetics of inulin. *Euopean Journal of Clinical Pharmacology* **40:**619-624.

Price GS and Frazier DL (1998) Use of body surface area (BSA)-based dosages to calculate chemotherapeutic drug dose in dogs: I. Potential problems with current BSA formulae. *J Vet Intern Med* **12:**267-271.

Proctor NJ, Tucker GT and Rostami-Hodjegan A (2004) Predicting drug clearance from recombinantly expressed CYPs: intersystem extrapolation factors. *Xenobiotica* **34:**151-178.

Rabik CA and Dolan ME (2007) Molecular mechanisms of resistance and toxicity associated with platinating agents. *Cancer Treat Rev* **33:**9-23.

Rahn KH, Heidenreich S and Bruckner D (1999) How to assess glomerula function and damage in humans. *Journal of Hypertension* **17:**309-317.

Ramirez J, Ogan K and Ratain MJ (1997) Determination of vinca alkaloids in human plasma by liquid chromatography/atmospheric pressure chemical ionization mass spectrometry. *Cancer Chemother Pharmacol* **39:**286-290.

Rassnick KM, Bailey DB, Flory AB, Balkman CE, Kiselow MA, Intile JL and Autio K (2008) Efficacy of vinblastine for treatment of canine mast cell tumors. *J Vet Intern Med* **22:**1390-1396.

Ratain MJ (1998) Body-surface area as a basis for dosing of anticancer agents: science, myth, or habit? *J Clin Oncol* **16:**2297-2298.

Rehberg PB (1926) Studies on Kidney Function: The Rate of Filtration and Reabsorption in the Human Kidney. *Biochem J* **20:**447-460.

Rehling M, Moller ML, Thamdrup B, Lund JO and Trap-Jensen J (1984) Simultaneous measurement of renal clearance and plasma clearance of 99mTc-labelled diethylenetriaminepenta-acetate, 51Cr-labelled ethylenediaminetetra-acetate and inulin in man. *Clin Sci (Lond)* **66:**613-619.

Richards MA and Hoe CM (1967) A long-term study of renal disease in the dog. *Vet Rec* **80:**640-646.

Ritschel WA, Vachharajani NN, Johnson RD and Hussain AS (1992) The allometric approach for interspecies scaling of pharmacokinetic parameters. *Comp Biochem Physiol C* **103:**249-253.

Robat C, London C, Bunting L, McCartan L, Stingle N, Selting K, Kurzman I and Vail DM Safety evaluation of combination vinblastine and toceranib phosphate (Palladia(R)) in dogs: a phase I dose-finding study(*). *Vet Comp Oncol*.

Roberts MS and Rowland M (1986) Correlation between in-vitro microsomal enzyme activity and whole organ hepatic elimination kinetics: analysis with a dispersion model. *J Pharm Pharmacol* **38:**177-181.

Rogers KS, Komkov A, Brown SA, Lees GE, Hightower D and Russo EA (1991) Comparison of four methods of estimating glomerular filtration rate in cats. *Am J Vet Res* **52:**961-964.

Rosenberg B, Vancamp L and Krigas T (1965) Inhibition of Cell Division in Escherichia Coli by Electrolysis Products from a Platinum Electrode. *Nature* **205:**698-699.

Rothwell TL, Howlett CR, Middleton DJ, Griffiths DA and Duff BC (1987) Skin neoplasms of dogs in Sydney. *Aust Vet J* **64:**161-164.

Rottem M, Kirshenbaum AS and Metcalfe DD (1991) Early development of mast cells. *Int Arch Allergy Appl Immunol* **94:**104-109.

Sawyer M and Ratain MJ (2001) Body surface area as a determinant of pharmacokinetics and drug dosing. *Invest New Drugs* **19:**171-177.

Schaeppi U, Heyman IA, Fleischman RW, Rosenkrantz H, Ilievski V, Phelan R, Cooney DA and Davis RD (1973) cis-Dichlorodiammineplatinum(II) (NSC-119 875): preclinical toxicologic evaluation of intravenous injection in dogs, monkeys and mice. *Toxicol Appl Pharmacol* **25:**230-241.

Schmidt-Nielsen K (1984) Scaling: Why is animal size is so important.13-78.

Schneider-Affeld F, von Fournier D, Wurster KH, Huter J and Kubli F (1977) [Preoperative diagnosis and histological findings in 51 subcutaneous mastectomies (proceedings)]. *Arch Gynakol* **224:**339-340.

Schneider WC (1948) Intracellular distribution of enzymes; the oxidation of octanoic acid by rat liver fractions. *J Biol Chem* **176:**259-266.

Schoning P, Erickson H and Milliken GA (1995) Body weight, heart weight, and heart-to-body weight ratio in greyhounds. *Am J Vet Res* **56:**420-422.

Sheiner LB and Beal SL (1981) Some suggestions for measuring predictive performance. *J Pharmacokinet Biopharm* **9:**503-512.

Shnurr E, Lahme W and Kuppers H (1980) Measurement of renal clearance of inulin and PAH in the steady state without urine collection. *Clinical nephrology* **13:**26-29.

Smith HW, Goldring W and Chasis H (1938) THE MEASUREMENT OF THE TUBULAR EXCRETORY MASS, EFFECTIVE BLOOD FLOW AND FILTRATION RATE IN THE NORMAL HUMAN KIDNEY. *J Clin Invest* **17:**263-278.

Smith R, Jones RD, Ballard PG and Griffiths HH (2008) Determination of microsome and hepatocyte scaling factors for in vitro/in vivo extrapolation in the rat and dog. *Xenobiotica* **38:**1386-1398.

Smith SH, Goldschmidt MH and McManus PM (2002) A comparative review of melanocytic neoplasms. *Vet Pathol* **39:**651-678.

Steel JD, Taylor RI, Davis PE, Stewart GA and Salmon PW (1976) Relationships between heart score, heart weight and body weight in Greyhound dogs. *Aust Vet J* **52:**561-564.

Steward A, Allott PR and Mapleson WW (1975) Organ weights in the dog. *Res Vet Sci* **19:**341-342.

Stringer RA, Strain-Damerell C, Nicklin P and Houston JB (2009) Evaluation of recombinant cytochrome P450 enzymes as an in vitro system for metabolic clearance predictions. *Drug Metab Dispos* **37:**1025-1034.

Tenstad O, Roald AB, Grubb A and Aukland K (1996) Renal handling of radiolabelled human cystatin C in the rat. *Scand J Clin Lab Invest* **56:**409-414.

Thamm DH, Turek MM and Vail DM (2006) Outcome and prognostic factors following adjuvant prednisone/vinblastine chemotherapy for high-risk canine mast cell tumour: 61 cases. *J Vet Med Sci* **68:**581-587.

Townsend DM, Tew KD, He L, King JB and Hanigan MH (2009) Role of glutathione S-transferase Pi in cisplatin-induced nephrotoxicity. *Biomed Pharmacother* **63:**79-85.

Van Acker BA, Koomen GC and Arisz L (1995) Drawbacks of the constant-infusion technique for measurement of renal function. *Am J Physiol* **268:**F543-552.

van den Bongard HJ, Mathot RA, Beijnen JH and Schellens JH (2000) Pharmacokinetically guided administration of chemotherapeutic agents. *Clin Pharmacokinet* **39:**345-367.

van Tellingen O, Beijnen JH, Baurain R, ten Bokkel Huinink WW, van der Woude HR and Nooyen WJ (1991) High-performance liquid chromatographic determination of

vinblastine, 4-O-deacetylvinblastine and the potential metabolite 4-O-deacetylvinblastine-3-oic acid in biological fluids. *J Chromatogr* **553:**47-53.

Venkatakrishnan K, Von Moltke LL and Greenblatt DJ (2001) Human drug metabolism and the cytochromes P450: application and relevance of in vitro models. *J Clin Pharmacol* **41:**1149-1179.

Venkatakrishnan K, von Moltke LL, Obach RS and Greenblatt DJ (2003) Drug metabolism and drug interactions: application and clinical value of in vitro models. *Curr Drug Metab* **4:**423-459.

Verbraecken J, Van de Heyning P, De Backer W and Van Gaal L (2006) Body surface area in normal-weight, overweight, and obese adults. A comparison study. *Metabolism* **55:**515-524.

Vickery KR, Wilson H, Vail DM and Thamm DH (2008) Dose-escalating vinblastine for the treatment of canine mast cell tumour. *Vet Comp Oncol* **6:**111-119.

Volkov SK and Grodnitskaya EI (1994) Application of high-performance liquid chromatography to the determination of vinblastine in Catharanthus roseus. *J Chromatogr B Biomed Appl* **660:**405-408.

Vriesendorp HM (1985) Optimal prescription method for cancer chemotherapy. *Exp Hematol* **13 Suppl 16:**57-63.

Wang J and Hihara E (2004) A unified formula for calculating body surface area of humans and animals. *Eur J Appl Physiol* **92:**13-17.

Wedemeyer J, Tsai M and Galli SJ (2000) Roles of mast cells and basophils in innate and acquired immunity. *Curr Opin Immunol* **12:**624-631.

Welle MM, Bley CR, Howard J and Rufenacht S (2008) Canine mast cell tumours: a review of the pathogenesis, clinical features, pathology and treatment. *Vet Dermatol* **19:**321-339.

West GB, Brown JH and Enquist BJ (1997) A general model for the origin of allometric scaling laws in biology. *Science* **276:**122-126.

White CR and Seymour RS (2003) Mammalian basal metabolic rate is proportional to body mass2/3. *Proc Natl Acad Sci U S A* **100:**4046-4049.

White CR and Seymour RS (2005) Allometric scaling of mammalian metabolism. *J Exp Biol* **208:**1611-1619.

Zhou H, Tai Y, Sun C and Pan Y (2005) Rapid identification of vinca alkaloids by direct-injection electrospray ionisation tandem mass spectrometry and confirmation by high-performance liquid chromatography-mass spectrometry. *Phytochem Anal* **16:**328-333.

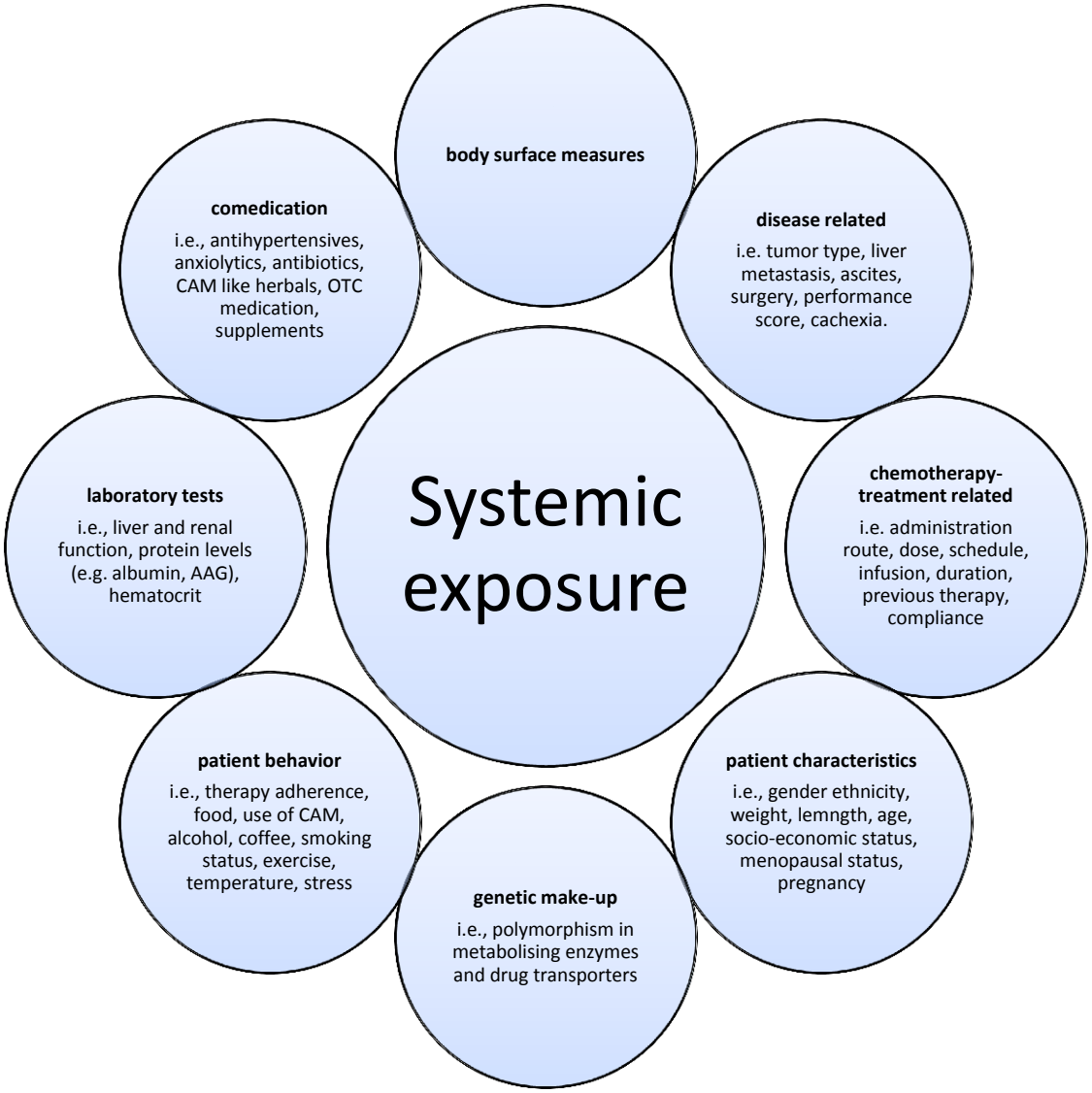

(Adapted from Mathijssen, et al., 2007)

Figure 1. Factors affecting the drug exposure of anticancer drugs

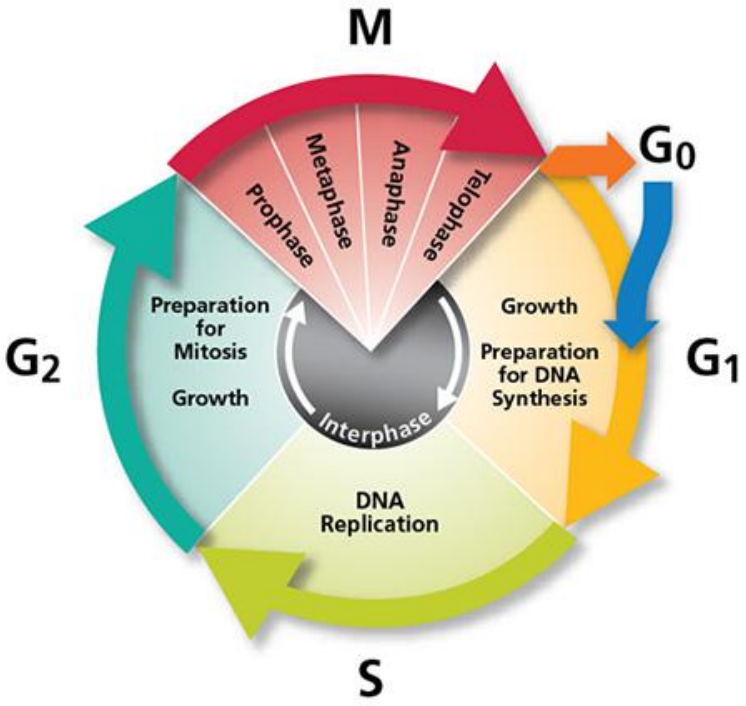

Where, G_0 = resting phase; G_1 = protein synthesis; RNA transcription; S = DNA synthesis; G_2 = protein synthesis; RNA transcription; M = Mitosis; and G_1+S+G_2 = Interphase.

Figure 2. Different phases of cell cycle

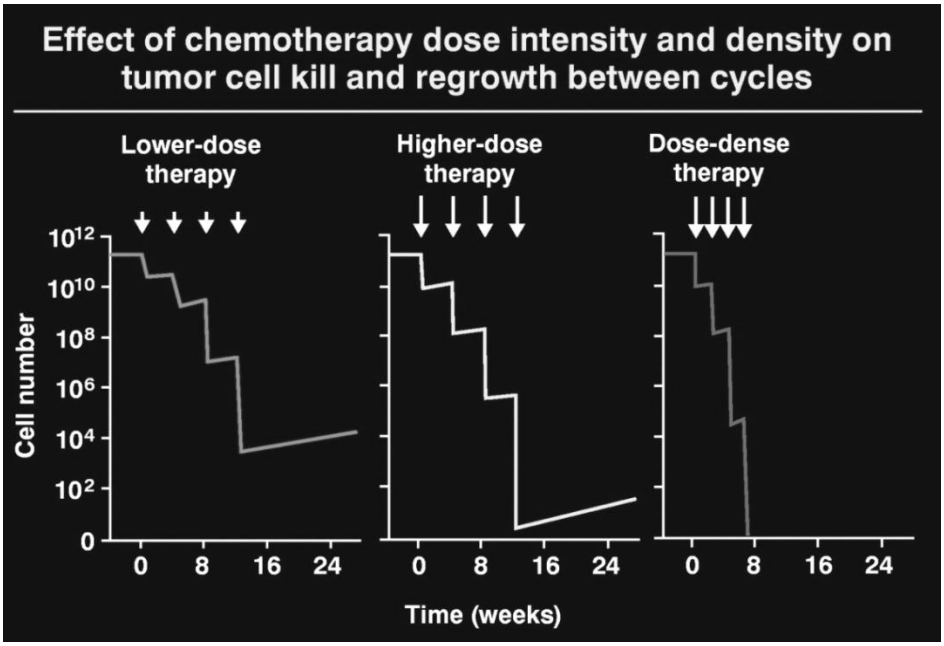

Figure 3. Effect of chemotherapy dose intensity and density on tumor cell kill and regrowth between cycles (Adapted from Norton, 1997 and Foote et al., 1998).

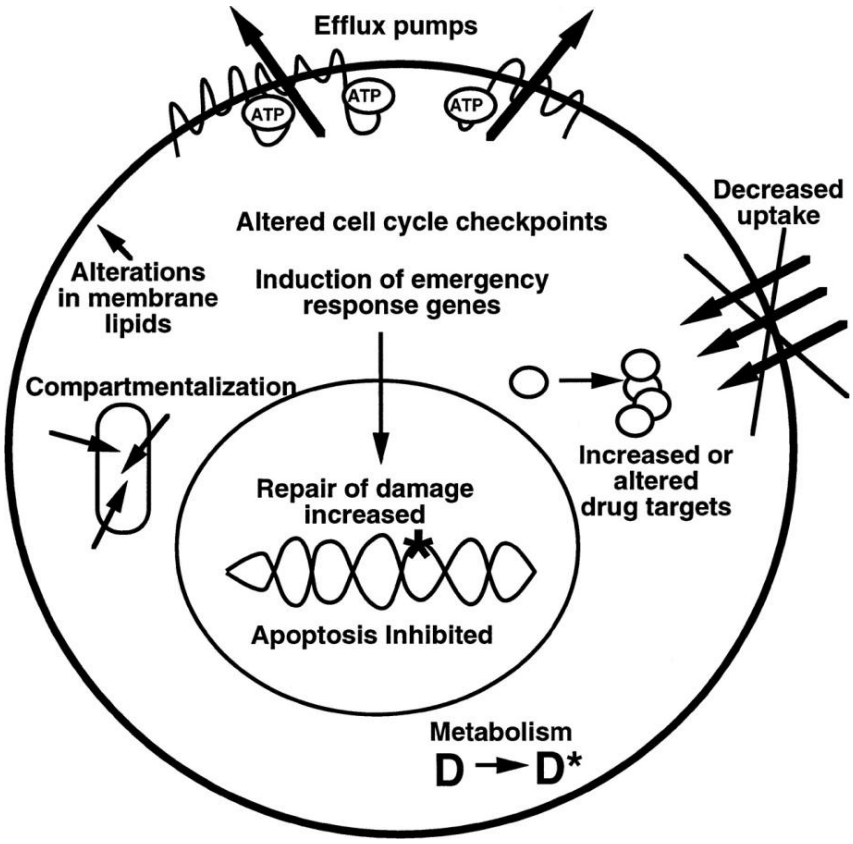

Figure 4. Summary of many of the ways of development of drug resistance to chemotherapeutics. (Adapted from Gottesman, 2002).

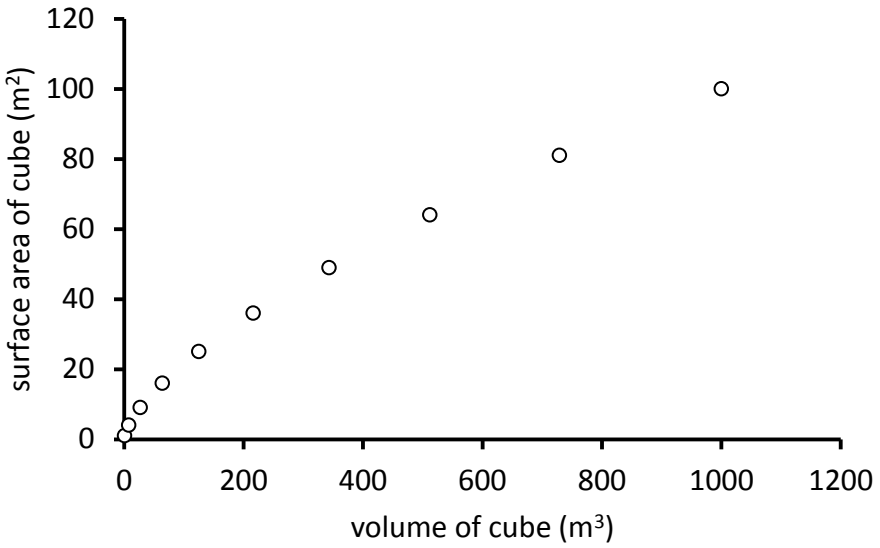

Figure 5. Illustration of allometric relationship in terms of volume and surface area of cube

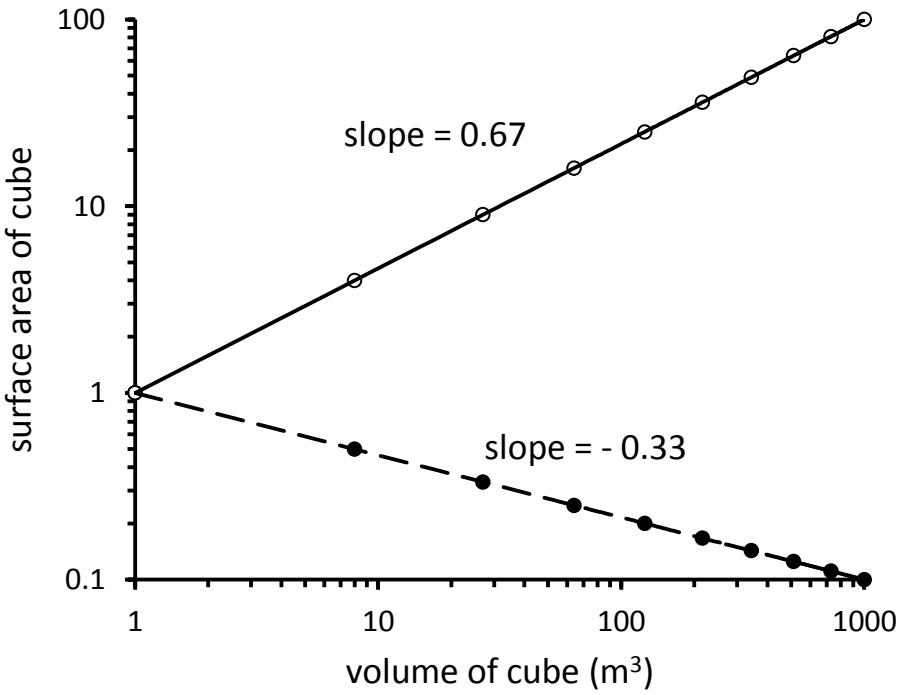

Figure 6. Illustration of allometric relationship and the concept of body surface area

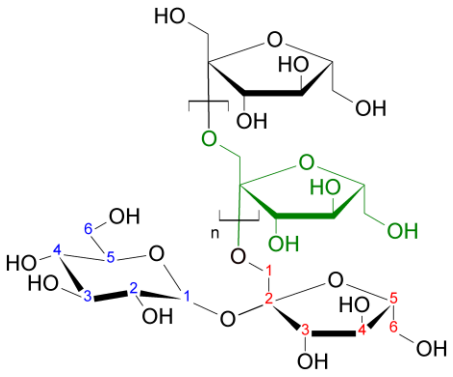

Figure 7. Chemical structure of inulin ($C_{6n}H_{10n+2}O_{5n+1}$)

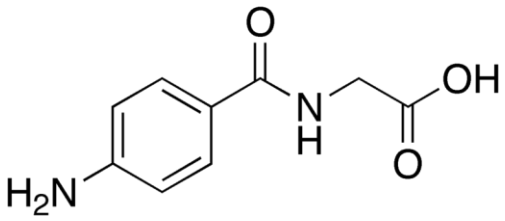

Figure 8. Chemical structure of para amino hippuric acid (PAH)

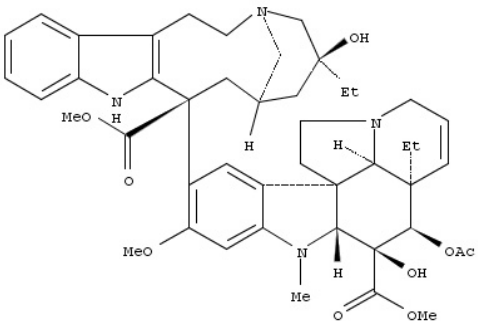

Figure 9. Chemical structure of vinblastine (molecular weight: 811)

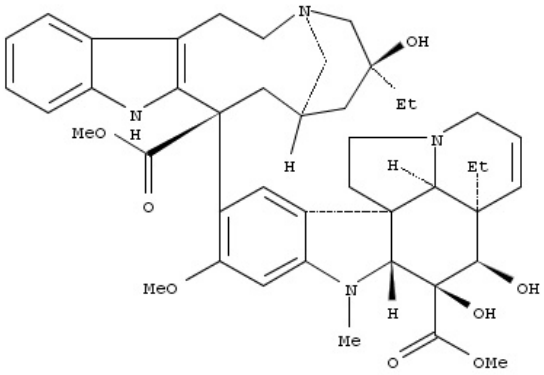

Figure 10. Chemical structure of desacetylvinblastine (molecular weight: 769)

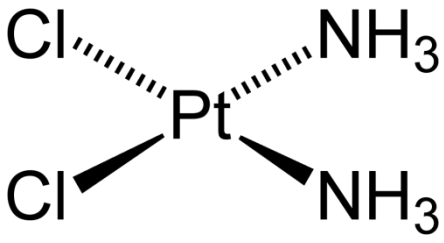

Figure 11. Chemical structure of cisplatin (molecular weight: 301.1)

CHAPTER III

ALLOMETRIC SCALING OF RENAL CLEARANCE OF CISPLATIN IN DOGS

Abstract

Cisplatin is a platinum containing anticancer drug indicated for the treatment of solid tumors in both veterinary and human patients. Cisplatin kinetics has been highly variable among disparate patients and difficult to predict. Current methods of dosing, such as body surface area (BSA) based dosing, do not fully standardize drug exposure between patients for most anticancer drugs. The purpose of this study was to test whether concomitant consideration of the effects of body weight and ontogeny on renal anatomy, physiology, and drug handling would accurately predict the clearance of cisplatin and to investigate whether clearance of cisplatin correlates with standard allometry or not. Post mortem body weight and organ weights were collected from 364 dogs (127 juveniles and 237 adults, including 51 geriatric dogs). Renal physiological and cisplatin pharmacokinetic studies were conducted in ten male intact dogs including two juvenile and eight adult dogs (4-55 kg). Glomerular filtration rate (GFR), effective renal plasma flow (ERPF), effective renal blood flow (ERBF), renal cisplatin clearance, and total cisplatin clearance were allometrically related to body weight with similar powers of 0.75, 0.59, 0.61, 0.71, and 0.70 respectively ($p<0.05$). In contrast to previous studies where cisplatin clearance was poorly predicted from GFR, these data showed good correlation between the allometry of kidney weight, GFR, renal cisplatin clearance, and total cisplatin clearance. The similar values of these diverse mass exponents suggest a common underlying basis for the allometry of kidney size, renal physiology, and renal drug handling.

Introduction

Cisplatin (*cis*-Diamminedicholoroplatinum II, *cis* $PtCl_2(NH_3)_2$) is a platinum containing alkylating - like agent that acts by establishing cross links within and between DNA strands with more guanine – guanine intra-strand cross linking (Legendre et al., 2000; Kostova, 2006). Cisplatin hydrates with and then forms adducts with purine bases, thus interferes with cell division. When the rate of DNA platination exceeds the rate of DNA repair, the cells will enter

into apoptosis and die (Bellon et al., 1991; Rabik and Dolan, 2007). Cisplatin was the prototypic platinum containing anticancer drug developed among its class of anticancer drugs. Cisplatin is primarily indicated for the treatment of solid tumors both in dogs and human patients as a single agent or in combination protocols. The aquated forms of cisplatin are highly nephrotoxic (Litterst, 1981; Rabik and Dolan, 2007; Hanigan et al., 2009) and other toxicities of cisplatin include, but are not limited to, peripheral neurotoxicity, ototoxicity, and myelosuppression(Rabik and Dolan, 2007). Cisplatin has been replaced by carboplatin, a sister analogue of cisplatin, in veterinary oncology because of its dose limiting severe nephrotoxicity. However, there is a resurgence of interest for cisplatin in veterinary oncology due to its efficacy against solid tumors, such as ovarian, testicular, and transitional cell carcinoma (Barabas et al., 2008; McDuffie et al., 2010). Cisplatin is continued to treat several solid tumors in human oncology, particularly in pediatric oncology, such as testicular tumor, medulloblastoma, neuroblastomas, hepatoblastomas, osteosarcomas, and brain tumors.(Fouladi et al., 2008).

The narrow therapeutic indices of cytotoxic anticancer drugs, such as cisplatin demand accurate calculation of doses to optimize drug exposure. The minimum lethal dose of cisplatin in dogs is 2.5 mg/kg (≈80 mg/m^2) (Schaeppi et al., 1973) while the therapeutic dose is 60 – 70 mg/ m^2 (Knapp et al., 1988). Currently, the doses of anticancer drugs are calculated as a function of body surface area (BSA) (Pinkel, 1958). There are approximately 400 dog breeds worldwide, with156 breeds recognized by American Kennel Club (The Complete Dog Book, AKC publication) (http://www.akc.org/breeds/complete_breed_list.cfm). As there is a wide variation in the body sizes of dogs from two pound Chihuahuas to 200 pound Great Dane, current dosing methodology based on body surface area had been failing to explain the reported therapeutic failure, toxicity, and disposition of several cytotoxic drugs (Page et al., 1988; Arrington et al., 1994; Gurney, 1996; Frazier and Price, 1998; Price and Frazier, 1998; Ratain, 1998; de Jongh et al., 2001; A. Felici et al., 2002; Smorenburg et al., 2003). Several alternative dosing equations

were proposed to optimize drug exposure, such as flat fixed dosing, fixed dosing for BSA clusters, toxicity adjusted dosing, therapeutic drug monitoring, and retrospective dosing but none of them had optimized drug exposure (Gurney, 1996; van Warmerdam, 1997; Warmerdam, 1997; Canal et al., 1998a; Canal et al., 1998b; Gao et al., 2004). However, the integration of *in vivo* data with *in vitro* studies might increase the predictive ability of the resulting pharmacokinetic scaling equations (Lave et al., 1999; Houston and Galetin, 2008).

Unlike some therapeutic drugs, the efficacy of anticancer drugs correlates with drug exposure, which is mathematically quantified as area under the plasma concentration versus time curve (Moore and Erlichman, 1987; Calvert et al., 1989) Carboplatin and oxaliplatin are sister analogues of cisplatin with reduced nephrotoxicity and their clearance correlates with the glomerular filtration unlike cisplatin clearance (Calvert et al., 1989; Peng et al., 1997; de Jongh et al., 2001). Prospective pharmacokinetic studies in human patients revealed that glomerular filtration rate correlated well with the clearance of carboplatin, resulting in development of a dosing equation as a function of creatinine clearance and area under plasma concentration versus time curve: Dose (mg) = target area under plasma concentration versus time curve (AUC) x (GFR + 25) (Calvert et al., 1989). Unfortunately, studies in humans have shown that glomerular filtration rate does not correlate with the clearance of cisplatin, making it unsuitable to develop similar dosing equations for cisplatin as a function of AUC and glomerular filtration rate (Peng et al., 1997; de Jongh et al., 2001; Loos et al., 2006).

Currently, prospective pharmacokinetic studies with toxicity adjusted dosing are considered to optimize drug exposure between disparate canine patients. But unfortunately, these studies require several *in vivo* studies which will be expensive and cumbersome. In light of wide variation in body sizes of dog breeds, combined with inter individual idiosyncratic responses, a better alternative to optimize drug exposure may be to understand the factors that influence the clearance of anticancer drugs. If the clearance of a drug is accurately determined, then the dose

required to produce desirable drug exposure can be calculated more accurately. As cisplatin is excreted through the kidneys, establishing allometric relations between body size and kidney weights, renal physiological parameters, and cisplatin pharmacokinetic parameters would illustrate how these renal covariates impact the disposition of cisplatin.

Allometry is the study of non-proportionate relationships between dependent and independent variables. With the increase in independent variable, dependent variable also increases but with an exponent other than unity. In simple terms, when the relationship between two parameters is not in direct proportion, the relationship is said to be an allometric or non-proportionate relationship. Mathematically, the dependence of a scalable variable, *Y* on body weight, *M* is represented by allometric form of equation: $Y = aM^b$ where, a = mass coefficient; b = mass exponent (West et al., 1997; White and Seymour, 2005; Mahmood, 2007). Many anatomical parameters (body surface area, liver weight, kidney weight, and heart weight), physiological parameters (basal metabolic rate, glomerular filtration rate, renal blood flow, hepatic blood flow, and cardiac output), and important pharmacokinetic parameters (clearance, volume of distribution, and elimination half life) are allometrically related with body weight.

Body size and functional organ mass of important organs, such as kidney and liver, which are responsible for metabolism of many drugs, influence the disposition of many anticancer drugs. The current literature on organ scaling studies in dogs is limited to few subjects in the study or homogenous subjects (Jackson and Cappiello, 1964; Steward et al., 1975; Lutzen et al., 1976). Pathologists estimate the weight of kidney as 1.13% and 0.4% of body weight in juveniles and adults, respectively; heart weight as 0.75% of body weight (Joseph, 1908; Steward et al., 1975). These estimations might be acceptable in assessing the gross pathology of organs based on size to some extent. However, these fixed proportions of body weights may not give accurate estimates of organ weights for use in predictive software programs such as physiological based

pharmacokinetic and population pharmacokinetic software programs particularly in species like dogs in which there is a wide variation in their body weights.

We hypothesize that the concomitant consideration of the effects of signalment, such as body weight, gender, and ontogeny on organ physiology and drug handling will accurately predict the clearance of anticancer drugs. The rationale for our hypothesis was based on the fact that drug clearance depends on functional organ mass and blood flow. (Hanigan et al., 2009; Townsend et al., 2009).

Dogs were declared as laboratory model animals to study pathophysiology and treatment of human cancer by National Cancer Institute, Bethesda, MD, USA and the Canine Comparative Oncology and Genomics Consortium (CCOGC). The results obtained from these canine species can be extrapolated to human beings using interspecies scaling methods (Mahmood, 2007). Most of the studies in laboratory animals limit to beagle dogs of 10 kg body weight and extrapolating those results to all sizes of dogs result in either under or over dosing of anticancer drugs. Our studies are unique in considering different body sizes into account to accommodate their functional organ mass, physiology, and pharmacokinetics through allometric relationships. Also, this study would give estimates of pharmacokinetic parameters of cisplatin in dogs of different body sizes *per se*. This work would be a step along the continuous efforts to optimize the drug exposure in disparate canine patients.

Materials and methods

Laboratory supplies: Inulin, para amino hippuric acid, and para amino benzoic acid were purchased from Sigma-Aldrich, Inc., St. Louis, MO, USA; all organic solvents were of HPLC grade, purchased from Fisher Scientific Inc., Pittsburgh, PA, USA; Vascular access ports were purchased from Access Technologies, Skokie, IL, USA; Centrifree® ultrafiltration devices were purchased from Millipore, Bedford, MA, USA.

Organ weights data collection: Post mortem body weights and organ weights were collected from dogs euthanized at Oklahoma City animal shelter, Tulsa animal shelter, and Oklahoma Animal Disease Diagnostic Laboratory (OADDL), Stillwater, Oklahoma. Dogs were euthanized as a part of a population control program at the shelters; and as patients submitted to OADDL for postmortem examination. The data collected from animal shelters was used as training data set and the data collected for OADDL was used as validation data set. Dogs above 1 year of age and less than 8 years of were considered as the adult group; dogs in the age group of 2 to 5 months were considered to be juvenile dogs. There are different opinions about considering a dog as geriatric, such as large breeds have shorter life span and attain geriatric phase earlier than small breeds (Patronek et al., 1997; Speakman et al., 2003; Galis et al., 2007; Greer et al., 2007). We assumed that dogs above 8 years old as geriatric (Cummings et al., 1996a; Cummings et al., 1996b; Studzinski et al., 2006; Cotman and Head, 2008). For the estimation of age of dogs, patient history and or age based on dentition (Merck veterinary manual) were used. The gender and reproductive status (neutered/spayed/intact) of the dogs were noted. Concurrent with the collection of kidney weights, heart weights were also collected to see if there is any correlation with renal physiological parameters. As cardiac output is dependent on heart weight healthy animals, the latter will influence renal blood flow as well. Body weight and organ weights were accurately collected. For the determination of kidney weights, peri-renal fat, capsules, major blood vessels supplying the kidneys, and ureters were removed. For the determination of heart weight, the heart was cut opened, blood clots were removed and great vessels were trimmed close to the base of the heart. A series of *a priori* inclusion criteria were defined before starting the collection of organ weights. The body condition score (BCS) of dogs was recorded on a scale of 1 - 9, and dogs with a BCS of 4, 5, and 6 were included in the study (Laflamme, 1997; Parker and Freeman, 2011). Exclusion criteria for dogs euthanized at the shelters included gross pathological lesions. Along with signalment, body weight, and organ weights, tissue specimens

were collected from shelter dogs. Histopathology reports were examined for all dogs which were collected from OADDL.

SigmaStat® 3.0, SPSS Inc., Chicago, IL was used to analyze the data. The normal distribution of the data was tested by Shapiro-Wilk normality test. The training data was $\log_{10}$ transformed and step wise multiple linear regressions were performed with organ weight as the dependent variable and gender, ontogeny, and body weight as independent variables to see which individual factors significantly influenced organ weight. Gender and ontogeny were represented as nominal variables with standard denotation: females were denoted as '1' and males were denoted as '0'; juveniles were denoted as '1' and adults were denoted as '0'. Ontogeny is the study of development of an individual from embryo to adult. An *F*-test was used as an indication of predictive ability of model. Stepwise multiple linear regression analyses were performed separately for juveniles and adults. The slopes of juveniles and adults were tested for differences by ANCOVA (SAS 9.2, SAS Institute Inc., Cary, NC, USA). Outliers were detected by Studentized residuals and Cook's distance. Based on a *priori* inclusion criteria, data having a Studentized residual more than +/- 2 were considered to be outliers. Tissue samples from the dogs determined to be outliers were examined histopathologically for evidence of disease. Collinearity was tested to see if independent variables have any correlation which might interfere with regression analysis. Statistically significant predictors of kidney weight and heart weight were retained in the final regression equation. Study significance was set *a priori* to alpha=*0.05*. The predictive ability of the newly developed allometric equations was validated by comparing to *per se* and validation data set. The sum of residuals of organ weights predicted with newly developed allometric equations and fixed proportions of body weights were compared. Log_{10} transformed residuals of organ weights predicted were plotted against $\log_{10}$ transformed body weights. A paired t- test was performed between $\log_{10}$ residual errors and zero to determine the predictability of the allometric equations in the validation data set for both organ weights.

***In vivo* animal studies**: Ten experimental intact adult male dogs (two juvenile: 8 -12 week old, and eight adults: above one year and below three years) were included in the *in vivo* portion of the study. The body weights of these dogs ranged from 4.25 – 56 kg. Eight dogs were mixed breed and two dogs were laboratory beagles. The BCS of dogs were within 4 – 6 out of 10 scale system. The Institutional Animal Care and Use Committee approved the husbandry and procedures utilized in this study. Separate subcutaneous vascular access ports (VAPs) (Access Technologies®, Skokie, IL, USA) were implanted in each jugular vein. The length of tubing of left side VAP was kept shorter than tubing on right side to ensure that they would not communicate in cranial vena cava. The VAPs were maintained using standard procedures for aseptic access and heparin lock. When there were problems in keeping Huber infusion sets in place, either long term percutaneous jugular catheters or cephalic catheters were used.

***In vivo* renal physiological studies**: Dogs were fasted overnight with *ad libitum* access to water. Sterile inulin and para amino huppuric acid (PAH) solutions were prepared and administered as intravenous bolus at a dose rate of 58.5 mg/kg and 9.3 mg/kg, respectively. Then, followed by a constant rate infusion (CRI) at a dose rate of 50 mg/kg/hr and 18 mg/kg/hr of inulin and PAH, respectively, for 180 minutes with a total fluid rate of 8.4 mL/kg/hr (Fischer Patricia A et al., 2000). Blood samples were collected at 80, 90, 100, 120, and 150 minutes during the infusion and hematocrit was determined at each sampling point. Plasma steady state inulin and PAH concentrations were determined by a reversed phase high performance liquid chromatography using modified previously published papers (Pastore et al., 2001; Meucci et al., 2004). Briefly, 100 µL of plasma samples were diluted with 100 µL of water. Plasma samples were spiked with 50 µL of para amino benzoic acid (PABA) as an internal standard. Plasma proteins were precipitated with 70% perchloric acid. After centrifugation, the supernatant was transferred into disposable borosilicate glass tubes, covered with aluminum foil, and placed into boiling water for 10 minutes. Five microliters of supernatant were injected onto the high performance liquid

chromatography system, using a C18 column (Altech® 250 mm x 4.6 mm and 5 μm particle size). Separation was achieved with isocratic elution using 87% of 50 mM of sodium phosphate buffer (pH: 4.1) and 13% of methanol. Ultraviolet detection was performed at 254 nm. Glomerular filtration rate (GFR) was calculated as the ratio of infusion rate of inulin to plasma steady state concentration ($C_{p(ss)}$) of inulin (Fischer Patricia A et al., 2000).

$$GFR\ (mL/\text{min}) = \frac{Infusion\ rate\ of\ inulin\ (mg/\text{min})}{C_{p(ss)}\ (mg/\text{mL})}$$

Similarly, the effective renal plasma flow (ERPF) was calculated as the ratio of infusion rate of PAH to steady state plasma concentration of PAH. ERPF was corrected to the extraction ratio (ER) of PAH with a value of 0.74 (Chiu et al., 1976; Fischer Patricia A et al., 2000)

$$ERPF\ (mL/\text{min}) = \frac{Infusion\ rate\ of\ PAH\ (mg/\text{min})}{ER\ C_{p(ss)}\ (mg/\text{mL})}$$

Effective renal blood flow (ERBF) was calculated by dividing the value of ERPF with (1 – *Hct/100*) (Fischer Patricia A et al., 2000)

$$ERBF\ (mL/\text{min}) = \frac{Infusion\ rate\ of\ PAH\ (mg/\text{min})}{(ER)C_{p(ss)}(1 - Hct/100)}$$

Where, Hct is the hematocrit determined for each sample collected. These equations were primarily derived from the standard equation to calculate clearance as a ratio of infusion rate to plasma steady state concentration of a drug (Earle and Berliner, 1946; Shnurr et al., 1980). Renal physiological parameters were $\log_{10}$ transformed and regressed against $\log_{10}$ transformed body weights (SigmaStat® 3.0, SPSS, Chicago, IL).

Cisplatin pharmacokinetic studies: Dogs were fasted overnight with *ad libitum* access to fresh drinking water. Dogs were housed in metabolic cages beginning 24 hours prior to cisplatin administration. Two days prior to and two weeks after performing cisplatin pharmacokinetic

studies, complete blood counts and renal biochemistry parameters were tested to confirm that values were within normal limits. Dogs were premedicated with ondansetron at a dose rate of 0.3 mg/kg intravenously to reduce emesis. Cisplatin was administered as a CRI for 20 minutes at a dose rate of 1 mg/kg. Prior to and after administration of cisplatin, dogs were given saline diuresis for 5 hours and 2 hours, respectively at a dose rate of 18.3 mL/min/kg. Blood samples were collected in heparinized tubes at 0, 10, and 20 minutes during the cisplatin infusion, and at 5, 15, 30 minutes, and 1, 2, 3, 4, 6, 8, 12, 24, 32, and 48 hours post infusion. As cisplatin is a highly protein bound drug, plasma was subjected to ultra-filtration harvested from plasma samples by centrifugation (2000 g for 30 min at 4 ^{0}C) using Centrifree® tubes having molecular weight cut off of 30,000 Daltons (Millipore®, Bedford, MA) in a fixed angle rotors (Eppendorf® Centrifuge 5403) and stored at –20^0 C until analysis. Urine samples (1.2 mL) were collected for 72 hours and volume of urine voided was recorded at each sampling time point. Metabolic cages were washed with 100 mL of water at each sampling time and urine wash samples were collected. Elemental platinum concentrations in urine and plasma ultra filtrate samples were quantified by using inductively coupled plasma mass spectrometry (ICP-MS) at Utah State Veterinary Diagnostic Laboratory, Logan, UT. For all analytical methods, accuracy within 20% of the nominal concentration at the lower limit of quantitation (LLOQ) and 15% of the nominal concentration at all higher concentrations were set as the acceptable limits. Similarly, an RSD of 20% at the LLOQ and 15% at higher concentrations were set as the acceptable parameters. Compartmental analysis of the data was performed to determine pharmacokinetic parameters with models in the format of $C = \sum_{i=1}^{n} A_i e^{-\lambda_i t}$ using WinNonlin® 5.2 (Pharsight Corp., Mountain View, CA). The best compartmental model was chosen using Akaike's information criteria (AIC), co-efficient variation values, and inspection of concentration versus time plots and residual plots (Yamaoka et al., 1978). The total and renal clearance of cisplatin values were calculated by compartmental and non-compartmental approaches, respectively. The renal

clearance of cisplatin was calculated by using the equation: $CL_{renal} = X_{u(72)} / AUC_{72}$ where, $X_{u(72)}$ is the total amount of platinum excreted in urine over 72 hour period, AUC_{72} is the area under the plasma platinum concentration versus time curve from time zero to 72 hours (Gibaldi and Perrier, 1982). The total and renal platinum clearance values were $\log_{10}$ transformed and regressed against $\log_{10}$ body weights (SigmaStat® 3.0, SPSS Inc., Chicago, IL).

Results

***Organ scaling*:** Data were collected from a total of 364 dogs including 237 adult dogs and 127 juvenile dogs over a period of six years. Based on the *a priori* inclusion and exclusion criteria, 237 kidney weight samples and 191 heart weight samples were retained for analysis (Table 1). There was no statistical difference between right and left kidney weights ($p>0.05$), so the weights of right and left kidneys were combined to get global kidney weight. Gender was not a significant predictor of kidney or heart weights in dogs ($p>0.05$), whereas body weight and age class affected organ weights ($p<0.05$). Collinearity was not observed among independent variables to interfere with regression analysis. There was no difference between the slopes of juveniles and adults ($p>0.05$), so one regression equation was utilized to describe the effect of body weight and age on kidney and heart sizes. The resulting allometric equation were: $\textbf{Kidney weight (g)} = \mathbf{9.35 \cdot BW^{0.789} \cdot 10^{0.095\ x\ ontogeny}}$ (where, a*dult*=0, *juvenile*=1) R^2 = 0.93, *Sy.x* = 0.088 (figure 1); $\textbf{Heart weight (g)} = \mathbf{10.86\ BW^{0.86}\ 10^{-0.095 x ontogeny}}$ (Where, *adult=0, juvenile=1*) R^2 = 0.98, *Sy.x* = 0.057 (figure 5). Sums of absolute residual errors of organ weights predicted with newly developed allometric equations and fixed proportion of body weight approach in training data set *per se* or validation data set were presented in tables 2, 3, 4, and 5. Sums of absolute residual errors of kidney and heart weights predicted with the allometric equations in training data set *per se* and validation data set had lower value compared to the fixed proportion of body weight approach. Residual plots of $\log_{10}$ transformed residuals of kidney and heart weights of training data set and validation data set against body weights were presented in figures 2, 3, 6, and 7. In figures 4 and

8, measured organ weights were plotted against body weight in comparison to predicted organ weights (allometric and fixed proportion) in validation data sets. The mean $\log_{10}$ residual errors of predicted kidney and heart weights with allometric equation in the validation data set were not significantly greater than zero ($p>0.05$). On the other hand, the mean of $\log_{10}$ residual errors of predicted kidney and heart weights with fixed proportion of body weight in the validation data set were significantly greater than zero and not significantly zero, respectively. However, the *p* – value of allometric residual error was higher than the fixed proportion indicating relative better predictive ability.

In vivo studies

Renal physiological parameters: One large adult dog (43 kg) was euthanized because of unmanageable discospondylitis of lumbar vertebrae. The *in vivo* data was presented from two juvenile and seven adult dogs. A highly sensitive analytical method was developed to determine the concentrations of inulin and PAH simultaneously in canine plasma using a reversed phase high performance liquid chromatography. The interday accuracy and precision (relative standard deviation) of the assay were within *a priori* acceptable limits (table 6). The limit of quantitation of the assay was 2.5 µg/mL and 3.125 µg/mL for inulin and PAH, respectively. The renal physiological parameters of juvenile dogs were not included in the regression analysis. However, data was included in the scatter plots to show how their values relate to weight matched adult dogs. The linear regressions of $\log_{10}$ transformed renal physiological parameters against $\log_{10}$ transformed body weights resulted in the following equations: $GFR = 0.5\ BW^{0.75}\ R^2 = 0.98$; $ERPF = 2.3\ BW^{0.59}\ R^2 = 0.95$; *and* $ERBF = 3.4\ BW^{0.61}\ R^2 = 0.94$ (figure 9).

Cisplatin pharmacokinetics: The accuracy and precision of the assay were within acceptable limits (table 7). The limit of quantitation of ICP-MS for platinum concentrations in both ultra filtrate and urine was 5 ng/mL. Cisplatin exhibited biphasic elimination. The peak plasma concentration of platinum was observed at the end of infusion of cisplatin. The plasma platinum

concentrations in small adult dogs had reached below limit of quantitation by 24 hours (figure 10). The initial plasma half life was short (0.26 ± 0.06 hr) and terminal half life was longer (23.95 ± 9.73 hr). In the compartmental analysis of cisplatin plasma concentrations versus time data, two compartmental modeling with 1/y weighting scheme had emerged as the best model fitting (figure 10). Best model was chosen based on the model fitting, R^2 values, co-efficient of variation values, Akaike's information criteria (AIC), and residual plots. The mean pharmacokinetic parameters of cisplatin after fitting to two-compartmental model were presented in table 8.

The platinum clearance depended on body weight with the allometric equation: CL_{total} = 1.08 $BW^{0.72}$ R^2 = 0.86; CL_{renal} = 0.35 $BW^{0.77}$ R^2 = 0.84 (figure 11). There was a good correlation between renal physiological parameters and total, and renal platinum clearance (figures 12 and 13). The cumulative % recovery of platinum in urine was 35.4 ± 4.5 of total dose administered. The % cumulative recovery of platinum in urine was higher in smaller individuals compared to larger individuals. The total platinum clearance exceeded the renal platinum clearance about 2.7 ± 0.3 (mean ± SD) fold indicating additional pathways of platinum elimination.

Discussion

Organ scaling: In humans and most domestic animals, the variation in adult body weights is narrow, limiting allometric effects. Dogs and horses are the two common domesticated animals in which a wide range of body weights are noted. Allometric scaling is very useful in extrapolating the results from one species to another species through interspecies allometric scaling; and within a species, in which a wide variation of body sizes is noted as in dogs and horses through intra-species allometric scaling (Ritschel et al., 1992; Mahmood, 2007). With the increase in concern over live animal studies and ethical issues, computer modeling and simulations with limited data from at least one species is gaining more impetus to extrapolate data to other species and within the same species. To avoid overlapping of age groups, dogs of 2 – 5 months age were classified as juveniles and dogs above one year and less than 8 years were classified as adult dogs. As there

are different opinions about defining geriatric status in dogs, dogs above eight years old were considered as geriatric dogs in this study. Both body weight and ontogeny affected kidney and heart weight ($p<0.05$). In contrast to previous studies, gender was not a significant predictor ($p>0.05$) of heart weight (Lutzen et al., 1976; Steel et al., 1976). As reported in previous studies, gender was not a significant predictor of kidney weight (Prothero, 1984). The canine intra-species allometric exponents of body weight for kidney and heart weights were 0.79 and 0.86, whereas the previously reported interspecies allometric exponents were 0.85 and 0.99, respectively (Prothero, 1979; Prothero, 1984). The allometric equations developed in this study to predict the organ weights were robust having data from 237 dogs ranging from 0.34 kg to 72 kg body weights and representing several breeds. There were few studies describing the allometric relationship between organ weights and body weights in dogs. In the previously published reports, the data was either collected from a homogenous population or few numbers of subjects were included in the study (Jackson and Cappiello, 1964; Deavers et al., 1972; Steward et al., 1975; Lutzen et al., 1976; Nemec and Vortel, 1981; Korhonen and Harri, 1985). Such data may not give better estimates of organ weights. Human and veterinary pathologists estimate kidney and heart size as a function of fixed proportion of body weight. Kidney weights are estimated as 1.13 % and 0.4% of body weight in juvenile and adult dogs, respectively; Heart weights are estimated as 0.75% of body weight (Steward et al., 1975). The allometric equation developed from the training set was used to predict the kidney and heart weights in the training data set *per se* and in the validation data set. The residual plots of both training and validation data sets (figures 2, 3, 6, and 7) showed that the residuals of kidney and heart weights determined from allometric equations were randomly distributed, in contrast to the residuals of organ weights predicted as a fixed proportion of body weights, which had a diagonal and skewed distribution. As further support for the greater utility of the allometric approach, the absolute sum of residual errors associated with allometric equations were lower than those from the estimates from a fixed proportion of body weights (table 2, 3, 4, and 5). Both the lower sum of absolute residual errors,

lack of bias in the distribution of residuals, and statistical tests demonstrate that allometric equations to predict kidney weights is better than conventional fixed proportion body weight approach. The allometric equations developed in this study can be used in estimating organ volume or size for donor and recipient during organ transplantation (Gregory et al., 1987; Phillips and Aronson, 2012); assessing the organ size for toxicological studies(Wolfsegger et al., 2009), during post mortem, and surgical procedures; can be incorporated into population based pharmacokinetic software programs and physiological based pharmacokinetic software programs. These robust and novel allometric equations would replace current allometric equations to predict kidney weights.

Renal physiological parameters: Understanding the renal physiological covariates which might correlate with the clearance of cisplatin is important to optimize drug exposure. Creatinine is a poor marker of GFR as increased serum creatinine levels occur only with marked damage to nephrons making it less sensitive diagnostic marker (Braun et al., 2003; McDuffie et al., 2010). Inulin is a non-toxic, inert fructose polysaccharide which is mainly obtained from tubers of Dahlia and Chicory, and a dozen of other tubers, roots and artichokes of plants. Inulin is freely filtered by glomerular filtration, neither absorbed nor secreted by renal tubules (Brochner-Mortensen, 1985; Perrone et al., 1990; Prescott et al., 1991). Therefore, the clearance of inulin is considered to be the gold standard for the measurement of glomerular filtration rate (Brochner-Mortensen, 1985; Toto, 1995; Rahn et al., 1999; Finco, 2005). PAH is an organic anion that is freely filtered by glomerulus and extensively secreted into the proximal convoluted tubules and very poorly reabsorbed. As PAH is removed from the blood by the kidneys and is nearly removed from renal plasma in one passage through the kidney, the renal clearance of PAH is approximately equal to effective renal plasma flow (Shnurr et al., 1980; Mann and Kinter, 1993; Toto, 1995). During the period of infusion of inulin and PAH as constant rate infusion, plasma steady state was achieved within 80 minutes after initiation of administration. In one dog (11.4

kg), after receiving loading bolus dose of inulin and PAH, adverse reactions were noticed. Dog recovered uneventfully after treatment with dexamethasone and Benadryl; received CRI within 1 hr of bolus dose. The same dog received constant rate infusion alone to see any difference in the values of ERPF with and without receiving bolus dose. GFR allometrically related with body weight with a mass exponent of 0.75 which was very similar to $3/4^{th}$ power of standard allometry (West et al., 1997; White and Seymour, 2005). The 3/4 power is widely accepted as the theoretical and experimental interspecific mass exponent relating several allometric relationships to body weight (West et al., 1997; Mahmood, 2007). ERPF and ERBF depended on body weight with a power of 0.6 which is closer to $2/3^{rd}$ power of intraspecies scaling. The mass exponents of ERPF and ERBF were lower than that of GFR. PAH is transported by organic anion transporters (OATs) across proximal convoluted tubules (PCTs). OATs are ATP dependent and reach saturation at higher doses of PAH leading to transport maximum of OATs ($T_{m(PAH)}$). In previous studies, it was shown that with the increase in plasma concentrations of PAH above 30 μg/mL, the clearance of PAH had decreased (Mann and Kinter, 1993). In the large dog (55 kg body weight), the plasma steady state PAH concentration was 50 μg/mL which was above $T_{m(PAH)}$. The lower allometric exponent of ERPF could be due to the higher doses of PAH in the large dog beyond the $T_{m(PAH)}$ (transport maximum) of the OATs. The dose of PAH would have been adjusted in larger dog without saturating OATs.

Cisplatin pharmacokinetics: The unbound plasma platinum concentrations in small adult dogs (4.25 – 4.7 kg) were below the limit of quantitation by 24 hours after cisplatin infusion, whereas the plasma platinum concentrations were above the limit of quantitation until 48 hours in larger dogs (10 – 55 kg). The total body clearance of unbound platinum per unit body weight had decreased with the increase in body weight. On the other hand, AUC, which is a dose dependent parameter, had increased with the increase in body weight (table 7). AUC has been considered as one of the important pharmacokinetic parameter as a predictor of therapeutic efficacy and

toxicity. There was a 2.8 fold difference in values of AUC between subjects in this study. The total body clearance of platinum exceeded renal platinum clearance, suggesting that there are nonrenal routes of elimination of cisplatin in conformation with previous studies in different species (Reece et al., 1989; Erdlenbruch et al., 2001). Both total body clearance and renal clearance of cisplatin were allometrically related to body weight by approximately the ¾ power of standard allometry. In contrast to previous studies (Reece et al., 1987; Peng et al., 1997), the clearance of cisplatin correlated well with GFR. The similar allometric powers of total body and renal clearance of cisplatin, as well as that of glomerular filtration rate, show cisplatin clearance did correlate well with renal markers, including GFR, in the dogs studied. This was a surprising finding suggesting that prime doses of cisplatin may follow standard allometry. It may be that multiple doses of cisplatin might result in alteration of kidney form and function resulting in a different relationship (Aleksunes et al., 2008)(Aleksunes et al., 2008). Some studies have shown that multiple doses of cisplatin cause down regulation of molecular biomarkers, organic anion and cation transporters responsible for the secretion of cisplatin in the renal tubules (Aleksunes et al., 2008; Morisaki et al., 2008; McDuffie et al., 2010). Studies involving prime dose and subsequent doses of cisplatin are suggested for better understanding about correlation of renal covariates and total and renal platinum clearance.

Conclusions

The allometric relationship of kidney weights, renal physiological parameters, and cisplatin renal and total clearance with body weight suggests a common underlying basis for the allometry of kidney form and function. Furthermore, the initial dose of cisplatin follows standard allometry and correlates well with GFR in dogs. Pharmacokinetic studies with multiple doses of cisplatin in dogs would be needed to determine whether successive doses continue to correlate well with GFR or whether cisplatin administration affects its own clearance with subsequent administrations.

References

A. Felici, J. Verweij and Sparreboom A (2002) Dosing strategies for anticancer drugs: the good, the bad and body-surface area

European Journal of Cancer **38:**1677-1684.

Aleksunes LM, Augustine LM, Scheffer GL, Cherrington NJ and Manautou JE (2008) Renal xenobiotic transporters are differentially expressed in mice following cisplatin treatment. *Toxicology* **250:**82-88.

Arrington KA, Legendre AM, Tabeling GS and Frazier DL (1994) Comparison of body surface area-based and weight-based dosage protocols for doxorubicin administration in dogs. *Am J Vet Res* **55:**1587-1592.

Barabas K, Milner R, Lurie D and Adin C (2008) Cisplatin: a review of toxicities and therapeutic applications. *Vet Comp Oncol* **6:**1-18.

Bellon SF, Coleman JH and Lippard SJ (1991) DNA unwinding produced by site-specific intrastrand cross-links of the antitumor drug cis-diamminedichloroplatinum(II). *Biochemistry* **30:**8026-8035.

Braun JP, Lefebvre HP and Watson AD (2003) Creatinine in the dog: a review. *Vet Clin Pathol* **32:**162-179.

Brochner-Mortensen J (1985) Current status on assessment and measurement of glomerular filtration rate. *Clin Physiol* **5:**1-17.

Calvert AH, Newell DR, Gumbrell LA, O'Reilly S, Burnell M, Boxall FE, Siddik ZH, Judson IR, Gore ME and Wiltshaw E (1989) Carboplatin dosage: prospective evaluation of a simple formula based on renal function. *J Clin Oncol* **7:**1748-1756.

Canal P, Chatelut E and Guichard S (1998a) Practical treatment guide for dose individualisation in cancer chemotherapy. *Drugs* **56:**1019-1041.

Canal P, Chatelut E and Guichard S (1998b) Practical treatment guide for dose individualisation in cancer chemotherapy. *Drugs* **56:**1019-1038.

Chiu PJ, Brown A, Miller G and Long JF (1976) Renal extraction of gentamicin in anesthetized dogs. *Antimicrob Agents Chemother* **10:**277-282.

Cotman CW and Head E (2008) The canine (dog) model of human aging and disease: dietary, environmental and immunotherapy approaches. *J Alzheimers Dis* **15:**685-707.

Cummings BJ, Head E, Afagh AJ, Milgram NW and Cotman CW (1996a) Beta-amyloid accumulation correlates with cognitive dysfunction in the aged canine. *Neurobiol Learn Mem* **66:**11-23.

Cummings BJ, Head E, Ruehl W, Milgram NW and Cotman CW (1996b) The canine as an animal model of human aging and dementia. *Neurobiol Aging* **17:**259-268.

de Jongh FE, Verweij J, Loos WJ, de Wit R, de Jonge MJ, Planting AS, Nooter K, Stoter G and Sparreboom A (2001) Body-surface area-based dosing does not increase accuracy of predicting cisplatin exposure. *J Clin Oncol* **19:**3733-3739.

Deavers S, Huggins RA and Smith EL (1972) Absolute and relative organ weights of the growing beagle. *Growth* **36:**195-208.

Earle DP, Jr. and Berliner RW (1946) A simplified clinical procedure for measurement of glomerular filtration rate and renal plasma flow. *Proc Soc Exp Biol Med* **62:**262-264.

Erdlenbruch B, Nier M, Kern W, Hiddemann W, Pekrun A and Lakomek M (2001) Pharmacokinetics of cisplatin and relation to nephrotoxicity in paediatric patients. *Eur J Clin Pharmacol* **57:**393-402.

Finco DR (2005) Measurement of glomerular filtration rate via urinary clearance of inulin and plasma clearance of technetium Tc 99m pentetate and exogenous creatinine in dogs. *Am J Vet Res* **66:**1046-1055.

Fischer Patricia A, Claudia B. Bogoliuk, Agusti'n J. Ramirez, Ramiro A Sa'nchez and Masnatta LD (2000) A new procedure for evaluation of renal function without urine collection in rat. *Kidney International* **58:**1336-1341.

Fouladi M, Chintagumpala M, Ashley D, Kellie S, Gururangan S, Hassall T, Gronewold L, Stewart CF, Wallace D, Broniscer A, Hale GA, Kasow KA, Merchant TE, Morris B, Krasin M, Kun LE, Boyett JM and Gajjar A (2008) Amifostine protects against cisplatin-induced ototoxicity in children with average-risk medulloblastoma. *J Clin Oncol* **26:**3749-3755.

Frazier DL and Price GS (1998) Use of body surface area to calculate chemotherapeutic drug dose in dogs: II. Limitations imposed by pharmacokinetic factors. *J Vet Intern Med* **12:**272-278.

Galis F, Van der Sluijs I, Van Dooren TJ, Metz JA and Nussbaumer M (2007) Do large dogs die young? *J Exp Zool B Mol Dev Evol* **308:**119-126.

Gao B, Klumpen H-J and Gurney H (2004) Dose calculation of anticancer drugs. *Drug Metab. Toxicol.* **4:**1307-1319.

Gibaldi M and Perrier D (1982) Pharmacokinetics. *Mercel Dekker, Newyork*.

Greer KA, Canterberry SC and Murphy KE (2007) Statistical analysis regarding the effects of height and weight on life span of the domestic dog. *Res Vet Sci* **82:**208-214.

Gregory CR, Gourley IM, Taylor NJ, Broaddus TW, Olds RB and Patz JD (1987) Preliminary results of clinical renal allograft transplantation in the dog and cat. *J Vet Intern Med* **1:**53-60.

Gurney H (1996) Dose calculation of anticancer drugs : a review of the current practice and introduction of an alternative. *Journal of clinica oncology* **14:**2590-2611.

Hanigan MH, Townsend DM and Cooper AJ (2009) Metabolism of cisplatin to a nephrotoxin. *Toxicology* **257:**174-175; author reply 176-177.

Houston JB and Galetin A (2008) Methods for predicting in vivo pharmacokinetics using data from in vitro assays. *Curr Drug Metab* **9:**940-951.

Jackson B and Cappiello VP (1964) Ranges of Normal Organ Weights of Dogs. *Toxicol Appl Pharmacol* **6:**664-668.

Joseph DR (1908) The Ratio between the Heart-Weight and Body-Weight in Various Animals. *J Exp Med* **10:**521-528.

Knapp DW, Richardson RC, Bonney PL and Hahn K (1988) Cisplatin therapy in 41 dogs with malignant tumors. *J Vet Intern Med* **2:**41-46.

Korhonen H and Harri H (1985) Organ scaling in the raccoon dog Nyctereutes procyonoides gray 1834, as monitored by influences of internal and external factors. *Comp Biochem Physiol A Comp Physiol* **82:**907-914.

Kostova I (2006) Platinum complexes as anticancer agents. *Recent Pat Anticancer Drug Discov* **1:**1-22.

Laflamme DP (1997) Development and Validation of a Body Condition Score System for Dogs. *Canine Practice* **22:**10-15.

Lave T, Coassolo P and Reigner B (1999) Prediction of hepatic metabolism clearance based on interspecies allometric scaling techniques and In-vitro-in vivo correlations. *Clinical pharmacokinetics* **36:**211-231.

Legendre F, Bas V, Kozelka J and Chottard JC (2000) A complete kinetic study of GG versus AG plantination suggests that the doubly aquated derivatives of cisplatin are the actual DNA binding species. *Chemistry* **6:**2002-2010.

Litterst CL (1981) Alterations in the toxicity of cis-dichlorodiammineplatinum-II and in tissue localization of platinum as a function of NaCl concentration in the vehicle of administration. *Toxicol Appl Pharmacol* **61:**99-108.

Loos WJ, de Jongh FE, Sparreboom A, de Wit R, van Boven-van Zomeren DM, Stoter G, Nooter K and Verweij J (2006) Evaluation of an alternate dosing strategy for cisplatin in patients with extreme body surface area values. *J Clin Oncol* **24:**1499-1506.

Lutzen L, Trieb G and Pappritz G (1976) Allometric analysis of organ weights: II. Beagle dogs. *Toxicol Appl Pharmacol* **35:**543-551.

Mahmood I (2007) Application of allometric principles for the prediction of pharmacokinetics in human and veterinary drug development. *Adv Drug Deliv Rev* **59:**1177-1192.

Mann WA and Kinter LB (1993) Characterization of the renal handling of p-aminohippurate (PAH) in the beagle dog (Canis familiaris). *Gen Pharmacol* **24:**367-372.

McDuffie JE, Sablad M, Ma J and Snook S (2010) Urinary parameters predictive of cisplatin-induced acute renal injury in dogs. *Cytokine* **52:**156-162.

Meucci V, Gasperini A, Soldani G, Guidi G and Giorgi M (2004) A new HPLC method to determine glomerular filtration rate and effective renal plasma flow in conscious dogs by single intravenous administration of iohexol and p-aminohippuric acid. *J Chromatogr Sci* **42:**107-111.

Moore MJ and Erlichman C (1987) Therapeutic drug monitoring in oncology. Problems and potential in antineoplastic therapy. *Clin Pharmacokinet* **13:**205-227.

Morisaki T, Matsuzaki T, Yokoo K, Kusumoto M, Iwata K, Hamada A and Saito H (2008) Regulation of renal organic ion transporters in cisplatin-induced acute kidney injury and uremia in rats. *Pharm Res* **25:**2526-2533.

Nemec J and Vortel V (1981) Absolute and relative organ weights of the beagle dog. *Z Versuchstierkd* **23:**333-336.

Page RL, Macy DW, Thrall DE, Dewhirst MW, Allen SL, Heidner GL, Sim DA, McGee ML and Gillette EL (1988) Unexpected toxicity associated with use of body surface area for dosing melphalan in the dog. *Cancer Res* **48:**288-290.

Parker VJ and Freeman LM (2011) Association between Body Condition and Survival in Dogs with Acquired Chronic Kidney Disease. *J Vet Intern Med* **25:**1306-1311.

Pastore A, Bernardini S, Dello Strologo L, Rizzoni G, Cortese C and Federici G (2001) Simultaneous determination of inulin and p-aminohippuric acid in plasma and urine by reversed-phase high-performance liquid chromatography. *J Chromatogr B Biomed Sci Appl* **751:**187-191.

Patronek GJ, Waters DJ and Glickman LT (1997) Comparative longevity of pet dogs and humans: implications for gerontology research. *J Gerontol A Biol Sci Med Sci* **52:**B171-178.

Peng B, English MW, Boddy AV, Price L, Wyllie R, Pearson AD, Tilby MJ and Newell DR (1997) Cisplatin pharmacokinetics in children with cancer. *Eur J Cancer* **33:**1823-1828.

Perrone RD, Steinman TI, Beck GJ, Skibinski CI, Royal HD, Lawlor M and Hunsicker LG (1990) Utility of radioisotopic filtration markers in chronic renal insufficiency: simultaneous comparison of 125I-iothalamate, 169Yb-DTPA, 99mTc-DTPA, and inulin. The Modification of Diet in Renal Disease Study. *Am J Kidney Dis* **16:**224-235.

Phillips H and Aronson LR (2012) Use of end-to-side arterial and venous anastomosis techniques for renal transplantation in two dogs. *J Am Vet Med Assoc* **240:**298-303.

Pinkel D (1958) The Use of Body Surface Area as a Criterion of Drug Dosage in Cancer Chemotherapy. *Cancer Research* **18:**853-856.

Prescott LF, McAuslane JAN and Freestone S (1991) The concentration-dependent disposition and kinetics of inulin. *Euopean Journal of Clinical Pharmacology* **40:**619-624.

Price GS and Frazier DL (1998) Use of body surface area (BSA)-based dosages to calculate chemotherapeutic drug dose in dogs: I. Potential problems with current BSA formulae. *J Vet Intern Med* **12:**267-271.

Prothero J (1979) Heart weight as a function of body weight in mammals. *Growth* **43:**139-150.

Prothero J (1984) Organ scaling in mammals: the kidneys. *Comp Biochem Physiol A Comp Physiol* **77:**133-138.

Rabik CA and Dolan ME (2007) Molecular mechanisms of resistance and toxicity associated with platinating agents. *Cancer Treat Rev* **33:**9-23.

Rahn KH, Heidenreich S and Bruckner D (1999) How to assess glomerular function and damage in humans. *J Hypertens* **17:**309-317.

Ratain MJ (1998) Body-surface area as a basis for dosing of anticancer agents: science, myth, or habit? *J Clin Oncol* **16:**2297-2298.

Reece PA, Stafford I, Davy M, Morris R and Freeman S (1989) Influence of infusion time on unchanged cisplatin disposition in patients with ovarian cancer. *Cancer Chemother Pharmacol* **24:**256-260.

Reece PA, Stafford I, Russell J, Khan M and Gill PG (1987) Creatinine clearance as a predictor of ultrafilterable platinum disposition in cancer patients treated with cisplatin: relationship between peak ultrafilterable platinum plasma levels and nephrotoxicity. *J Clin Oncol* **5:**304-309.

Ritschel WA, Vachharajani NN, Johnson RD and Hussain AS (1992) The allometric approach for interspecies scaling of pharmacokinetic parameters. *Comp Biochem Physiol C* **103:**249-253.

Schaeppi U, Heyman IA, Fleischman RW, Rosenkrantz H, Ilievski V, Phelan R, Cooney DA and Davis RD (1973) cis-Dichlorodiammineplatinum(II) (NSC-119 875): preclinical toxicologic evaluation of intravenous injection in dogs, monkeys and mice. *Toxicol Appl Pharmacol* **25:**230-241.

Shnurr E, Lahme W and Kuppers H (1980) Measurement of renal clearance of inulin and PAH in the steady state without urine collection. *Clinical nephrology* **13:**26-29.

Smorenburg CH, Sparreboom A, Bontenbal M, Stoter G, Nooter K and Verweij J (2003) Randomized cross-over evaluation of body-surface area-based dosing versus flat-fixed dosing of paclitaxel. *J Clin Oncol* **21:**197-202.

Speakman JR, van Acker A and Harper EJ (2003) Age-related changes in the metabolism and body composition of three dog breeds and their relationship to life expectancy. *Aging Cell* **2:**265-275.

Steel JD, Taylor RI, Davis PE, Stewart GA and Salmon PW (1976) Relationships between heart score, heart weight and body weight in Greyhound dogs. *Aust Vet J* **52:**561-564.

Steward A, Allott PR and Mapleson WW (1975) Organ weights in the dog. *Res Vet Sci* **19:**341-342.

Studzinski CM, Christie LA, Araujo JA, Burnham WM, Head E, Cotman CW and Milgram NW (2006) Visuospatial function in the beagle dog: an early marker of cognitive decline in a model of human aging and dementia. *Neurobiol Learn Mem* **86:**197-204.

Toto RD (1995) Conventional measurement of renal function utilizing serum creatinine, creatinine clearance, inulin and para-aminohippuric acid clearance. *Curr Opin Nephrol Hypertens* **4:**505-509; discussion 503-504.

Townsend DM, Tew KD, He L, King JB and Hanigan MH (2009) Role of glutathione S-transferase Pi in cisplatin-induced nephrotoxicity. *Biomed Pharmacother* **63:**79-85.

van Warmerdam LJ (1997) Tailor-made chemotherapy for cancer patients. *Neth J Med* **51:**30-35.

Warmerdam VL (1997) Tailor-made chemotherapy for cancer patients. *Netherlands Journal of Medicine* **51:**30-35.

West GB, Brown JH and Enquist BJ (1997) A general model for the origin of allometric scaling laws in biology. *Science* **276:**122-126.

White CR and Seymour RS (2005) Allometric scaling of mammalian metabolism. *J Exp Biol* **208:**1611-1619.

Wolfsegger MJ, Jaki T, Dietrich B, Kunzler JA and Barker K (2009) A note on statistical analysis of organ weights in non-clinical toxicological studies. *Toxicol Appl Pharmacol* **240:**117-122.

Yamaoka K, Nakagawa T and Uno T (1978) Application of Akaike's information criterion (AIC) in the evaluation of linear pharmacokinetic equations. *J Pharmacokinet Biopharm* **6:**165-175.

	Training data set		Validation data set	
	Kidney	**Heart**	**Kidney**	**Heart**
Juveniles	61	55	16	16
Adults	106	66	54	54
Total	167	121	70	70
Range of body weights (kg)	0.6 – 72		0.5 - 63	

Table 1. Number of animals included in the training data set and validation data set for organ scaling studies of kidney and heart weights.

		Allometric equation	**Fixed proportion of body weight**
Kidney	Juveniles	7.65	12.39
	Adults	4.14	8.42
	Total	11.79	20.81

Table 2. Sum of absolute residual errors from predictions of kidney weights using the newly developed allometric equations and fixed proportion of body weight (1.13 % and 0.4% of body weight, respectively for juveniles and adults) in the training data set *per se*.

		Allometric equation	**Fixed proportion of body weight**
Kidney	Juveniles	1.43	5.53
	Adults	5.75	9.17
	Total	7.17	14.70

Table 3. Sum of absolute residual errors from predictions of kidney weights in the validation data set using the newly developed allometric equations and fixed proportion of body weight (1.13 % and 0.4% of body weight, respectively for juveniles and adults).

		Allometric	0.75% of body weight
Heart	Juvenile	2.09	2.99
	Adult	3.29	3.90
	Total	5.38	6.88

Table 4. Sum of absolute residual errors from predictions of heart weights, using the newly developed allometric equations and fixed proportion of body weight (0.75 % of body weight for both juveniles and adults), in the training data set.

		Allometric	0.75% of body weight
Heart	Juvenile	0.83	0.62
	Adult	4.29	5.08
	Total	5.12	5.70

Table 5. Sum of absolute residual errors from predictions of heart weights, using the newly developed allometric equations and fixed proportion of body weight (0.75 % of body weight for both juveniles and adults), in the validation data set.

Analyte	Conc. (µg/mL)	Accuracy %	RSD %
Inulin	2.5	88	7
	3.75	93	4
	375	93	4
	750	92	6
PAH	3.125	98	9
	5	95	5
	50	90	2
	250	93	3

Table 6. Accuracy and precision of reversed phase high performance liquid chromatography to measure the concentrations of inulin and para amino hippuric acid in canine plasma samples. The values of accuracy and precision were within acceptable limits.

Pt conc. (ng/mL)	Accuracy %	RSD %
5	92	0.4
325	91	1
975	107	15

Table 7. Accuracy and precision of ICP-MS method to quantify the concentrations of cisplatin in canine ultrafiltrate samples.

Body weight (kg)	**4.25**	**4.7**	**10.5**	**10.9**	**20.8**	**23.4**	**55.4**
K10 (1/hr)	2.4	2.4	1.9	2.2	1.4	0.9	1.1
Alpha_HL (hr)	0.2	0.2	0.2	0.2	0.3	0.4	0.3
Beta_HL (hr)	16.4	14.6	19.1	13.5	21.9	49.1	28.5
Cmax (ng/mL)	1023.0	1391.7	1754.4	1699	963.2	663.6	1654.9
Vss (mL/kg)	6847.6	3841.4	4772.0	3434	9453.6	25167.7	6845.8
CL (mL/hr/kg)	899.5	701.7	451.0	509	628.4	682.9	285.7
AUC (hr*ng/mL)	722.6	926.3	1441.2	1276	1034.4	951.8	2275.0

Values are expressed as the mean ± SD. K10 = elimination rate constant; Alpha_HL = distribution half - life; Beta_HL = elimination half - life; $V_{d(ss)}$ = apparent volume of distribution at steady state; CL = total body clearance; AUC = area under the serum drug concentration-time curve, extrapolated to infinity.

Table 8. Mean pharmacokinetic parameters for platinum after IV administration of 1 mg/kg of cisplatin to seven adult dogs.

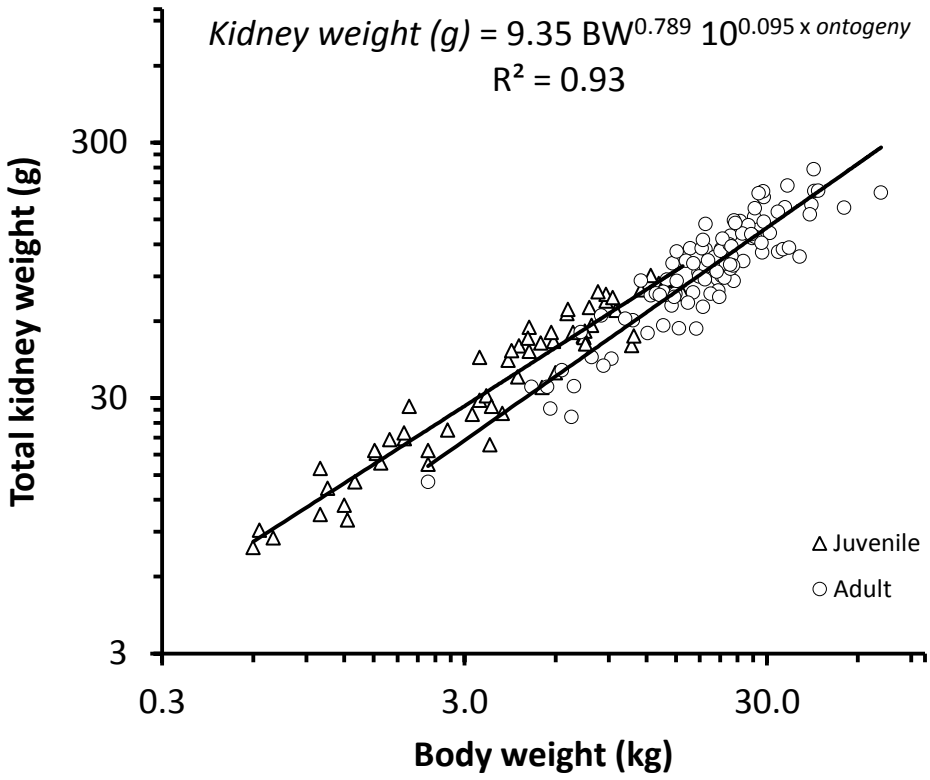

Figure 1: Scatter plot of kidney weight (g) against body weight (kg) from 61 juvenile and 106 adult dogs. The kidney weight allometrically related to body weight and ontogeny as: ***Kidney weight (g)* = 9.35· BW$^{0.789}$·10$^{0.095\ x\ ontogeny}$ *where, adult = 0, juvenile = 1,* R^2 = 0.93** (*p <0.05*).

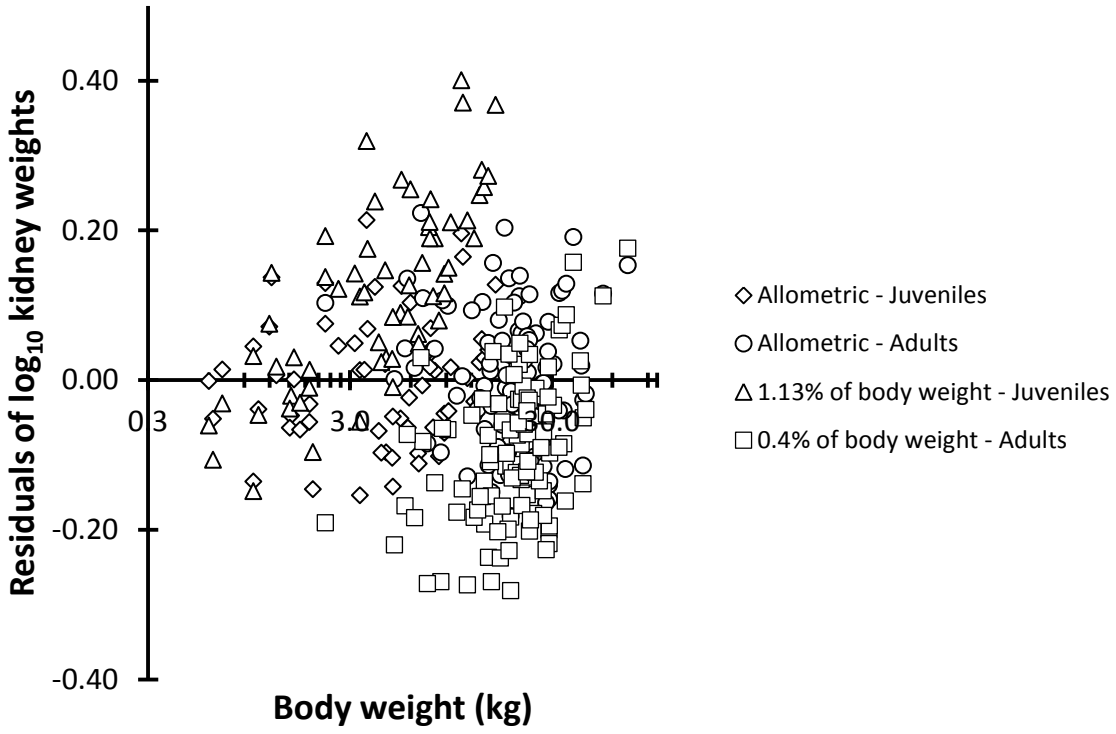

Figure 2. The residuals of $\log_{10}$ transformed kidney weights predicted with the newly developed allometric equation and fixed proportion of body weights were plotted against $\log_{10}$ transformed body weights in the training data set.

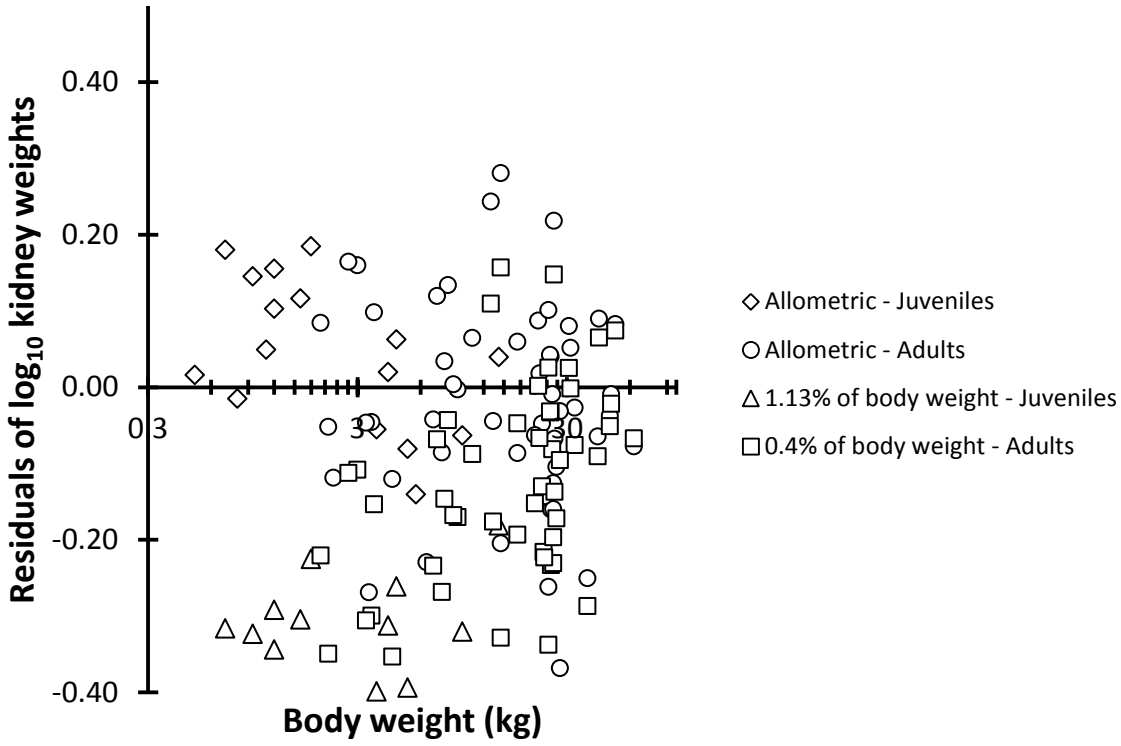

Figure 3. The residuals of $\log_{10}$ transformed kidney weights predicted in validation data set with the newly developed allometric equation and the fixed proportion of body weights were plotted against body weights.

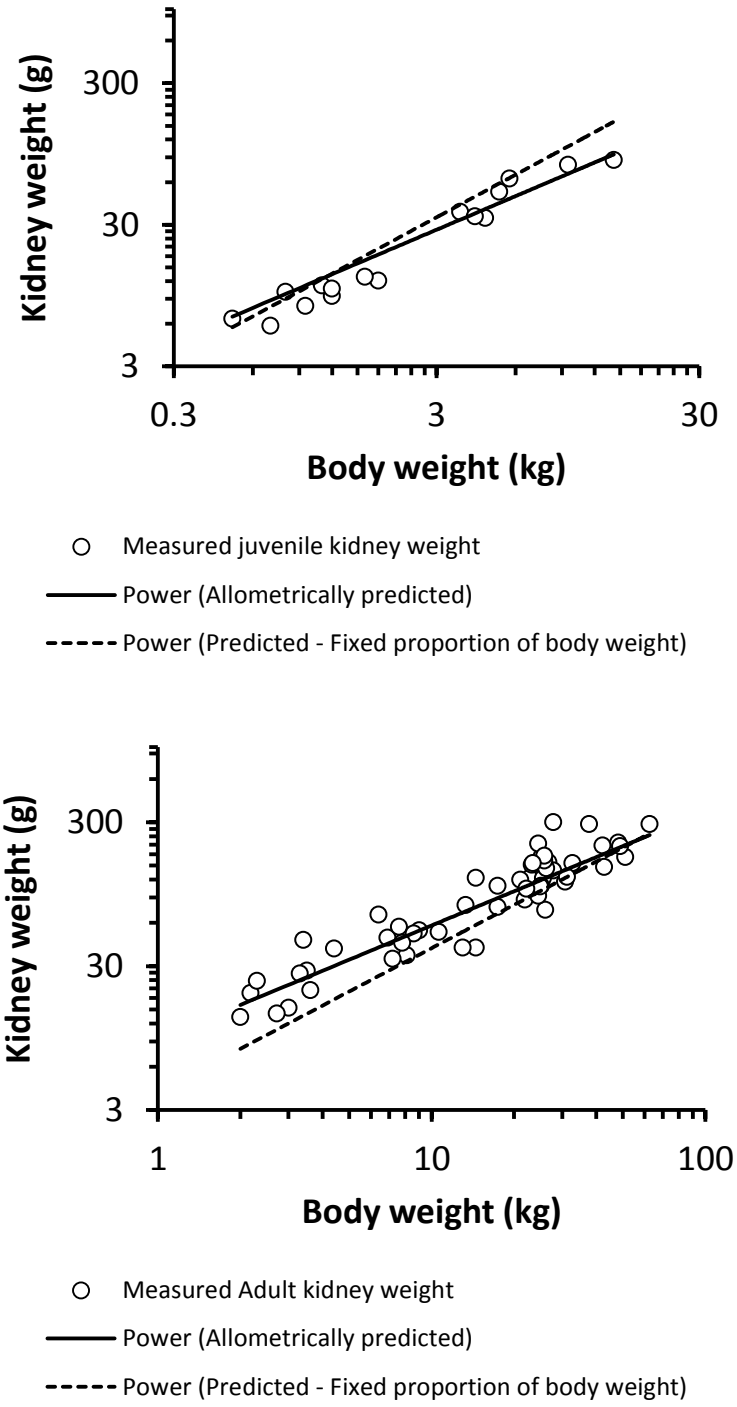

Figure 4: Scatter plots of measured kidney weight (g) against body weight (kg) of validation data set. The solid line indicates the predicted kidney weights using the newly developed allometric equation. The dashed line indicates predicted kidney weights using 1.13% and 0.4% of body weights for juveniles and adults, respectively.

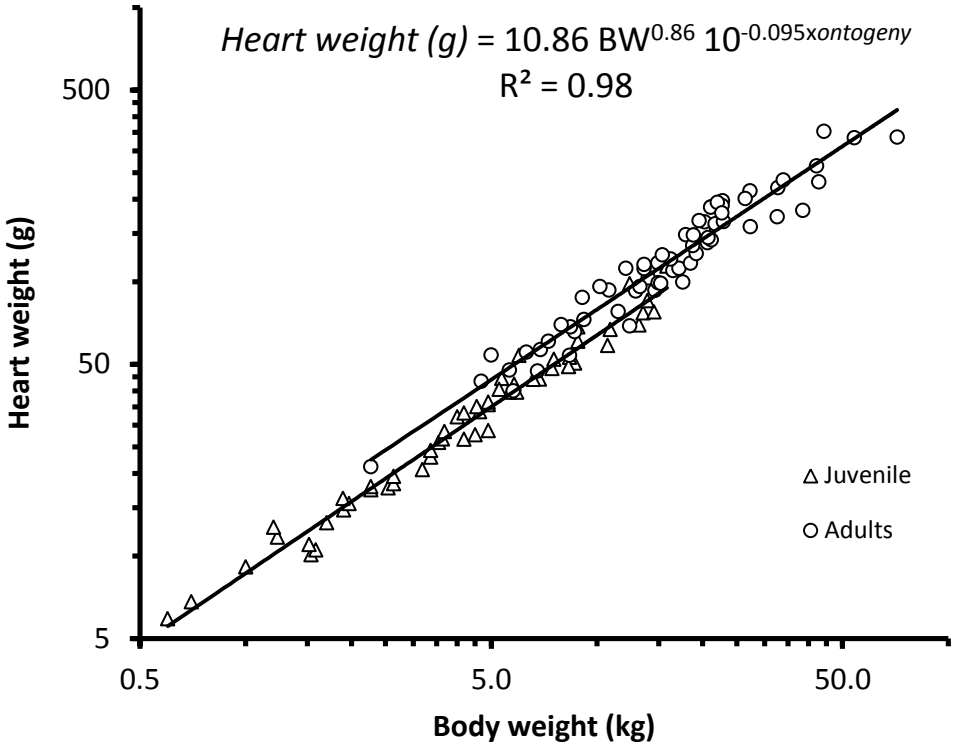

Figure 5: Scatter plot of $\log_{10}$ heart weight (g) against $\log_{10}$ body weight (kg) from 121 juvenile and adult dogs of training data set. The heart weight allometrically related to body weight and ontogeny as: ***Heart weight (g)* = 10.86 BW$^{0.86}$ 10$^{-0.095x ontogeny}$** *Where, Adult = 0, juvenile = 1,* R^2 = 0.98 ($p<0.05$).

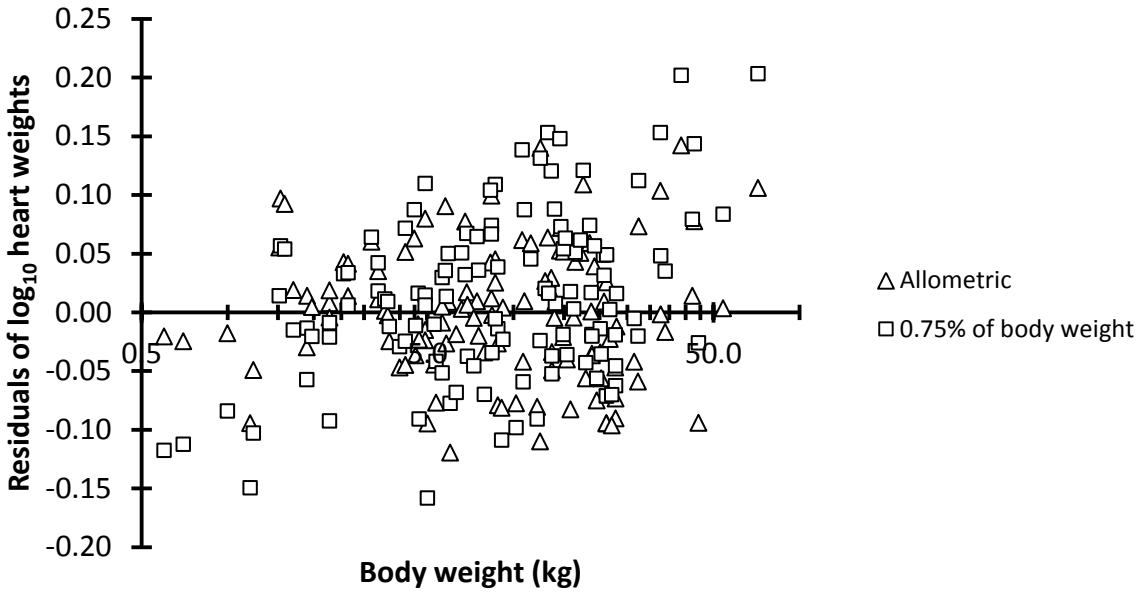

Figure 6. The residuals of $\log_{10}$ transformed heart weights predicted with the newly developed allometric equation and 0.75% of body weights were plotted against body weights in the training data set *per se*.

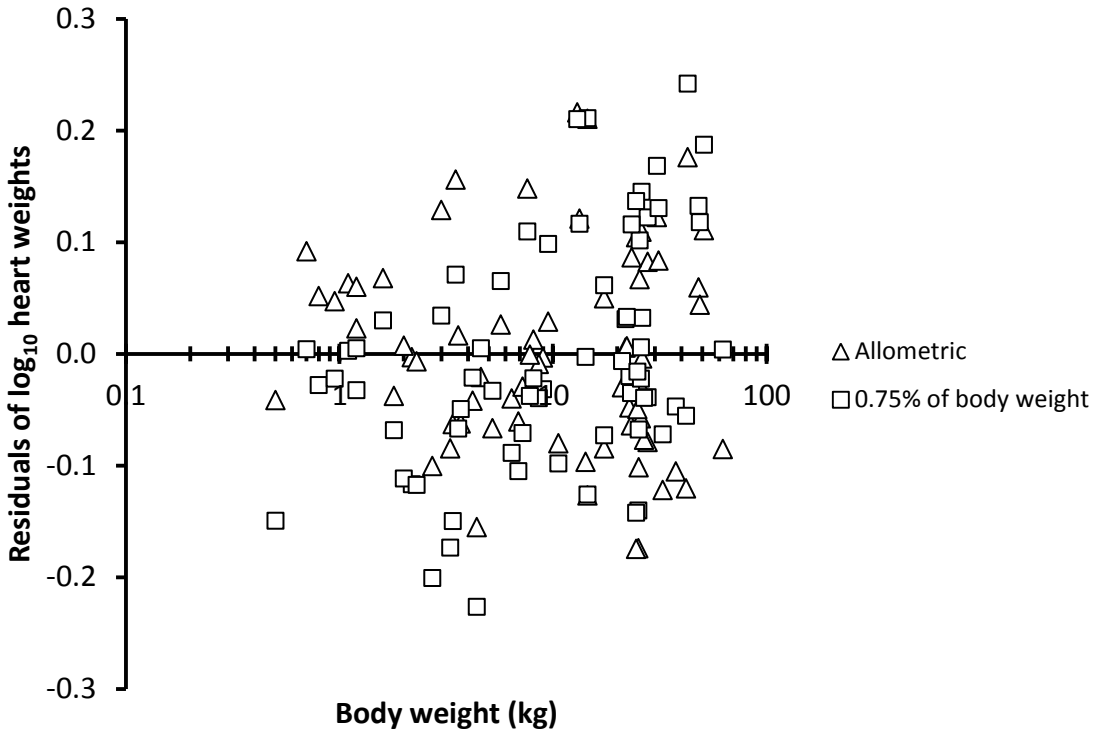

Figure 7. The residuals of $\log_{10}$ transformed heart weights predicted with the newly developed allometric equation and 0.75% of body weights were plotted against body weights in the validation data set.

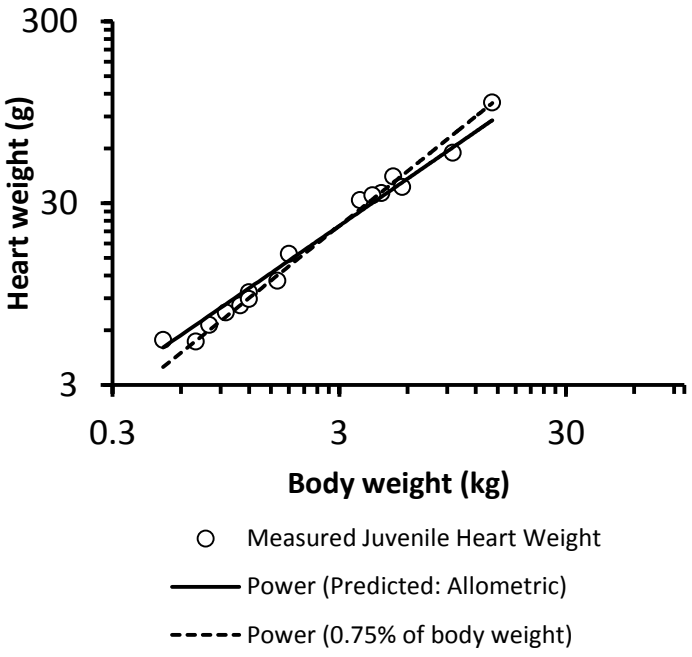

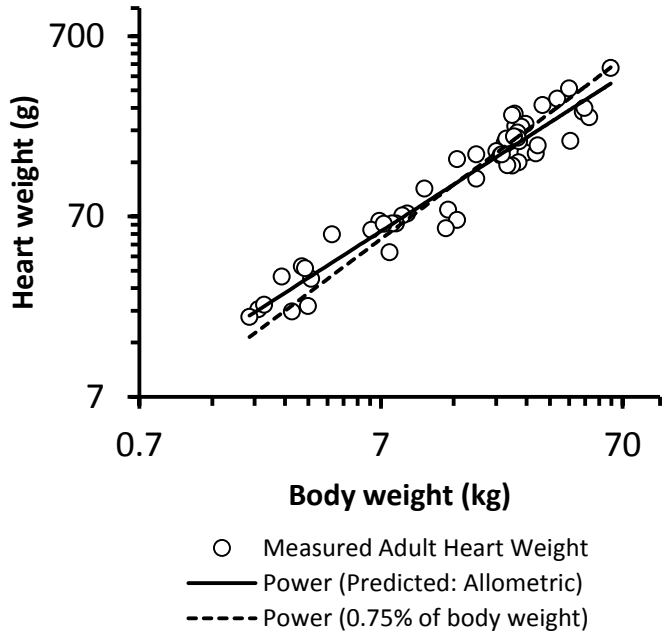

Figure 8: Scatter plots of measured heart weight (g) against body weight (kg) of validation data set. The solid line indicates the predicted heart weights using newly developed allometric equation with training data set. The dashed line indicates predicted heart weights using 0.75% fixed proportion of body weight.

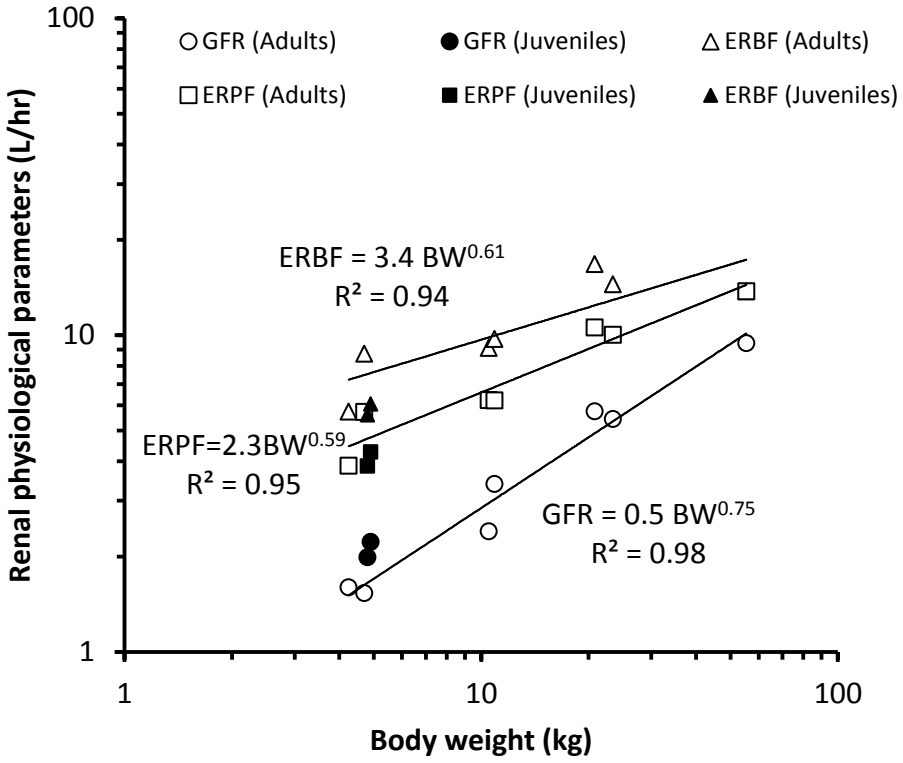

Figure 9: Log_{10} transformed renal physiological parameters were regressed against log_{10} transformed adult body weights

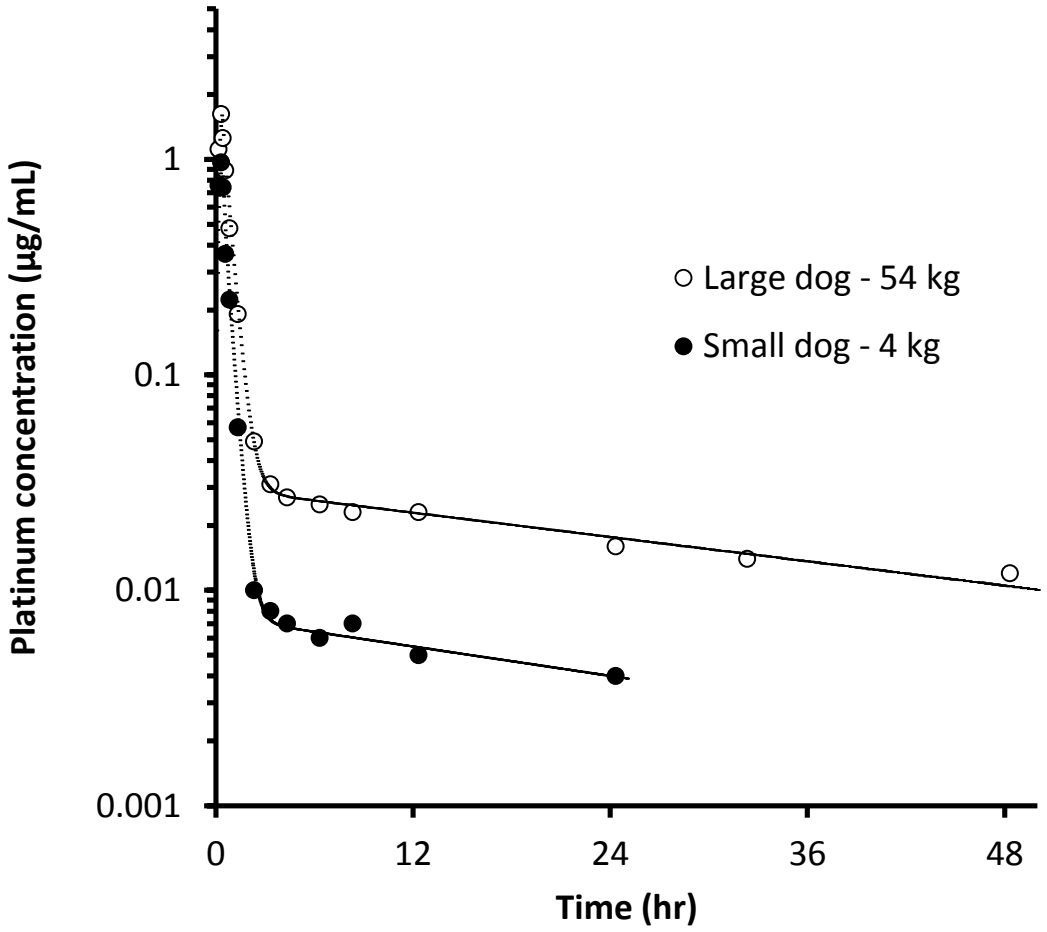

Figure 10: Two-compartmental model fitting of platinum concentrations in a large sized (55 kg) and small sized adult dogs (4.2 kg). Circles indicate observed concentrations and black dots indicate predicted concentrations

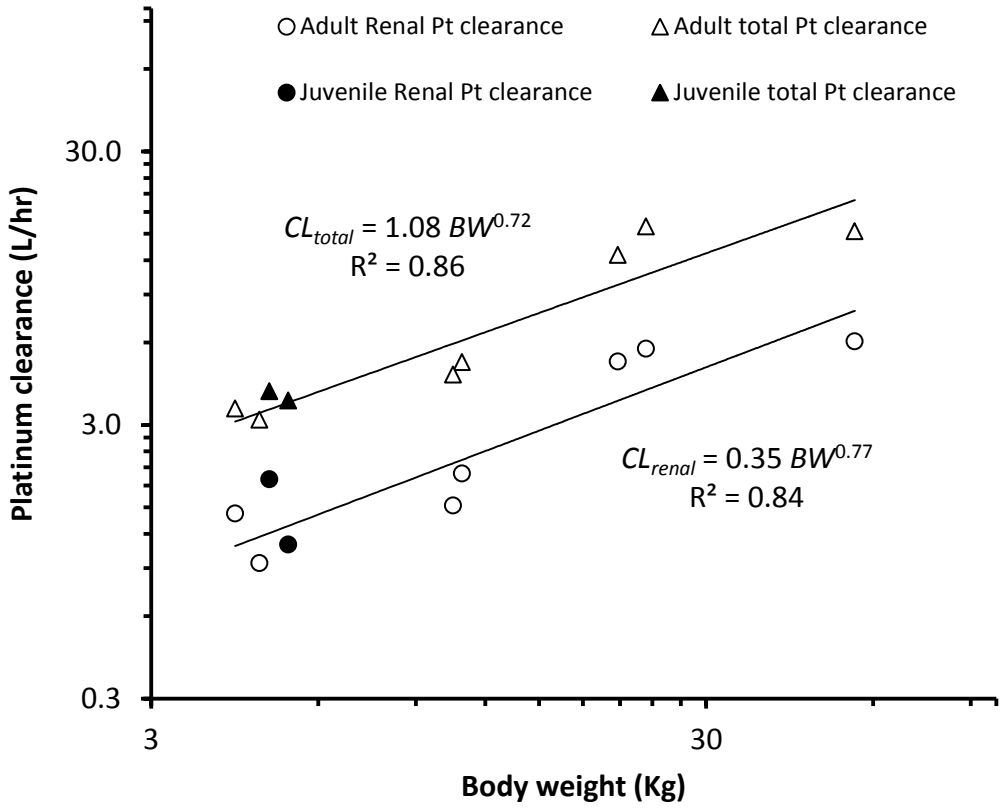

Figure 11: Relationship between total and renal platinum clearance, and body weight

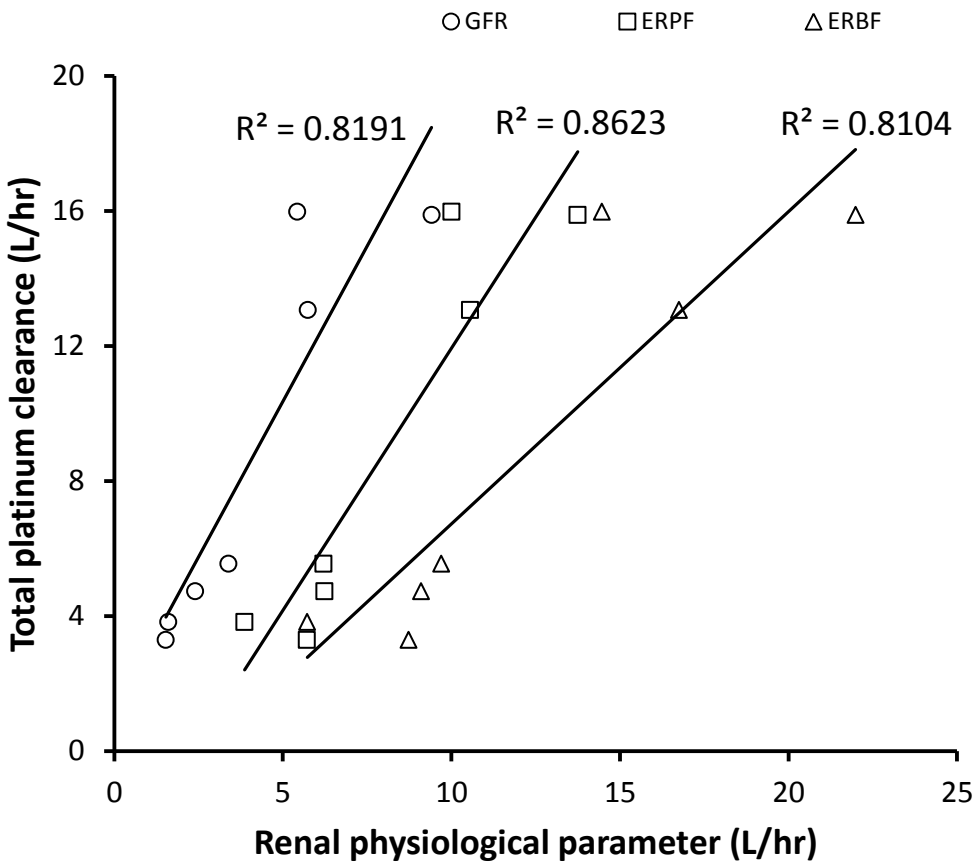

Figure 12: Correlation between total platinum clearance and renal physiological parameters

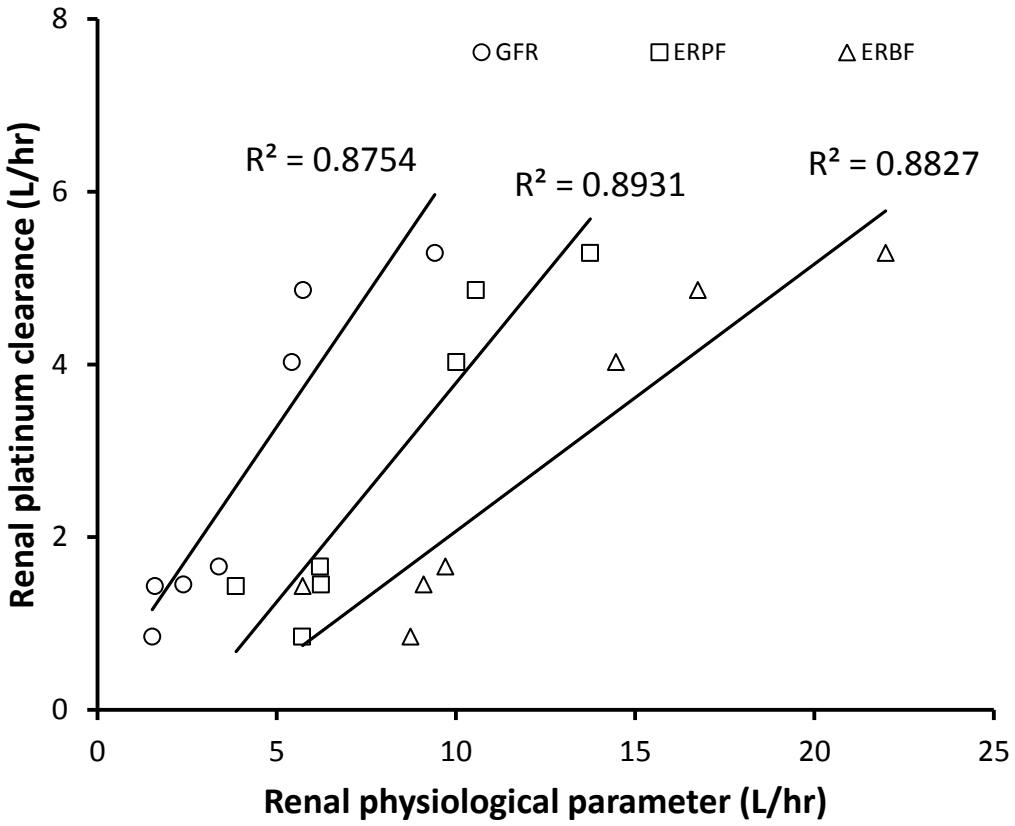

Figure 13: Correlation between renal platinum clearance and renal physiological parameters.

CHAPTER IV

ALLOMETRY OF HEPATIC METABOLISM OF VINBLASTINE IN DOGS

Abstract

Vinblastine and prednisone regimens are well tolerated by dogs with mast cell tumors but their efficacy is less than 50% of treated dogs indicating under-dosing with the current body surface area based dosing. We hypothesize that novel dosing equations that relate the pharmacokinetics of vinblastine to liver weight and drug metabolizing activity will yield more predictable plasma drug levels than current dosing formulae. Liver and body weights were collected from a total of 324 dogs and multiple linear regressions were performed. Microsomes were purified by differential centrifugation in twenty three liver samples. The density of cytochrome P450 enzymes in the microsomal samples was determined by ascorbate reduced dithionate difference spectra. The intrinsic clearance (CL_{int}) of vinblastine (0.025 – 61.65 μM) was determined by substrate depletion approach. The hepatic clearance (CL_{hep}) of vinblastine was predicted by well-stirred, parallel tube, and dispersion models. In order to compare *in vitro* metabolism studies, *in vivo* vinblastine pharmacokinetic studies were conducted in four adult male dogs (10 - 54 kg). A novel dosing equation was developed to calculate the doses of vinblastine as a function of clearance and area under plasma concentration versus time curve. Liver weight, density of cytochrome P450 enzymes, intrinsic clearance, and hepatic clearance of vinblastine were allometrically related to body weight. All three predictive models predicted CL_{hep} within acceptable limits. A novel dosing equation was developed: Dose = AUC*(21.6 $BW^{0.78}$) and shown that current doses are suboptimal. These are proof-of-concept studies and have to be tested in a large sample size for definitive results.

Introduction

Vinblastine is a vinca alkaloid isolated from the periwinkle plant, *Catharanthus rosesus.* Vinblastine is indicated for the treatment of several soft tissue tumors in both human and veterinary patients. Mast cell tumors are one of the most common cutaneous tumors in dogs of all

ages and breeds. However, mast cell tumors are more prevalent in geriatric dogs and some breeds, such as Boston terriers, Pugs, Boxers, and Labrador retrievers. Mast cell tumors are staged into different categories by different classification systems, such as World Health Organization (WHO) (Dobson and Scase, 2007), Patnaik grading (Patnaik et al., 1984), and 2 – tier grading system (Kiupel et al.). However, recent 2 – tier grading system of cutaneous mast cell tumors had replaced previous grading systems. Surgical excision with wide margins remains the mainstay of treatment for resectable mast cell tumors (Welle et al., 2008). In advanced stages, surgical excision or radiation therapy may be coupled with chemotherapy. Vinblastine combined with prednisone regimens are well tolerated but are effective in less than 50% of treated dogs (Thamm et al., 1999; Rassnick et al., 2008). Oral toceranib phosphate (Palladia®) is the only FDA approved drug with an indication to treat mast cell tumors in dogs. However, vinca alkaloid and prednisone regimens are still considered a standard of care for the treatment of certain presentations of mast cell tumors in dogs. Therapeutic efficacy of vinblastine and toceranib combinations were investigated in dogs with mast cell tumors (Robat et al.).

Currently, vinblastine exposure is normalized by calculation of the dose rate as a direct proportion of body surface area. However, few pharmacokinetic studies of vinblastine have been performed in dogs, and the ability of dosing on the basis of BSA to normalize drug exposure in disparate phenotypes of dogs is currently unknown (Creasey et al., 1975; de Lannoy et al., 1994). There are approximately 400 breeds of dogs worldwide and 156 are recognized by the American Kennel Club. Unlike many species, dogs exhibit wide variation in body weights, ranging from a 1 kg Chihuahua to a 100 kg pound Saint Bernard. Despite such profound variability, most of the pharmacokinetic studies are limited to one breed or size, such as beagle dogs as the model laboratory animal for this species. Results from such studies may be insufficient to determine whether drug exposure is normalized among disparate canine patients. The low risk for adverse effects and low therapeutic outcome with vinblastine / prednisone regimens suggest that most dogs may be receiving suboptimal doses of vinblastine. Therefore, the therapeutic outcome of

vinblastine and prednisone regimens may be improved if the vinblastine doses were optimized to produce drug exposure that was as similar as possible among different patients. The efficacy of anticancer drugs is correlated with the drug exposure unlike many therapeutic drugs (Moore and Erlichman, 1987; Calvert et al., 1989; van den Bongard et al., 2000). Mathematically, drug exposure is calculated as AUC (area under plasma concentration versus time curve) (Hempel and Boos, 2007). The doses of anticancer drugs are calculated as function of clearance and drug exposure, dose = AUC * clearance. Thus, to achieve a constant drug exposure in disparate patients, clearance is the important pharmacokinetic parameter. If the total body clearance of a drug is determined accurately, then the dose required to produce therapeutically relevant drug exposure can be calculated accurately.

We hypothesize that novel dosing equations that relate the pharmacokinetics of vinblastine to liver weight and drug metabolizing activity will yield more predictable plasma drug levels than current dosing formulae. The rationale for our studies was based on: vinblastine is primarily metabolized in the liver through oxidation reaction of phase I and excreted mostly in bile through feces and to some extent renal secretion. For xenobiotics that are cleared by the liver, the intrinsic hepatic clearance (CL_{int}) depends on drug metabolizing activity, the density of enzymes per volume of liver, and liver mass relative to body weight.

The success rate of drug development would be improved with decreased expenses if there are better *in vitro* approaches to predict *in vivo* pharmacokinetic parameters. Approximately 10% of the drug candidates that are selected for clinical development are marketed and out of those marketed, approximately 40% are discontinued because of unacceptable pharmacokinetic / toxicokinetic properties (Prentis et al., 1988; Obach et al., 1997). To decrease expenditures in drug development, the best approach would be to perform *in vitro / in vivo* correlation studies to test the suitability of *in vitro* studies to predict *in vivo* pharmacokinetic parameters. Because of the short amount of time it takes, less expenses, and easy applicability to *in vivo* pharmacokinetic

parameters, *in vitro* studies are becoming more popular in the preclinical screening of new chemical entities (NCEs) and to make go or no-go decisions in early drug discovery phases.

Physiologically based pharmacokinetics (PBPK) modeling and allometric scaling are the two common approaches to predict *in vivo* pharmacokinetic parameters from *in vitro* data. PBPK modeling is complex and requires lot of information, software programming, and expertise. On the other hand, allometric scaling is simple to use, requires minimal data, and less expertise to perform. Allometric scaling is particularly important in extrapolating results from one species to another species (*interspecies* allometric scaling) and within a species where there is a wide variation in body weights, in species, such as dogs and horses (*intraspecies* allometric scaling). However, PBPK modeling is a highly versatile and powerful tool in predicting absorption, distribution, metabolism, and excretion of a chemical compound or drug. In order to perform PBPK modeling to predict the disposition of a drug, accurate input of information on anatomical, physiological, and preliminary estimates of pharmacokinetic parameters are needed. Unfortunately, such information is available in the literature only for laboratory beagle sized dogs that may not predict required information for wide range of canine breeds.

Many anatomical (BSA, liver weight, kidney weight, and other organs), physiological (basal metabolic rate, glomerular filtration rate, renal blood flow, hepatic blood flow, and cardiac output), and pharmacokinetic parameters (clearance, volume of distribution, and elimination half-life) vary with body size in a disproportionate relationship which can be mathematically represented as $y = aW^b$, where 'y' is the dependent parameter, 'a' is the mass coefficient, 'W' is body weight, and 'b' is the mass exponent or power. Pharmacokinetic scaling has consistently revealed the inadequacy of any fixed mass exponent, such as 2/3 or ¾ powers, in predicting drug pharmacokinetic parameters as a function of body weight. Allometric or non-proportional relationships between body size and drug clearance are magnified when body weight varies widely. The effect of body weight on drug clearance is particularly important in dogs, where there

is wide range in body weights. Therefore, the accuracy of pharmacokinetic scaling can only be judged retrospectively and requires the construction of individual scaling relationships for each particular drug, based on multiple *in vivo* studies. Conducting such *in vivo* studies is not only expensive but also cumbersome. However, the integration of *in vivo* allometric considerations with *in vitro* studies increases the predictive power of the resulting equations. Once the true influence of individual factors such as, body weight, gender, and ontogeny are understood, drug doses can be individualized as a function of significant individual factors and in combination with other individual characteristics, such as disease status.

The current studies on organ scaling are limited to few subjects and homogenous population (Jackson and Cappiello, 1964; Steward et al., 1975; Lutzen et al., 1976). Pathologists estimate the weight of liver as 3.5% of body weight (Steward et al., 1975). However, these fixed proportions of body weights may not give good estimates of liver weights in dogs as there is wide variation in body weights.

The overall objective of this study was to develop novel dosing equations to accurately predict the dosages of vinca alkaloids in dogs and to establish in *vitro / in vivo* correlations of hepatic clearance of vinblastine in dogs.

Materials and methods

Materials: Vinblastine sulfate, dithionate, ascorbic acid were obtained from Sigma Aldrich Inc., St. Louis, MO, USA. Vindesine sulfate was obtained from LKT laboratories, Inc., St. Paul, MN, USA. Nicotinamide adenine dinucleotide phosphate - regenerating system (NADPH-RS) consisting of solution A (glucose-6-phosphate and nicotinamide adenine dinucleotide phosphate) and solution B (glucose-6-phosphate dehydrogenase) were purchased from BD Biosciences, San Jose, CA, USA. HPLC grade organic solvents and reagents were purchased from Fisher scientific, Pittsburgh, PA, USA.

Allometric scaling of liver weights: Post mortem body weights and liver weights were collected from dogs euthanized at the nearby urban animal shelters for population control and from submissions to the Oklahoma animal disease diagnostic laboratory (OADDL), Stillwater, Oklahoma for post mortem examination. Dogs above 1 year of age and less than 8 years of old were considered as adult group; dogs in the age group of 2 to 5 months age were considered as juvenile dogs. There are different opinions about considering a dog as geriatric, such as large breeds have shorter life span and attain geriatric phase earlier than small breeds (Patronek et al., 1997; Speakman et al., 2003; Galis et al., 2007). We assumed that dogs above 8 years old as geriatric (Cummings et al., 1996a; Cummings et al., 1996b; Studzinski et al., 2006; Cotman and Head, 2008). For the determination of age of dogs, patient history and or dentition (Merck veterinary manual) were used. The gender and reproductive status (neutered/spayed/intact) of the dogs were noted. For the determination of liver weights, gall bladder was cut opened, drained, and retained. Data were collected from a total of 364 dogs including 237 adult dogs and 127 juvenile dogs over a period of six years. A series of *a priori* inclusion criteria were defined before starting the collection of organ weights and data outside these criteria were omitted at the stage of data collection. The body condition score (BCS) of dogs was recorded on a scale of 1 – 9 (Laflamme, 1997; Parker and Freeman, 2011). Dogs with BCS of 4, 5, and 6 were included in the study. Tissue specimens were also collected along with the signalment of dogs for the collected from animal shelters. Histopathology reports were examined for all dogs which were collected from OADDL.

For the statistical analysis of the data, SigmaStat® 3.0, SPSS, Inc., Chicago, IL, USA and SAS 9.2, SAS Institute Inc., Cary, NC, USA were used. The normal distribution of the data was tested by Shapiro-Wilk normality test. Outliers were detected by Studentized residuals and Cook's distance. Based on a *priori* inclusion criteria, dogs having Studentized residual more than +/- 2 were considered as residuals. Residuals outside the inclusion criteria were removed and

analyzed again to detect outliers and the resulting outliers were examined histopathologically to consider inclusion in the model. Data were $\log_{10}$ transformed and step wise multiple linear regressions were performed with liver weight as dependent variable and gender, age class, and body weight as independent variables to see which individual factors influenced the organ weight. Gender and ontogeny were represented as nominal variables with standard denotation: females were denoted as '1' and males were denoted as '0'; juveniles were denoted as '1' and adults were denoted as '0'. *F*-test was used as an indication of predictive ability of model. Stepwise multiple linear regression analyses were performed separately for each group of juveniles and adults. Statistical significant predictors of liver weight were retained for the analysis. The statistical significant difference between the slopes of juveniles and adults was determined using ANCOVA (SAS 9.1, SAS Institute Inc., Cary, NC, USA). Collinearity was tested to see if independent variables have any correlation which might interfere with regression analysis. Study significance was set *a priori* to alpha=*0.05.* The data collected from animal shelters was used as training data set to perform multiple linear regression analysis and develop allometric equation. The data from the OADDL was used as validation data set to verify the resulting regression equations of shelter data. The predictive ability of the newly developed allometric equations was validated by comparing to training data set per *se* and validation data set. The sum of residuals of organ weights predicted with newly developed allometric equations and fixed proportions of body weights were compared. Log_{10} transformed residuals of organ weights predicted were plotted against $\log_{10}$ transformed body weights. A paired t- test was performed between $\log_{10}$ residual errors and zero to determine the predictability of the allometric equations in both training and validation data sets.

Microsomal purification: Liver samples were collected from twenty three adult dogs (2.3 - 54 kg) euthanized at the Oklahoma City Animal Shelter, Oklahoma City, OK within thirty minutes after euthanasia. Samples were plunged in ice cold Lactated Ringer's solution. Any apparent

vessels or bile ducts were flushed thoroughly with saline until sample became blanched. Samples were carried to the laboratory for microsomal purification either on ice or in liquid nitrogen. Microsomes were purified based on the standard procedure (Schneider, 1948). Approximately, 25 - 35 g of liver sample was finely chopped into small pieces with a scalpel blade. Using a clean scissors, any visible connective tissue was trimmed. Minced liver sample was transferred to Potter-Elvehjem homogenizer and homogenized with three volumes of homogenization buffer. The homogenate was centrifuged at 10,500 rpm for 20 minutes at 4 ^{0}C. The fatty layer from the supernatant was removed, which is the S9 fraction. Supernatant was transferred into cold ultracentrifuge tubes (16 – 26 mL) and centrifuged at 35,000 rpm for 65 minutes at 4 ^{0}C using 55.2 Ti rotor. Supernatant was poured off and an equal amount of (16 – 26 mL) ice cold homogenizing buffer was added. Pellet was resuspended and transferred to 30 mL homogenizer for gentle homogenization. The homogenate was centrifuged at 35,000 rpm for 65 minutes at 4 ^{0}C. Supernatant was poured off and microsomes were resuspended in storage solution. Pellets were homogenized in 15 mL homogenizer and microsomes were stored until use, at -80 ^{0}C.

Microsomal protein determination: The protein concentration microsomal samples was determined by Bradford protein assay in triplicate using Bio-Rad Protein Assay Kit, Hercules, CA (Bradford, 1976).

Cytochrome P450 density: The density of cytochrome P450 in microsomes was determined by ascorbate reduced dithionate - difference spectra (Matsubara et al., 1976; Johannesen and DePierre, 1978), a modified method of gold standard method (Omura and Sato, 1964a; Omura and Sato, 1964b) in duplicate using a Cary 300 UV – vis spectrophotometer. In brief, samples were diluted 1:10 with cytochrome P450 dilution buffer (100 mM sodium phosphate buffer, pH 7.4). Baseline was run with buffer from 400 to 500 nm. Ten microliters of ascorbic acid was added to microsomes to make final concentration of 250 µM and the baseline was recorded. Then carbon monoxide (CO) was bubbled into the microsomal suspension for about 1 minute and

spectrum was obtained. Few grains of sodium dithionate were added to the microsomal suspension in the cuvette. Then contents were mixed well and the spectrum was obtained after 2 minutes. The concentration of cytochrome P450 was determined from the spectrum using Beer's law with the molar extinction coefficient of 104 mM^{-1} cm^{-1} for the difference of absorption between peak position at 450 nm and 490 nm.

***In vitro* incubations**: The conditions for microsomal incubation of vinblastine, such as range of vinblastine concentrations for incubations, microsomal protein concentration, incubation temperature, time of pre-incubation and incubation, and stop solution to be used were optimized. All microsomal incubations were done in duplicate. Vinblastine sulfate (in methanol) was added to microsomal samples which were diluted to 0.5 mg/mL microsomal protein concentration with 100 mM sodium phosphate buffer (pH 7.4) in the final concentrations of 0.025 - 61.65 µM (final organic solvent concentration of 1%). Fortified microsomal samples were pre-incubated for 3 minutes at 37 ^{0}C in a shaking water incubation bath with open lid. Reaction was initiated by addition of NADPH - RS at the final concentration of 1.55 mM. Reactions were stopped by addition of 400 µL of ice cold acetonitrile containing internal standard, vindesine sulfate to 200 µL of microsomal incubate samples at pre, 3, 5, 10, 15, 20, and 30 minutes. Samples were vortex mixed and centrifuged at 10,000 g at room temperature for 10 minutes (Biofuge, Pico, Heraeus and Sorvall Company, Germany). To 200 µL of supernatant, 400 µL of 80 mM ammonium acetate (pH: 2.5) was added and vortex mixed. The concentrations of vinblastine in the microsomal incubate samples were determined by reversed phase high performance liquid chromatography (RP-HPLC). The Waters® RP - HPLC consisted of 1500 series binary pump, column heater set at 30 ^{0}C, in-flow degasser, 717 auto sampler set at 4 ^{0}C, and fluorescence detector at excitation wavelength of 254 nm and emission wavelength of 320 nm. Fifty micro liters of samples were injected onto C18 (250 mm x 4.6 mm and 5 µm particle size) column and separated under isocratic elution with mobile consisting of 53% of 80 mM ammonium acetate

(pH: 2.5) and 47% of acetonitrile and methanol (1:1). For all analytical methods, accuracy within 20% of nominal concentrations at the lower limit of quantitation (LLOQ) and 15% of the nominal concentrations at higher concentrations; similarly, an RSD of 20% at the LLOQ and 15% at higher concentrations were set as the acceptable limits.

The data was analyzed on WinNonlin® 5.2 pharmacokinetic software program (Pharsight Corp., Mountain View, CA) using pharmacodynamic model # 101: ($E = \frac{E_{max} \cdot C}{C + EC_{50}}$) to obtain the values of theoretical maximum rate of reaction (V_{max}) and Michaelis constant (K_m). *In vitro* intrinsic clearance of vinblastine was calculated as a ratio of V_{max} to K_m ($In\ vitro\ CL_{int} = \frac{V_{max}}{K_m}$). The values of *in vitro* intrinsic clearance were scaled to the whole animal using a scaling factor of 55 mg microsomal protein/g of liver to get *in vivo* intrinsic clearance of vinblastine: ($In\ vivo\ CL_{int} = In\ vitro\ CL_{int} \cdot \frac{55\ mg\ microsomal\ protein}{g\ of\ liver} \cdot \frac{g\ of\ liver}{kg\ of\ body\ weight}$) (Smith et al., 2008; Obach, 2011). Hepatic clearance of vinblastine was predicted using three predictive models, such as well stirred model, parallel tube model (undistributed sinusoidal model), and dispersion model (Pang and Rowland, 1977; Houston and Carlile, 1997).

Well stirred model (equation 1):
$$CL_{hepatic} = \frac{Q_h \bullet f_u \bullet CL_{\text{int}}}{Q_h + f_u \bullet CL_{\text{int}}}$$

Parallel tube model (equation 2):
$$CL_{hepatic} = Q_h \left[1 - \exp\left(\frac{f_u \bullet CL_{\text{int}}}{Q_h} \right) \right]$$

Dispersion model (equation 3):
$$CL_{hepatic} = Q_h \left[1 - \frac{4a}{(1+a)^2 \exp\left[\frac{a-1}{2Dn} \right] - (1-a)^2 \exp\left[-\frac{a+1}{2Dn} \right]} \right]$$

Where, f_u = fraction of unbound drug; Q_h = hepatic blood flow = 29.06 mL/min/kg hepatic blood flow was used (Hanna, 1984); $a = (1+4RnDn)^{1/2}$; $Rn= f_u \times Cl_{int} / Q_h$; Dn = dispersion number = 0.17.

***In vivo* vinblastine pharmacokinetic studies**: In order to compare hepatic clearance of vinblastine determined in the *in vitro* vinblastine metabolism studies, *in vivo* vinblastine pharmacokinetic studies were conducted in four adult male dogs (10 – 54 kg). All dogs had BCS of 4 – 6. Two small dogs (10 kg) were laboratory beagles and two dogs (43-54 kg) were mixed breeds. The Institutional Animal Care and Use Committee approved the husbandry and procedures utilized in this study. Indwelling vascular access ports (VAP) (Access Technologies®, Skokie, IL, USA) were implanted in jugular veins under anesthesia following standard procedures (Bagley, 1990; Henry et al., 2002; Cahalane et al., 2007). The Huber infusion sets (Access Technologies®, Skokie, IL, USA) were used to access ports to administration of drug and collection of blood samples. The VAPs were maintained using standard aseptic procedures for access and heparin lock. Dogs were kept in metabolic cages and fasted overnight with *ad libitum* access to water. Vinblastine sulfate (1 mg/mL) (APP Pharmaceuticals LLC, Schaumburg, IL, USA) was administered as a bolus dose at the rate of 0.075 mg/kg. Blood samples were collected at pre, 2 min, 5, 10, 15, 20, 30, 45 min, 1 hr, 2, 3, 4, 5, 6, 9, 12, and 24 hr post infusion. Urine samples were collected at 1hr, 3, 5, 7, 12, 24, 32, 48, 56, and 72 hr post infusion. Metabolic cages were washed with 100 mL of nanopure water to get wash sample at each urine sample collection time point. An analytical method was developed to quantify the concentrations of vinblastine and desacetylvinblastine (DVLB), a metabolite of vinblastine, in urine and plasma samples using liquid chromatography/atmospheric pressure chemical ionization – tandem mass spectrometry (LC/APCI-MS/MS). The system consisted of a Schimadzu HPLC system (Shimadzu corporation, Kyoto, Japan) having a system controller (CBM-20A), binary solvent delivery unit (LC-20AD), in-line degasser (DGU-20A5), an auto-sampler (SIL-20AC) with thermostatic injector set at 4 ^{0}C

and a column oven set at 40 ^{0}C (CTO-20AC) with a Restek Allure Pentafluorophenyl (PFP) Propyl 5 μm 50 x 2.1 mm column (Restek, Bellefonte, PA), and guard cartridge (Restek 5 μm, Ultra Biphenyl, 10 x 2.1 mm) were used. An Applied Biosystems 4000 Q-Trap MS/MS system (Applied Biosystems, Foster City, CA) equipped with an atmospheric pressure chemical ionization source and a NitroGen N300DR nitrogen generator was used (Peak Scientific Instruments Ltd, Paisley, United Kingdom). Analyst® 1.5 software for Windows® was used to acquire and analyze the data.

Plasma and urine samples were processed on Oasis® HLB solid phase extraction cartridges (Waters®, MA). Briefly, for calibrants and quality controls, 480 μL of blank plasma or urine were added to micro-centrifuge tubes. Ten microliters of vinblastine and 10 μL of desacetylvinblastine calibrator solutions in methanol were added to achieve final concentrations of 0.125 - 100 ng/mL and 1 – 2,000 ng/mL in plasma; 0.125 - 5 ng/mL and 0.5 - 100 ng/mL in urine samples, respectively. Incurred samples of *in vivo* vinblastine pharmacokinetic study were thawed at room temperature and 500 μL of sample matrix were added to the labeled micro centrifuge tubes. All samples were diluted with 500 μL of water containing 10 μL of 500 ng/mL vinorelbine and vortex mixed. Oasis® HLB cartridges were preconditioned with 1 mL of methanol and 1 mL of water. Samples were loaded onto the column slowly, at a rate of approximately 1 – 2 drops per second. Cartridges were washed with 2 mL of water, and then dried at maximum airflow for 30 minutes. Samples were slowly eluted with 2 mL of methanol into labeled silanized glass tubes. The eluted samples were dried under nitrogen at 30 0C and were resuspended in 150 μL of buffer, containing 50% 5 mM ammonium acetate, 25% acetonitrile, and 25% methanol. For plasma samples, 100 μL of the redissolved sample was injected onto the system, whereas 20 μL were injected for urine samples. Silanized glassware was used wherever possible during sample preparation to avoid systemic under-estimation of analyte concentration and to increase sensitivity (Trim et al., 2008; Damen et al., 2009; Damen et

al., 2010). The mobile phase consisted of 10% 5 mM ammonium acetate buffer, adjusted to a pH of 3.5 with glacial acetic acid, and 90% HPLC grade methanol. Separation was achieved by isocratic elution at a flow rate of 0.75 mL/min.

Pharmacokinetic parameters were calculated by compartmental analysis with the models of the form, $C = \sum_{i=1}^{n} A_i e^{-\lambda_i t}$ on WinNonlin® 5.2 pharmacokinetic software program (Pharsight Corp., Mountain View, CA) using pharmacokinetic model # 18. The appropriate compartment model was chosen based on Akaike's information criteria (AIC), co-efficient of variation values, and inspection of concentration versus time plots and residual plots (Yamaoka et al., 1978). The renal clearance of vinblastine was calculated using the equation: $CL_{renal} = X_{0\text{-}72}/AUC_{0\text{-}72}$, where $AUC_{0\text{-}72}$ is the area under plasma concentration versus time curve from 0 – 72 hr and $X_{0\text{-}72}$ is the total amount of drug excreted in the urine from time 0 – 72 hr. Hepatic clearance of vinblastine was determined by subtracting renal clearance from the total clearance of vinblastine. The total and hepatic clearance of vinblastine was regressed against body weights (SigmaStat® 3.0, SPSS Inc., Chicago, IL).

***In vitro/in vivo* correlations**: The values of hepatic clearance of vinblastine obtained in *in vitro* and *in vivo* studies were compared to see the utility of *in vitro* studies in predicting the *in vivo* pharmacokinetic parameters of vinblastine in dogs. The percent accuracy was calculated for each predictive model. The accuracy of predictions of hepatic clearance with these predictive models was tested by percent accuracy, root mean squared error (*rmse*), and the average fold-error (*afe*) which reflects precision and bias, respectively (Sheiner and Beal, 1981). The correlation analyses were also performed between the observed and predicted hepatic clearance values.

$$afe = 10^{\left|\frac{1}{n}\Sigma\frac{predicted}{observed}\right|}$$

$$mse = \frac{1}{n}\sum(predicted - observed)^2$$

$rmse = \sqrt{mse}$

Results

Organ scaling: The organ weights data had passed normality test. There was no difference between the slopes of juveniles and adults per ANCOVA results (SAS 9.2, SAS Institute Inc., Cary, NC, USA). The data was combined and multiple linear regression analysis was done for the combined data. Gender was not a predictor of liver weight ($p>0.05$) but body weight and ontogeny had significantly influenced the liver weight ($p < 0.001$). A regression equation was developed from data collected from the training data set, a total of 160 dogs (58 juveniles and 102 adults) (figure 1). Using the newly developed allometric equation, weight of the liver for a given body weight of dog can be predicted from the equation: $Liver\ weight\ (g) = 49.77 \cdot BW^{0.90} \cdot 10^{0.105 \cdot ontogeny}$ R^2 =0.93, $Sy.x$ = 0.094, Where, for ontogeny, adult =0 and juvenile =1. The allometric equation developed from the training data set was validated in the training data set *per se* and validation data set. Log_{10} transformed residuals of liver weights were plotted against body weights in both training and validation data set were presented in figures 2 and 3. Sums of absolute residual errors of predicted liver weights with newly developed allometric equation were lower compared to fixed proportion of body weights (tables 1 and 2). The mean of log_{10} residual errors of predicted liver weights with allometric equation in training and validation data sets were not significantly different from zero and significantly different from zero, respectively. In figure 4, measured liver weight was plotted against body weights on logarithmic coordinates in comparison with predicted liver weights with the newly developed allometric equation and 3.5% of fixed proportion of body weights. The average proportion of liver weight to body weight in training and validation data sets were 4.47% and 3.93%, respectively.

***In vitro* studies:**

Microsomal purification was done successfully with differential centrifugation method (Schneider, 1948). The concentrations of microsomal protein were in the range of 12.35 mg/mL to 36 mg/mL.

Cytochrome P450 density: the density of cytochrome P450 enzymes in the hepatic microsomes was determined by gold standard method, carbon monoxide difference spectrum. Microsomal samples which were processed from frozen liver samples had hemoglobin contamination and such samples had a prominent peak at 420 nm while obscuring the peak at 450 nm. In order to reduce the peak at 420 nm without affecting the peak at 450 nm, different methods were tested, such as dithionate difference spectra, ascorbate reduced dithionate difference spectra, and ascorbate and PES reduced dithionate difference spectra (figures 5, 6, 7, and 8). Out of these four methods, ascorbate reduced dithionate difference spectra and carbon monoxide difference spectra had given similar results in non - hemoglobin contaminated samples (table 3 and 4). The density of cytochrome P450 enzymes were in the range of 0.28 - 0.99 nmole/mg of protein. The density of cytochrome P450 enzymes was allometrically related with the body weight ($p<0.05$) (figure 9).

Substrate depletion approach: The incubation conditions for substrate depletion approach were optimized, such as optimal microsomal concentration for incubation (0.5 mg/mL); time of pre-incubation (3 min); temperature of incubation (37 ^{0}C); the range of vinblastine concentrations to be used (0.025 – 61.65 μM), time points to stop; and stop solution to use. The concentrations of vinblastine in the incubate samples were quantified by a RP-HPLC. The intraday and interday accuracy and precision were within the acceptable limits. A typical substrate depletion profile of vinblastine in microsomal incubations was shown in figure 11. $1/x^2$ weighting scheme was used for the quantification. The limit of quantitation of the assay was 10 ng/mL. No metabolite was

seen either with fluorescence or ultra violet (UV) detection (figure 10). The best model for fitting of substrate depletion data to determine the values of V_{max} and K_m was chosen based on coefficient of variation (CV) %, residual plots, and inspection of the fitted plots. 1/y weighting scheme was used for model fitting of the substrate depletion data. A representative model fitting of substrate depletion data was presented in figure 12 similar to a Michaelis-Menten enzyme kinetic profile. The range of values of V_{max}, K_m, and intrinsic clearance (CL_{int}) of vinblastine were 22 – 265 pmoles/min/mg of protein, 2.5 – 40 μM, and 5.25 – 70.12 mL/min/kg, respectively. The *in vivo* CL_{int} and hepatic clearance of vinblastine determined *in vitro* were allometrically related to body weight ($p<0.05$) (figures 13 and 14).

***In vivo* vinblastine pharmacokinetic studies**: Pharmacokinetics of vinblastine in dogs was best described by three – compartmental model with 1/y weighting scheme, and Gauss-Newton (Levenberg and Hartley) integration method. Appropriate model was chosen based on low CV%, AIC values, and inspection of residual plots and plasma concentration versus time plots. Plasma concentrations of vinblastine declined sharply following the bolus administration of vinblastine sulfate (figure 15). The concentrations of vinblastine were above the limit of quantitation in both plasma and urine samples in all dogs. The pharmacokinetic parameters of vinblastine were presented in table 5. The excretion profile of vinblastine in urine was presented in figure 16. The percent recovery of vinblastine in urine out of total dose administered was 11.6 ± 2.1 (mean ± SD). Although desacetylvinblastine (DVLB) was noticed in plasma and urine samples, the appearance of DVLB did not give any information in terms of rate of metabolism. Hepatic clearance of vinblastine was determined by subtracting the renal clearance of vinblastine from the total clearance of vinblastine and was plotted against the body weight to establish the allometric relationship (figure 17).

***In vitro / in vivo* correlations**:

In vitro / in vivo correlations were established for hepatic clearance of vinblastine. In table 6, the percent accuracy of prediction of hepatic clearance of vinblastine with different predictive models was presented. Parallel tube model predicted hepatic clearance of vinblastine with better accuracy compared to the other two models. Different statistical tests, such as *afe, mse, and rmse* were performed and presented in table 7. In corroboration with percent accuracy of predictive models in table 6, the statistical methods also gave similar results. The co-efficient of determination between predicted hepatic clearance and observed hepatic clearance of vinblastine was 1 (figure 18).

Discussion

Organ scaling: No difference was noted between the slopes and y-intercepts of adults and juveniles. Therefore, the data was combined and analyzed as a single data with the inclusion of significant factor ontogeny term in the final regression equation. In conformation with previous studies, gender was not a significant predictor of liver weight ($p>0.05$) (Prothero, 1982). The canine intraspecies allometric exponent of liver was 0.9, whereas the previously reported interspecies allometric exponent of liver was 0.886. The newly developed allometric equation was validated using both training data set *per se* and validation data set. For the data in validation data set, detailed histopathology and post-mortem reports were available. The residual plots of both training and validation data set showed that the residuals of liver weights determined from allometric equation were randomly distributed. In contrast, residuals of liver weights determined as a function of fixed proportion of body weight had diagonal and skewed distribution (figures 2 and 3). Further, the sums of absolute residuals have shown the better predictive ability of the newly developed equation compared to the 3.5 % fixed proportion of body weight in both training and validation data sets. The average % relative weights of liver (that is, liver weight (g)*10^{-3} ÷ body weight (kg)) in training and validation data sets were 4.47 and 3.93, respectively. As demonstrated in the residual and scatter plots (figures 2, 3, and 4), and the values of % relative

liver weights in this studies, 3.5% of fixed proportion of body weights is under estimating the weights of liver. The percent fixed proportion of body weights for liver reported in the previous studies based on few number of subjects were 2.36 ± 0.38 (mean ± SD) (Steward et al., 1975), 3.04 (Jackson and Cappiello, 1964), and 3.29 (Reber et al., 1961). Fixed proportions of body weight approach considers only body weight as significant determinant of liver weight whereas allometric equation developed in this study considers both body weight and ontogeny which were significant determinants of liver weights. The newly developed allometric equation is more robust compared to previous similar studies in terms of number, pool of different breeds, and range of body weights considered. The newly developed equations could be used in predictive software programs, such as physiologically based pharmacokinetic, population pharmacokinetic, and SimCYP®.

Microsomal purification: Purification of microsomes was done successfully. The values of microsomal protein concentrations and density of cytochrome P450 enzymes were within the reported literature values (Smith et al., 2008). In order to achieve good quality of microsomes, exposure to air should be minimized as exposure might reduce the potency of enzymes through oxidation.

Cytochrome P450 density: Hemoglobin contamination was noticed in microsomal samples which were purified from frozen liver samples. Hemoglobin contamination was evidenced by the appearance of a peak at 420 nm, altered peak shape at 450 nm with classical carbon monoxide difference spectra (Omura and Sato, 1964b; Omura and Sato, 1964a). Also, the microsomal samples processed from fresh liver samples were light straw colored while microsomes purified from frozen liver samples were dark red in color. The density of cytochrome P450 enzymes allometrically related to body weight ($p<0.05$). With the increase in body weight, the density of cytochrome P450 enzymes had decreased. This phenomenon is in conformation with the earlier findings that cellular metabolism is allometrically related to body size (Porter, 2001). Also, this

allometric dependence of cytochrome P450 enzymes answers why larger individuals receive lesser dose per unit body weight compared to smaller individuals within the same species.

Intrinsic clearance: Ideally, the kinetic behavior of an enzyme is assessed by monitoring rates of product or metabolite formation at various substrate concentrations. However, standards for metabolites may not be available or metabolites may not be identified. In such cases, alternative approaches, such as substrate depletion approach and *in vitro* half - life methods are used. In the preliminary studies, no metabolite was recognized which could be used to perform classical Michaelis-Menten kinetics based on the rate of product or metabolite formation. Therefore, substrate depletion approach which is emerging as a potential *in vitro* method to characterize kinetic behavior of an enzyme was used (Obach and Reed-Hagen, 2002; Komura et al., 2005; Nath and Atkins, 2006). As kinetic characterization of metabolite or product is not required, this method is well suited for the new chemical entities (NCEs) and drugs for which standards of metabolites are not available. There are some studies which have shown similar results with substrate depletion approach and classical Michaelis-Menten kinetics (Stringer et al., 2009). To the best of authors' knowledge, studies on *in vitro* metabolism of vinblastine in dogs were not published elsewhere. As there was no published literature on microsomal incubations in dogs, the microsomal incubation conditions were optimized and incubations were conducted successfully. Optimization of initial conditions is important as Michaelis - Menten parameters are determined *in vitro* under linear conditions with respect to time of incubation and microsomal protein concentration. In microsomal substrate depletion studies, an initial apparent rise in the concentrations of substrate was observed which might be due to slow solubilization of drug into microsomes. Similar observations were found elsewhere also (Obach, 2011). To avoid errors, substrate depletion up to 20% of initial concentration was considered for the calculation of rate of reaction (Nath and Atkins, 2006). This study is the first of its kind to consider different body weights in *in vitro* drug metabolism studies. The study had produced robust estimates of V_{max}, K_m,

and intrinsic clearance of vinblastine in 23 dogs weighing from 2.3 – 54 kg. It is noteworthy to recognize that both density of cytochrome P450 enzymes and intrinsic clearance of vinblastine were allometrically related to body weight. These findings explain allometric dependence of hepatic enzymes which explains why larger individuals receive lesser dose per unit body weight.

Hepatic clearance: The intrinsic clearance of vinblastine was integrated with other physiological parameters which influence clearance, such as hepatic blood flow and fraction of free drug in plasma to determine hepatic clearance. Considering the simple forms of hepatic predictive models, the fraction of unbound drug in microsomes was assumed as 1. Three different predictive models were used. There are underlying assumptions for each predictive model but all of them share some common assumptions, such as perfusion rate limited distribution of drug, rapid diffusion of drug into hepatocytes, and homogenous distribution of enzymes in the liver (Houston and Carlile, 1997; Ito and Houston, 2004). Well-stirred model (equation 1) which is the simplest of three models assumes that the liver is a single well-stirred compartment and drug is mixed infinitely well inside the liver. Parallel tube model (equation 2) assumes that the liver is composed of a number of identical and parallel tubes with enzymes distributed evenly in each cross-section, and blood flows in one direction. The drugs are mixed along a flow path from input to output of the liver only in the infinitely small section. Dispersion model (equation 3) is described based on the analysis on the distribution of the hepatic residence time of drugs after the bolus injection into the liver. Dispersion model is considered to be described based on the flow dynamics in the liver more relevant than the other two models. Dispersion number (D_N) indicates the extent of dispersion of drugs in the liver. The dispersion model becomes well stirred model when the dispersion is infinite and parallel tube model when no dispersion is noticed (Pang and Rowland, 1977; Chiba et al., 2009). As expected, based on the results of allometry of cytochrome P450 density and intrinsic clearance with body weight, hepatic clearance of vinblastine allometrically related with body weight ($p<0.05$).

***In vivo* studies:** A highly sensitive and specific analytical method - liquid chromatography/atmospheric pressure chemical ionization-tandem mass spectrometry, was developed with the limit of quantitation of 0.125 ng/mL for both VLB and DVLB and in both urine and plasma matrices. To the best of authors' knowledge, this was the first analytical method developed to quantify the concentrations of VLB and DVLB simultaneously in plasma and urine samples of dogs. As described previously in humans, the disposition of vinblastine following IV administration was best described by a three-compartmental model (Owellen et al., 1977). However, two compartmental modeling of disposition was also reported in dogs (Creasey et al., 1975). With the increase in body weight, the total clearance of vinblastine per unit body weight had decreased while AUC, a dose dependent parameter had increased with the increase in body weight. Unlike other drugs, AUC correlates with the therapeutic efficacy and toxicity of cancer chemotherapic drugs (Moore and Erlichman, 1987; Calvert et al., 1989; Warmerdam, 1997; Hempel and Boos, 2007). The percent recovery of vinblastine in urine samples was 11.6 ± 2.1 (mean ± SD). These values indicate that approximately 12% of the total dose administered is excreted in the urine. Similar percent recoveries were reported in humans (Owellen et al., 1977). The mechanism of renal excretion of vinblastine was established as renal secretion (de Lannoy et al., 1994). Also, these results support that hepatic metabolism is the major route of metabolism for vinca alkaloids. The *in vivo* vinblastine pharmacokinetic study would have been strengthened by more number of animals with different body weights for a robust allometric equation. However, these studies are proof-of-concept studies to lay foundation for a definitive research in large number of dogs.

***In vitro/in vivo* correlations: C**orrelations between *in vitro* studies and *in vivo* studies in limited sample size are gaining more importance because of their wide applicability. Such correlations would decrease number of live animal studies and increase the speed of pre-clinical drug development process. The percent of accuracy and statistical tests performed to test the predictive

ability of *in vitro* metabolism studies also had given satisfactory results for all three predictive models. In fact, all these predictive models are derived from mass balance relationships. If the predicted value is equal to actual value, then the average fold error would be equal to one. The *afe* would be equal to 2 if the predicted value is within 100% above or 50% below the observed value (Sheiner and Beal, 1981). Similar statistical analysis to evaluate *in vitro* methods were done and an afe value ≤ 2 was considered successful (Obach et al., 1997). Correlation coefficient values were similar for all three predictive models. Based on *afe*, and *rmse* values, the predictive ability of the models is in the order of parallel tube > dispersion model > well-stirred model. Previous work also reported similar results (Ito and Houston, 2004). These studies have clearly shown the applicability of *in vitro* studies in predicting *in vivo* pharmacokinetic parameters successfully.

Clinical applicability

Using the standard equation, $Dose = AUC \cdot CL_{total}$ and by substituting the clearance term with the allometric equation developed in this study as a function of body weight, the dose of vinblastine for a desired therapeutically relevant drug exposure can be accurately calculated: $Dose = AUC \cdot (21.6 \cdot BW^{0.78})$. *In silico* calculations were performed to demonstrate the utility of this novel approach to determine the doses of vinblastine to treat mast cell tumors in dogs. Based on the current dose rate of vinblastine, 2 mg/m^2 to treat mast cell tumors in dogs (Rassnick et al. 2008) and clearance predicted from the novel allometric equations, the drug exposure (AUC) was calculated in a 20 kg body weight dog.

Approximate body surface area in m^2 = (10.1 x (weight in grams)$^{2/3}$)/10000

= (10.1 x (20000) $^{2/3}$)/10000 = 0.74417 m^2

AUC (drug exposure) = Dose / Clearance = (0.744 x 2) / (21.6 x (20$^{0.78}$)) = 0.00666 mg·min/mL

Using this value of drug exposure as target value, doses of vinblastine were calculated using both BSA dosing methodology and new dosing equation. The percent difference between the drug exposure calculated by the current BSA dosing methodology and target drug exposure calculated by the newly developed allometric equation were presented in table 8. As expected, the percent difference of AUC calculated with BSA approach from the target drug exposure was more at the extremes of body weights of dogs. From these values, it could be concluded that smaller dogs are over dosed and larger dogs are under dosed. Therefore, dog breeds, such as boxers, Labrador retrievers, golden retrievers, Schnauzers, and Shar peis which have higher predilection for mast cell tumors are receiving subtherapeutic doses. The newly developed allometric equation for the accurate calculation of doses of vinblastine in dogs to treat mast cell tumors and other responsive modalities is expected to normalize the drug exposure between disparate canine patients. Clinical studies are suggested to test the newly developed dosing equations.

Conclusions

In summary, a robust allometric equation was developed to predict the weight of liver in dogs. For the first time, allometric dependence of density of cytochrome P450 enzymes on body weight was shown in dogs; intrinsic clearance of vinblastine was determined in dogs using substrate depletion approach. Hepatic clearance of vinblastine was predicted using well-stirred model, parallel tube model, and dispersion model with acceptable predictive ability. An allometric equation was developed to determine the value of hepatic clearance of vinblastine in dogs for a given body weight. *In vivo* vinblastine pharmacokinetic studies were conducted to compare the results of *in vitro* studies. *In vitro/in vivo* correlations were established for the hepatic clearance of vinblastine in dogs. A new dosing equation was developed to accurately calculate the doses of vinblastine in dogs.

References

Bagley RSF, J.A (1990) The totally implantable vascular access systems. *The compendium Small Animal* **12:**22-27.

Bradford MM (1976) A rapid and sensitive method for the quantitation of microgram quantities of protein utilizing the principle of protein-dye binding. *Anal Biochem* **72:**248-254.

Cahalane AK, Rassnick KM and Flanders JA (2007) Use of vascular access ports in femoral veins of dogs and cats with cancer. *J Am Vet Med Assoc* **231:**1354-1360.

Calvert AH, Newell DR, Gumbrell LA, O'Reilly S, Burnell M, Boxall FE, Siddik ZH, Judson IR, Gore ME and Wiltshaw E (1989) Carboplatin dosage: prospective evaluation of a simple formula based on renal function. *J Clin Oncol* **7:**1748-1756.

Chiba M, Ishii Y and Sugiyama Y (2009) Prediction of hepatic clearance in human from in vitro data for successful drug development. *AAPS J* **11:**262-276.

Cotman CW and Head E (2008) The canine (dog) model of human aging and disease: dietary, environmental and immunotherapy approaches. *J Alzheimers Dis* **15:**685-707.

Creasey WA, Scott AI, Wei CC, Kutcher J, Schwartz A and Marsh JC (1975) Pharmacological studies with vinblastine in the dog. *Cancer Res* **35:**1116-1120.

Cummings BJ, Head E, Afagh AJ, Milgram NW and Cotman CW (1996a) Beta-amyloid accumulation correlates with cognitive dysfunction in the aged canine. *Neurobiol Learn Mem* **66:**11-23.

Cummings BJ, Head E, Ruehl W, Milgram NW and Cotman CW (1996b) The canine as an animal model of human aging and dementia. *Neurobiol Aging* **17:**259-268.

Damen CW, Lagas JS, Rosing H, Schellens JH and Beijnen JH (2009) The bioanalysis of vinorelbine and 4-O-deacetylvinorelbine in human and mouse plasma using high-performance liquid chromatography coupled with heated electrospray ionization tandem mass-spectrometry. *Biomed Chromatogr* **23:**1316-1325.

Damen CW, Rosing H, Schellens JH and Beijnen JH (2010) High-performance liquid chromatography coupled with mass spectrometry for the quantitative analysis of vinca-alkaloids in biological matrices: a concise survey from the literature. *Biomed Chromatogr* **24:**83-90.

de Lannoy IA, Mandin RS and Silverman M (1994) Renal secretion of vinblastine, vincristine and colchicine in vivo. *J Pharmacol Exp Ther* **268:**388-395.

Dobson JM and Scase TJ (2007) Advances in the diagnosis and management of cutaneous mast cell tumours in dogs. *J Small Anim Pract* **48:**424-431.

Galis F, Van der Sluijs I, Van Dooren TJ, Metz JA and Nussbaumer M (2007) Do large dogs die young? *J Exp Zool B Mol Dev Evol* **308:**119-126.

Hanna SS (1984) Measurement of liver blood flow by galactose clearance. *Can J Surg* **27:**218-220.

Hempel G and Boos J (2007) Flat-fixed dosing versus body surface area based dosing of anticancer drugs: there is a difference. *Oncologist* **12:**924-926.

Henry CJ, Russell LE, Tyler JW, Buss MS, Seguin B, Cambridge AJ and Moore ME (2002) Comparison of hematologic and biochemical values for blood samples obtained via jugular venipuncture and via vascular access ports in cats. *J Am Vet Med Assoc* **220:**482-485.

Houston JB and Carlile DJ (1997) Prediction of hepatic clearance from microsomes, hepatocytes, and liver slices. *Drug Metab Rev* **29:**891-922.

Ito K and Houston JB (2004) Comparison of the use of liver models for predicting drug clearance using in vitro kinetic data from hepatic microsomes and isolated hepatocytes. *Pharm Res* **21:**785-792.

Jackson B and Cappiello VP (1964) Ranges of Normal Organ Weights of Dogs. *Toxicol Appl Pharmacol* **6:**664-668.

Johannesen KA and DePierre JW (1978) Measurement of cytochrome P-450 in the presence of large amounts of contaminating hemoglobin and methemoglobin. *Anal Biochem* **86:**725-732.

Kiupel M, Webster JD, Bailey KL, Best S, DeLay J, Detrisac CJ, Fitzgerald SD, Gamble D, Ginn PE, Goldschmidt MH, Hendrick MJ, Howerth EW, Janovitz EB, Langohr I, Lenz SD, Lipscomb TP, Miller MA, Misdorp W, Moroff S, Mullaney TP, Neyens I, O'Toole D, Ramos-Vara J, Scase TJ, Schulman FY, Sledge D, Smedley RC, Smith K, P WS, Southorn E, Stedman NL, Steficek BA, Stromberg PC, Valli VE, Weisbrode SE, Yager J, Heller J and Miller R Proposal of a 2-tier histologic grading system for canine cutaneous mast cell tumors to more accurately predict biological behavior. *Vet Pathol* **48:**147-155.

Komura H, Kawase A and Iwaki M (2005) Application of substrate depletion assay for early prediction of nonlinear pharmacokinetics in drug discovery: assessment of nonlinearity of metoprolol, timolol, and propranolol. *J Pharm Sci* **94:**2656-2666.

Laflamme DP (1997) Development and Validation of a Body Condition Score System for Dogs. *Canine Practice* **22:**10-15.

Lutzen L, Trieb G and Pappritz G (1976) Allometric analysis of organ weights: II. Beagle dogs. *Toxicol Appl Pharmacol* **35:**543-551.

Matsubara T, Koike M, Touchi A, Tochino Y and Sugeno K (1976) Quantitative determination of cytochrome P-450 in rat liver homogenate. *Anal Biochem* **75:**596-603.

Moore MJ and Erlichman C (1987) Therapeutic drug monitoring in oncology. Problems and potential in antineoplastic therapy. *Clin Pharmacokinet* **13:**205-227.

Nath A and Atkins WM (2006) A theoretical validation of the substrate depletion approach to determining kinetic parameters. *Drug Metab Dispos* **34:**1433-1435.

Obach RS (2011) Predicting clearance in humans from in vitro data. *Curr Top Med Chem* **11:**334-339.

Obach RS, Baxter JG, Liston TE, Silber BM, Jones BC, MacIntyre F, Rance DJ and Wastall P (1997) The prediction of human pharmacokinetic parameters from preclinical and in vitro metabolism data. *J Pharmacol Exp Ther* **283:**46-58.

Obach RS and Reed-Hagen AE (2002) Measurement of Michaelis constants for cytochrome P450-mediated biotransformation reactions using a substrate depletion approach. *Drug Metab Dispos* **30:**831-837.

Omura T and Sato R (1964a) The Carbon Monoxide-Binding Pigment of Liver Microsomes. I. Evidence for Its Hemoprotein Nature. *J Biol Chem* **239:**2370-2378.

Omura T and Sato R (1964b) The Carbon Monoxide-Binding Pigment of Liver Microsomes. II. Solubilization, Purification, and Properties. *J Biol Chem* **239:**2379-2385.

Owellen RJ, Hartke CA and Hains FO (1977) Pharmacokinetics and metabolism of vinblastine in humans. *Cancer Res* **37:**2597-2602.

Pang KS and Rowland M (1977) Hepatic clearance of drugs. I. Theoretical considerations of a "well-stirred" model and a "parallel tube" model. Influence of hepatic blood flow, plasma and blood cell binding, and the hepatocellular enzymatic activity on hepatic drug clearance. *J Pharmacokinet Biopharm* **5:**625-653.

Parker VJ and Freeman LM (2011) Association between Body Condition and Survival in Dogs with Acquired Chronic Kidney Disease. *J Vet Intern Med* **25:**1306-1311.

Patnaik AK, Ehler WJ and MacEwen EG (1984) Canine cutaneous mast cell tumor: morphologic grading and survival time in 83 dogs. *Vet Pathol* **21:**469-474.

Patronek GJ, Waters DJ and Glickman LT (1997) Comparative longevity of pet dogs and humans: implications for gerontology research. *J Gerontol A Biol Sci Med Sci* **52:**B171-178.

Porter RK (2001) Allometry of mammalian cellular oxygen consumption. *Cell Mol Life Sci* **58:**815-822.

Prentis RA, Lis Y and Walker SR (1988) Pharmaceutical innovation by the seven UK-owned pharmaceutical companies (1964-1985). *Br J Clin Pharmacol* **25:**387-396.

Prothero JW (1982) Organ scaling in mammals: the liver. *Comp Biochem Physiol A Comp Physiol* **71:**567-577.

Rassnick KM, Bailey DB, Flory AB, Balkman CE, Kiselow MA, Intile JL and Autio K (2008) Efficacy of vinblastine for treatment of canine mast cell tumors. *J Vet Intern Med* **22:**1390-1396.

Reber EF, Malhotra OP, Simon J, Kreier JP, Beamer PD and Norton HW (1961) The effects of feeding irradiated flour to dogs. II. Reproduction and pathology. *Toxicol Appl Pharmacol* **3:**568-573.

Robat C, London C, Bunting L, McCartan L, Stingle N, Selting K, Kurzman I and Vail DM Safety evaluation of combination vinblastine and toceranib phosphate (Palladia(R)) in dogs: a phase I dose-finding study(*). *Vet Comp Oncol*.

Schneider WC (1948) Intracellular distribution of enzymes; the oxidation of octanoic acid by rat liver fractions. *J Biol Chem* **176:**259-266.

Sheiner LB and Beal SL (1981) Some suggestions for measuring predictive performance. *J Pharmacokinet Biopharm* **9:**503-512.

Smith R, Jones RD, Ballard PG and Griffiths HH (2008) Determination of microsome and hepatocyte scaling factors for in vitro/in vivo extrapolation in the rat and dog. *Xenobiotica* **38:**1386-1398.

Speakman JR, van Acker A and Harper EJ (2003) Age-related changes in the metabolism and body composition of three dog breeds and their relationship to life expectancy. *Aging Cell* **2:**265-275.

Steward A, Allott PR and Mapleson WW (1975) Organ weights in the dog. *Res Vet Sci* **19:**341-342.

Stringer RA, Strain-Damerell C, Nicklin P and Houston JB (2009) Evaluation of recombinant cytochrome P450 enzymes as an in vitro system for metabolic clearance predictions. *Drug Metab Dispos* **37:**1025-1034.

Studzinski CM, Christie LA, Araujo JA, Burnham WM, Head E, Cotman CW and Milgram NW (2006) Visuospatial function in the beagle dog: an early marker of cognitive decline in a model of human aging and dementia. *Neurobiol Learn Mem* **86:**197-204.

Thamm DH, Mauldin EA and Vail DM (1999) Prednisone and vinblastine chemotherapy for canine mast cell tumor--41 cases (1992-1997). *J Vet Intern Med* **13:**491-497.

Trim PJ, Henson CM, Avery JL, McEwen A, Snel MF, Claude E, Marshall PS, West A, Princivalle AP and Clench MR (2008) Matrix-assisted laser desorption/ionization-ion mobility separation-mass spectrometry imaging of vinblastine in whole body tissue sections. *Anal Chem* **80:**8628-8634.

van den Bongard HJ, Mathot RA, Beijnen JH and Schellens JH (2000) Pharmacokinetically guided administration of chemotherapeutic agents. *Clin Pharmacokinet* **39:**345-367.

Warmerdam VL (1997) Tailor-made chemotherapy for cancer patients. *Netherlands Journal of Medicine* **51:**30-35.

Welle MM, Bley CR, Howard J and Rufenacht S (2008) Canine mast cell tumours: a review of the pathogenesis, clinical features, pathology and treatment. *Vet Dermatol* **19:**321-339.

Yamaoka K, Nakagawa T and Uno T (1978) Application of Akaike's information criterion (AIC) in the evaluation of linear pharmacokinetic equations. *J Pharmacokinet Biopharm* **6:**165-175.

		Allometric	3.5% of body weight
Liver	Juvenile	3.8	11.4
	Adult	8.1	8.5
	Total	11.9	19.9

Table 1. Sum of absolute residual errors from predictions of liver weights using newly developed allometric equation and 3.5% fixed proportion of body weight in the training data set *per se*.

		Allometric	3.5% of body weight
Liver	Juvenile	1.7	2.7
	Adult	7.1	6.6
	Total	8.8	9.2

Table 2. Sum of absolute residual errors from predictions of liver weights using the newly developed allometric equation and 3.5 % fixed proportion of body weight in the validation data set.

Animal ID	CO difference spectra	Dithionate difference spectra	Ascorbate reduced dithionate difference spectra	Ascorbate and PES reduced dithionate difference spectra
B3040	**20.5 ± 1.2**	17.7 ± 0.8	**19.1 ± 0.8**	17.3 ± 0.4
7950	**17.7 ± 0.4**	16.2 ± 0.6	**17.3 ± 0.2**	16.1 ± 0.2
55-82-91	**21.2 ± 0.6**	20.7 ± 0.6	**19.6 ± 0.8**	19.3 ± 0.4

Table 3. The cytochrome P450 density determined in duplicate in non-hemoglobin contaminated microsomal samples by four methods revealed that the carbon monoxide difference spectra and ascorbate reduced dithionate difference spectra had given similar values (see figures 5 and 8).

Animal ID	CO difference spectra	Dithionate difference spectra	Ascorbate reduced dithionate difference spectra	Ascorbate and PES reduced dithionate difference spectra
08OKC51	16.7 ± 1.5	**21.3 ± 0.2**	**20.1 ± 1.4**	18.3 ± 0.7
08OK52	10.5 ± 0.3	**15.8 ± 0.4**	**15.8 ± 1.2**	14.3 ± 0.1
08OKC84	10.3 ± 0.4	**11.3 ± 0.1**	**10.4 ± 0.8**	10.0 ± 0.1

Table 4. The cytochrome P450 density in microsomal samples contaminated with hemoglobin was also compared by all four methods. Dithionate difference spectra and dithionate difference spectra reduced with ascorbic acid had similar values to one another without interference from the P420 peak (see figures 7 and 8).

Body weight (kg)	**10.6**	**11.3**	**43**	**54**
K10 (1/hr)	1.0	0.9	0.52	0.51
alpha_HL (hr)	0.02	0.02	0.04	0.01
beta_HL (hr)	0.45	0.37	0.4	0.81
gamma_HL(hr)	19	16	20	29
Cmax (ng/mL)	106	75	76.75	64.45
Vss (mL/kg)	18039	18817	13234	23719
CL (mL/hr/kg)	703	858	508	598
AUC (ng.hr/mL)	107	87	148	125
AUMC (ng.hr.hr/mL)	2735.9	1918.2	3842	4980
MRT (hr)	25.65	21.94	26	40

Observed maximum plasma concentration (C_{max}), Elimination rate constant (K10), half - life of rapid distribution phase (Alpha_HL), half – life of slow distribution phase (Beta_HL), half-life of elimination phase (Gamma_HL), Volume of distribution at steady state (V_{ss}), Plasma clearance (CL), Area under the curve from administration to infinity (AUC), Area under moment curve (AUMC), Mean residence time (MRT)

Table 5. Important pharmacokinetic parameters (mean ± SD) of vinblastine estimated by compartmental analysis in four adult male dogs (10 -54 kg) after an intravenous bolus administration of vinblastine sulfate at the dose rate of 0.075 mg/kg.

Body weight (kg)	Actual hepatic clearance (mL/min)	Well-stirred (mL/min)	Parallel tube (mL/min)	Dispersion (mL/min)
11.3	148.47	111 (-25%)	131 (-12%)	124 (-17%)
10.6	110.47	106 (-3.9%)	125 (13%)	118 (7%)
43	324.41	291 (-10%)	325 (0.2%)	311 (-4%)
53.64	447.67	341 (-24%)	378 (-16%)	363 (-19%)

Table 6. Table showing the actual hepatic clearance of vinblastine measured in four adult male dogs (10 - 54) and predictive ability of three predictive models. Out of three predictive models, parallel tube model had predicted hepatic clearance with less % difference from the observed values.

	Well-stirred model	Parallel tube model	Dispersion model
afe	1.19	1.03	1.08
rmse	1.96	1.20	1.35
r^2	0.85	0.85	0.85

Table 7. Statistical data comparing the accuracy of predictions with the three predictive models. All three models have predicted hepatic clearance with acceptable statistics. However, parallel tube model had predicted better than other two models.

BW	clearance	Dose (allometric)	Dose (allometric)	BSA	Dose (BSA)	Dose (BSA)	AUC (BSA)	% diff
kg	mL/min/kg	mg	mg/kg	m^2	2 mg/m^2	mg/kg	mg.min /mL	
0.9	22.1	0.1	0.15	0.09	0.19	0.21	0.0095	42.1
5	15.2	0.5	0.10	0.30	0.59	0.12	0.0078	17.0
10.6	12.8	0.9	0.09	0.49	0.97	0.09	0.0072	7.5
11.3	12.7	1.0	0.08	0.51	1.02	0.09	0.0071	6.7
20	11.2	1.5	0.07	0.74	1.49	0.07	0.0067	0.0
43	9.4	2.7	0.06	1.24	2.48	0.06	0.0061	-8.3
53.6	9.0	3.2	0.06	1.44	2.87	0.05	0.0060	-10.6
60	8.8	3.5	0.06	1.55	3.10	0.05	0.0059	-11.7
90	8.0	4.8	0.05	2.03	4.06	0.05	0.0056	-15.7

Table 8. Comparison of current BSA dosing methodology and newly developed allometric equation. Drug exposure calculated using BSA dosing approach was compared with the target drug exposure (0.00667 mg.min/mL) calculated in a 20 kg body weight dog. The percent difference of AUC calculated with BSA dosing approach was more pronounced at the extremes of body weights of dogs.

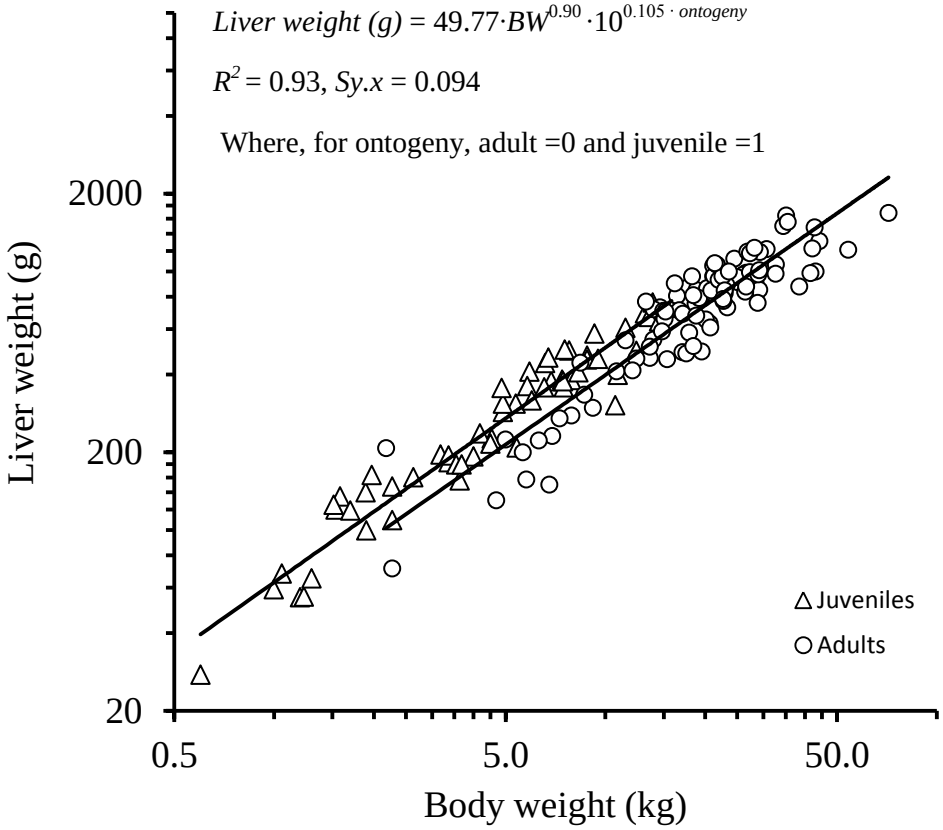

Figure 1. Intraspecific allometry of liver weights in dogs. The data was collected from a total of 160 dogs (58 juveniles and 102 adults). Log_{10} transformed liver weights were regressed against log_{10} transformed body weights. The liver weight allometrically related to body weight and ontogeny as: $Liver\ weight\ (g) = 49.77 \cdot BW^{0.90} \cdot 10^{0.105 \cdot ontogeny}$ R^2 =0.93, *Sy.x* = 0.094, Where, for ontogeny, adult =0 and juvenile =1

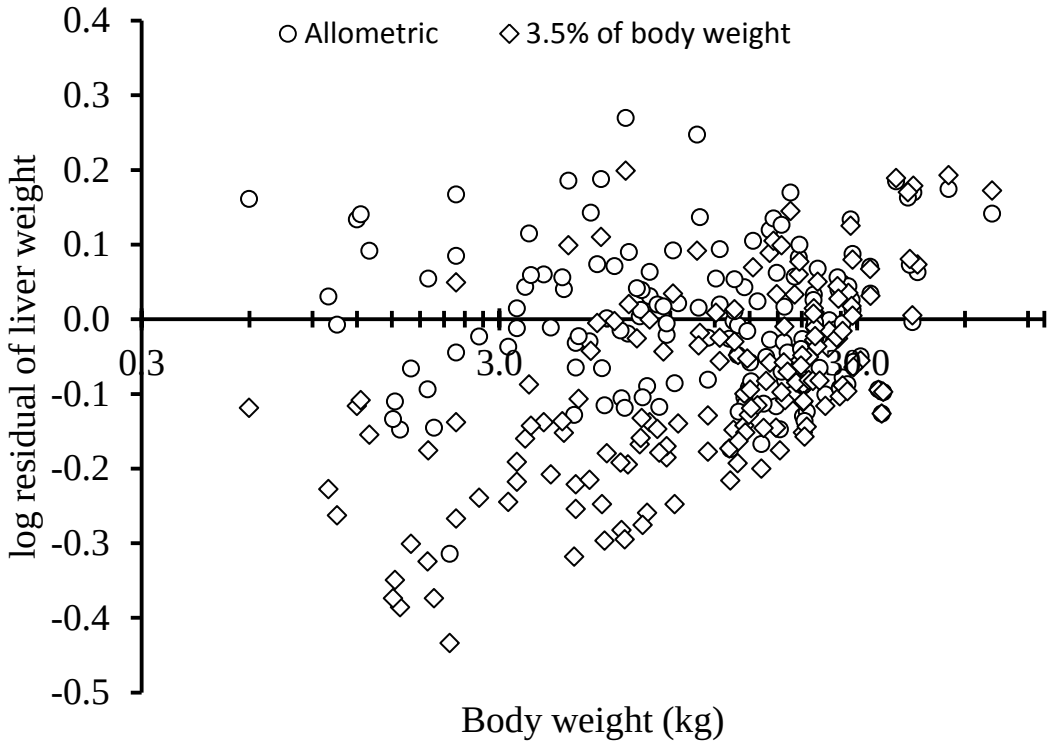

Figure 2. The residuals of $\log_{10}$ transformed liver weights predicted with newly developed allometric equation and 3.5% fixed proportion of body weights were plotted against body weights in the training data set *per se*.

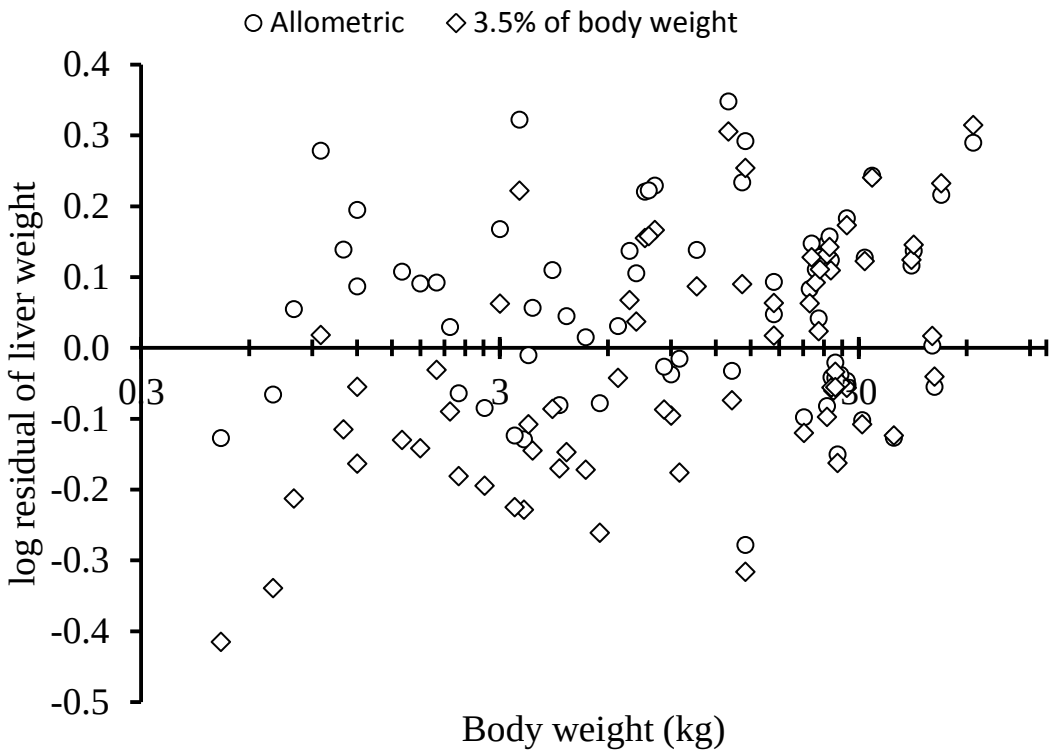

Figure 3. The residuals of $\log_{10}$ transformed liver weights predicted with newly developed allometric equation and 3.5% fixed proportion of body weights were plotted against body weights in the validation data set.

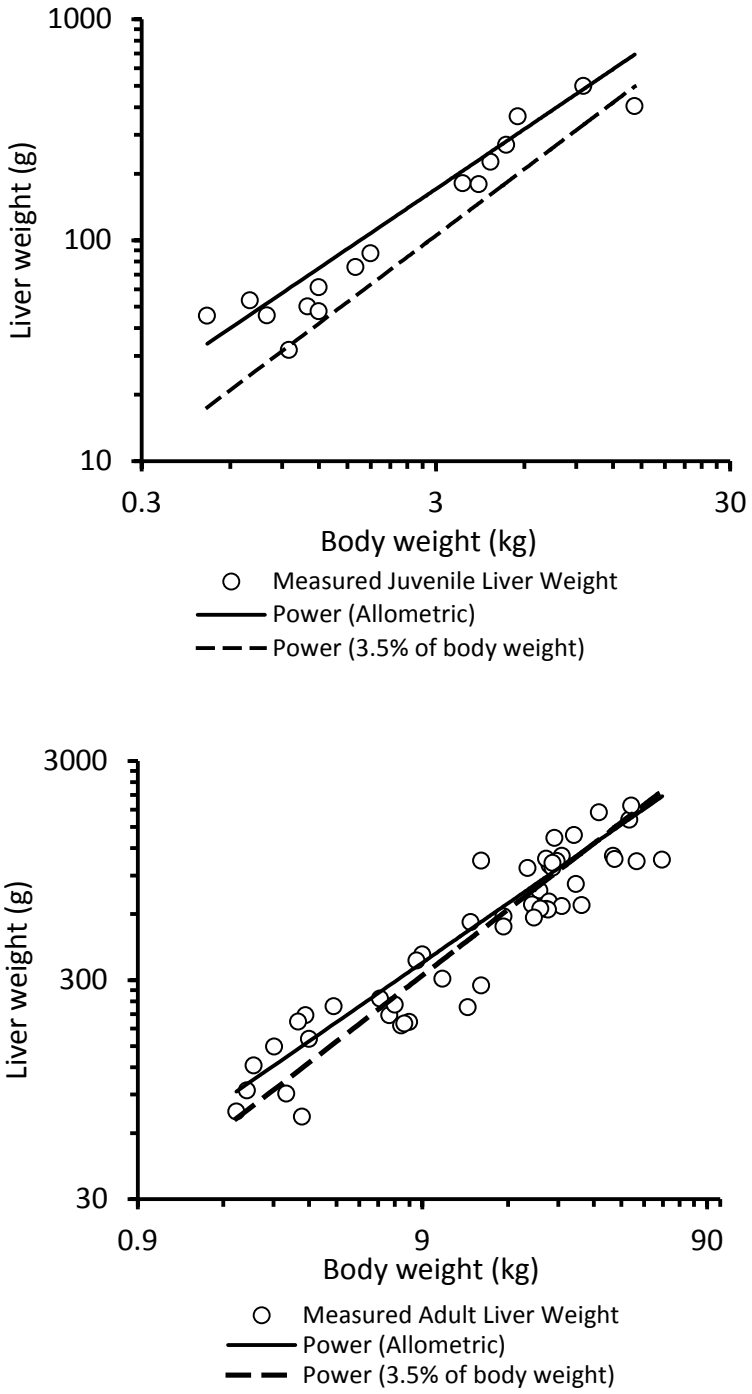

Figure 4. Scatter plots of measured liver weight (g) against body weight (kg) of validation data set. The solid line indicates the regression line of predicted liver weight using the newly developed allometric equation. The dashed line indicates predicted liver weights as 3.5% fixed proportion of body weight.

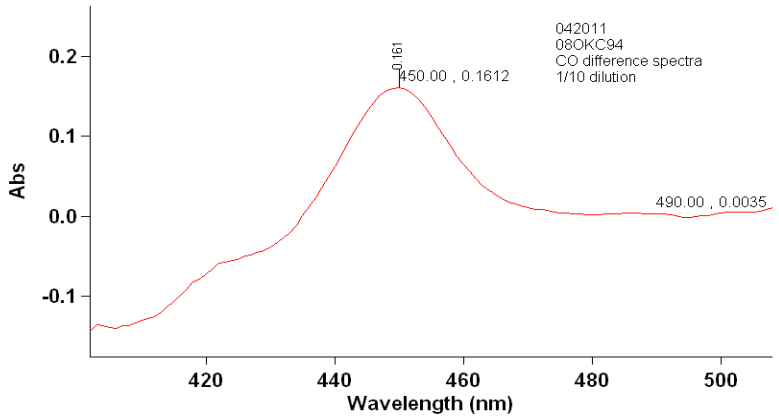

Figure 5. A representative spectrophotograph showing the peak at 450 nm with carbon monoxide difference spectrum.

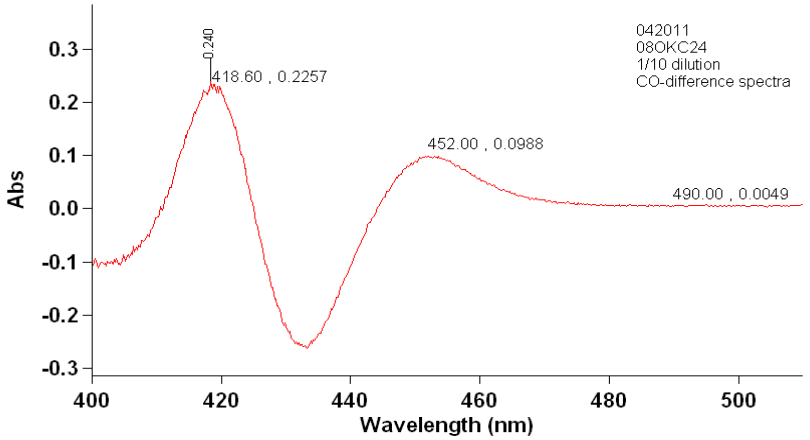

Figure 6. A representative spectrophotograph showing the obscured peak at 450 nm and a more pronounced peak at 419 nm in hemoglobin contaminated microsomal sample using carbon monoxide difference spectrum.

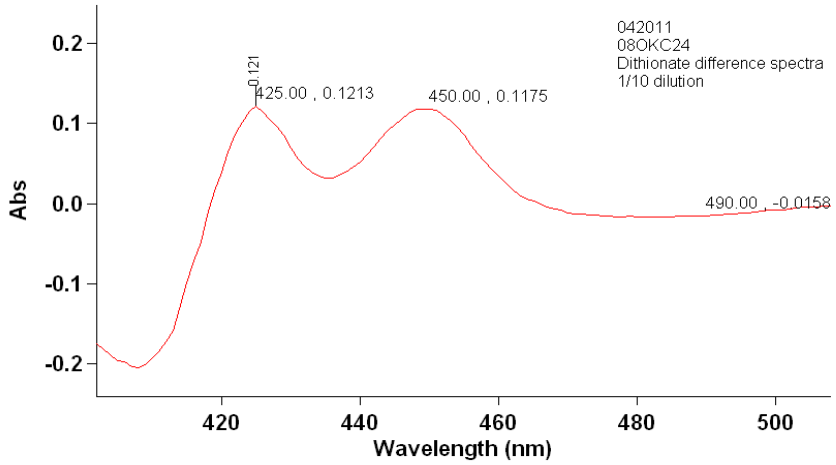

Figure 7. A representative spectrophotograph showing the reduced peak at 425 nm without affecting peak at 450 nm in hemoglobin contaminated microsomal sample using dithionate difference spectra.

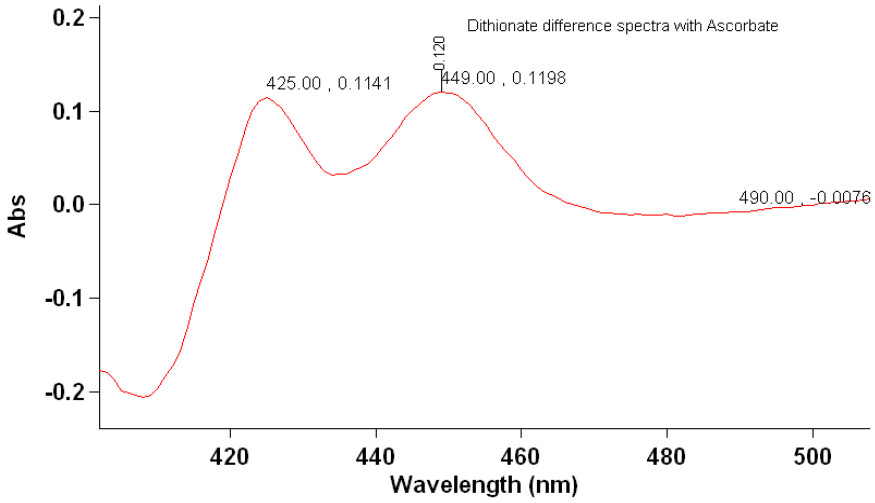

Figure 8. A representative spectrophotograph showing the reduced peak at 425 nm without affecting peak at 450 nm in hemoglobin contaminated microsomal sample using ascorbate reduced dithionate difference spectra.

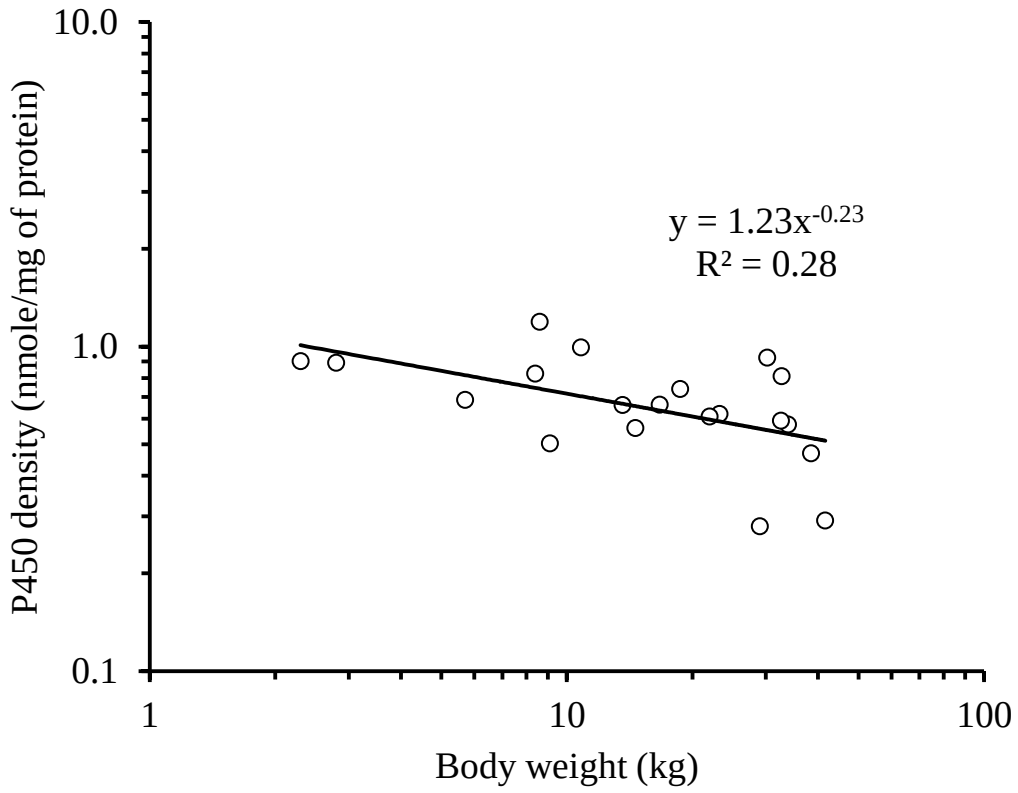

Figure 9. Scatter plot showing the allometric relationship between cytochrome P450 density (nmole/mg of protein) and body weight (kg). With the increase in body weight, the density of cytochrome P450 enzymes had decreased ($p<0.05$).

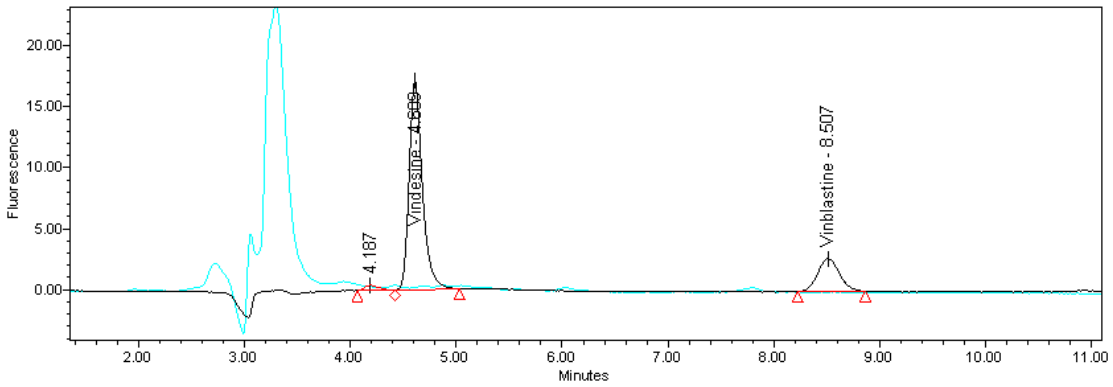

Figure 10. A representative chromatogram of vinblastine incubate sample overlaid on blank microsomal sample.

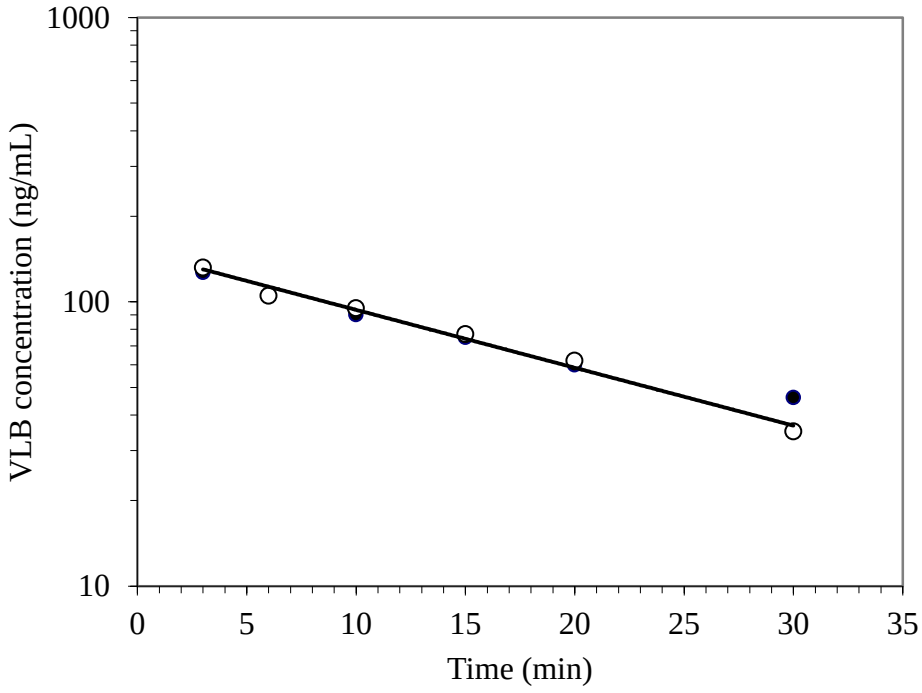

Figure 11. A representative substrate depletion profile of vinblastine in hepatic microsomes in duplicate.

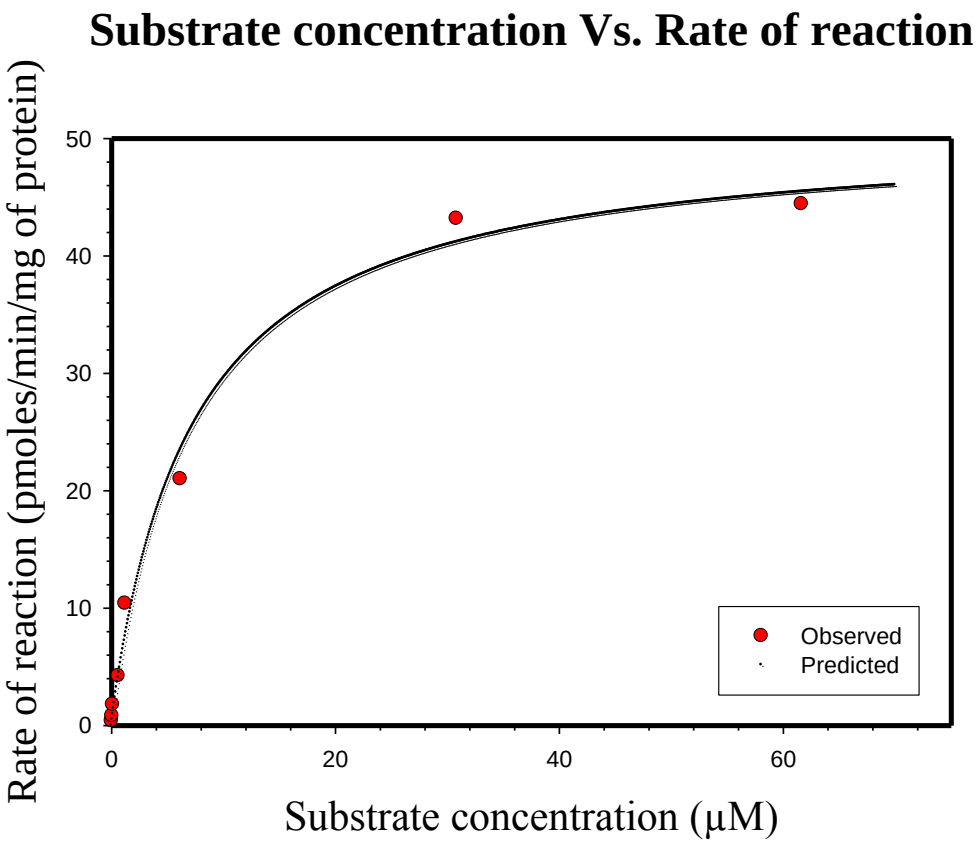

Figure 12. A representative model fitting of substrate depletion approach data of vinblastine microsomal incubations similar to Michaelis-Menten enzyme kinetics. The rate of reaction had increased with the increase in the substrate concentration reaching the theoretical maximum rate of reaction (V_{max}).

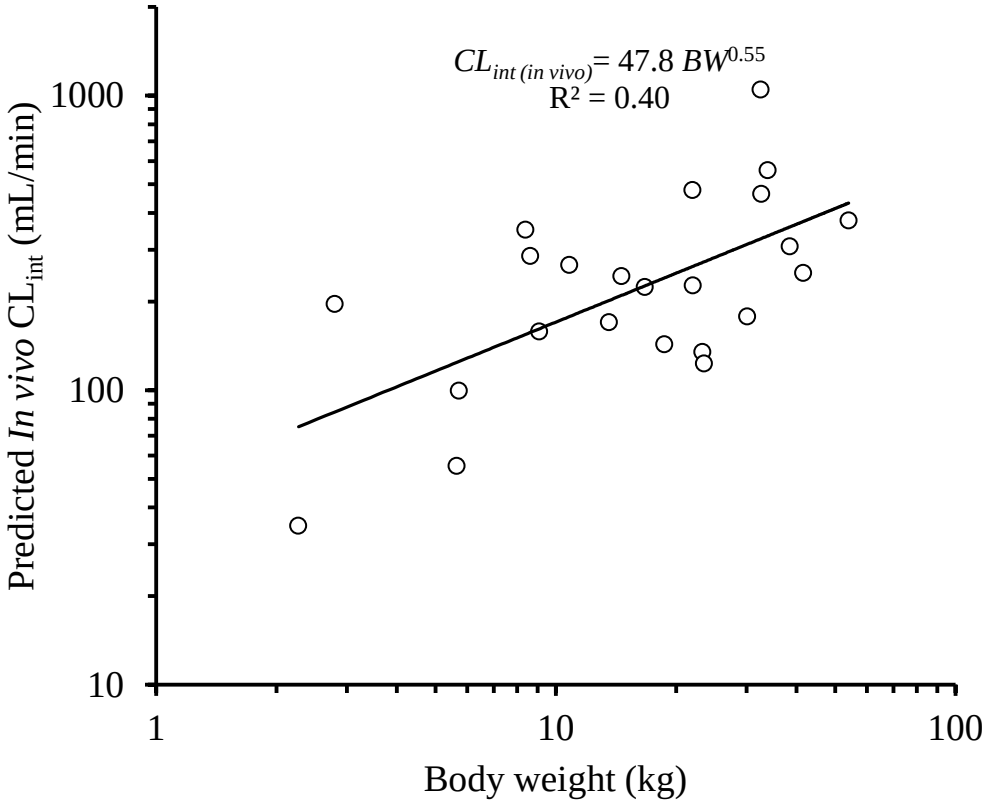

Figure 13. Scatter plot showing the allometric relationship between body weight (kg) and predicted *in vivo* intrinsic clearance of vinblastine (mL/min/kg) on logarithmic coordinates. With the increase in body weight, the *in vivo* CL_{int} had decreased ($p<0.05$).

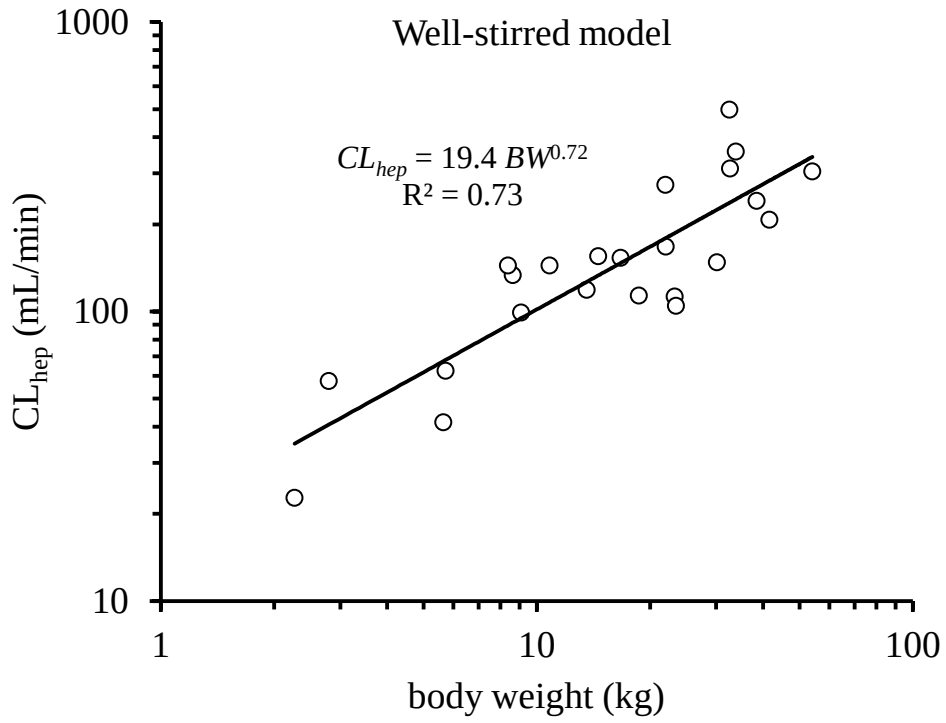
Well-stirred model
CL_{hep} = 19.4 $BW^{0.72}$
R² = 0.73
1000
100
10
CL_{hep} (mL/min)
1
10
100
body weight (kg)

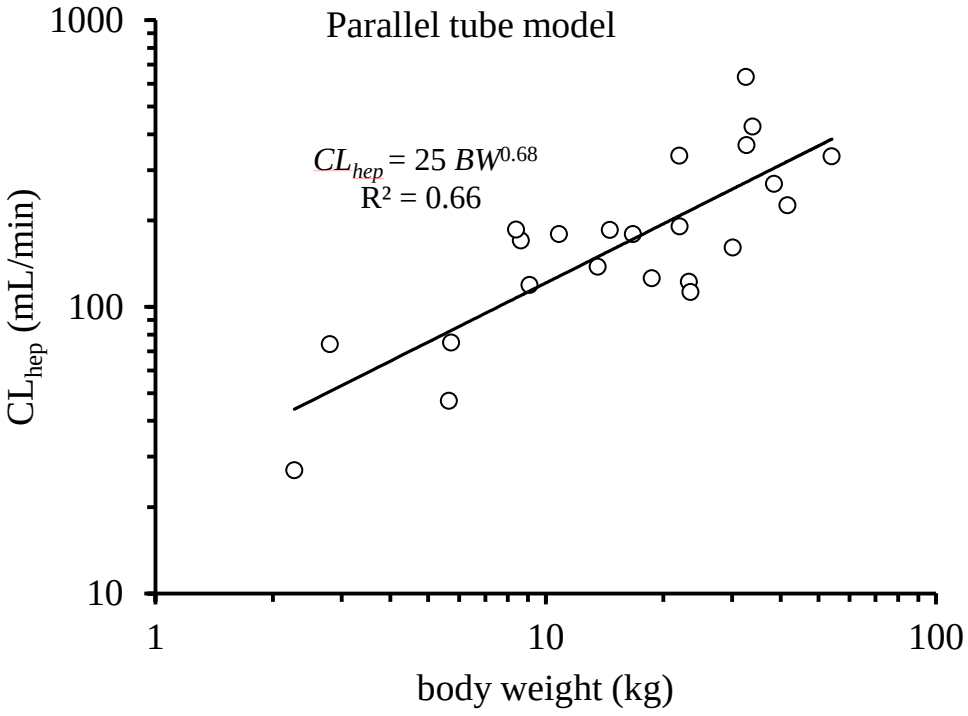
Parallel tube model
CL_{hep} = 25 $BW^{0.68}$
R² = 0.66
1000
100
10
CL_{hep} (mL/min)
1
10
100
body weight (kg)

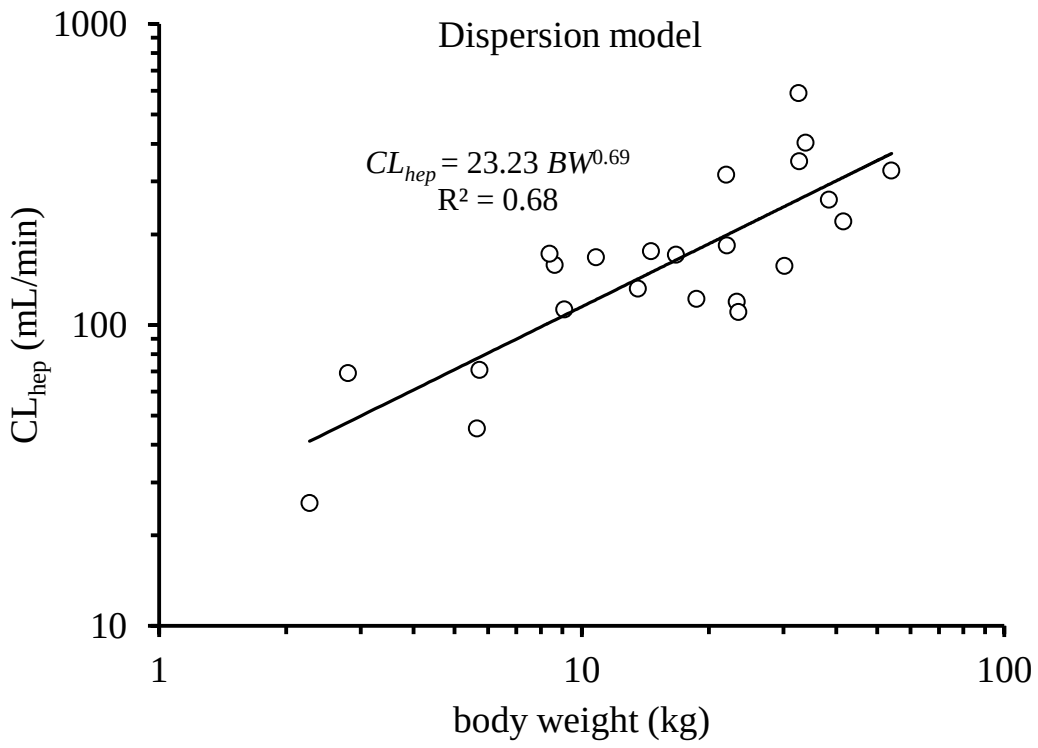

Figure 14. Scatter plots showing the allometric relationship between hepatic clearances of vinblastine (mL/min) predicted *in vitro* using well-stirred model (equation 1), parallel tube model (equation 2), and dispersion model (equation 3) and body weight (kg) on logarithmic coordinates. With the increase in body weight, the hepatic clearance of vinblastine per unit body weight determined *in vitro* had decreased ($p<0.05$).

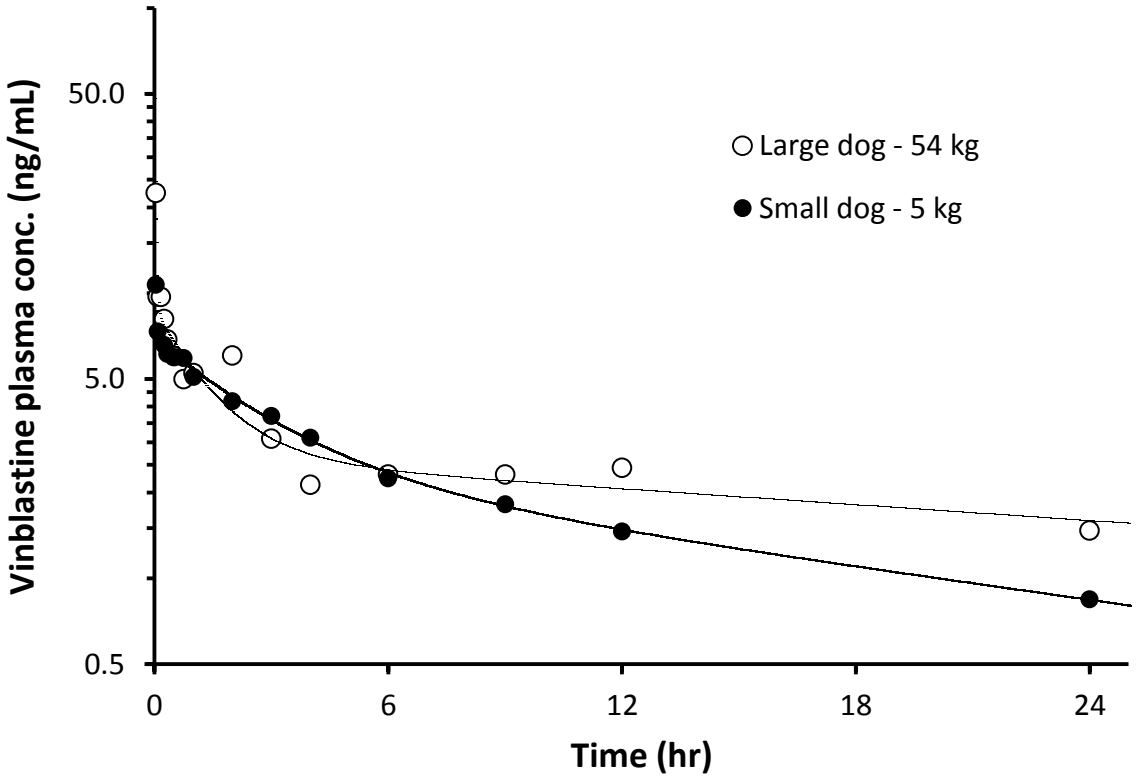

Figure 15: A representative 3-compartmental model fitting of vinblastine in a 54 kg body weight adult and 5 kg body weight juvenile dog following intravenous bolus administration of vinblastine at the rate of 0.075 mg/kg. Circles represent observed concentrations and dots indicate predicted vinblastine concentrations.

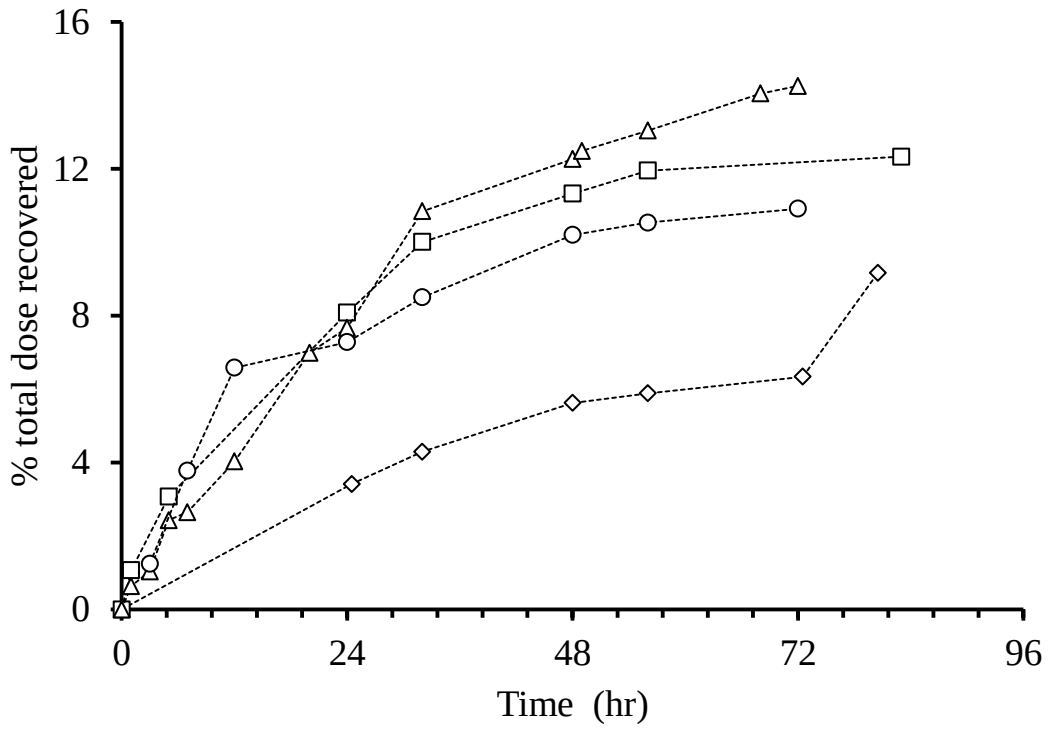

Figure 16. Excretion of vinblastine in urine following an intravenous dose of 0.075 mg/kg vinblastine. The percent recovery of vinblastine in urine was 11.6 ± 2.1 (mean ± SD) out of total dose administered.

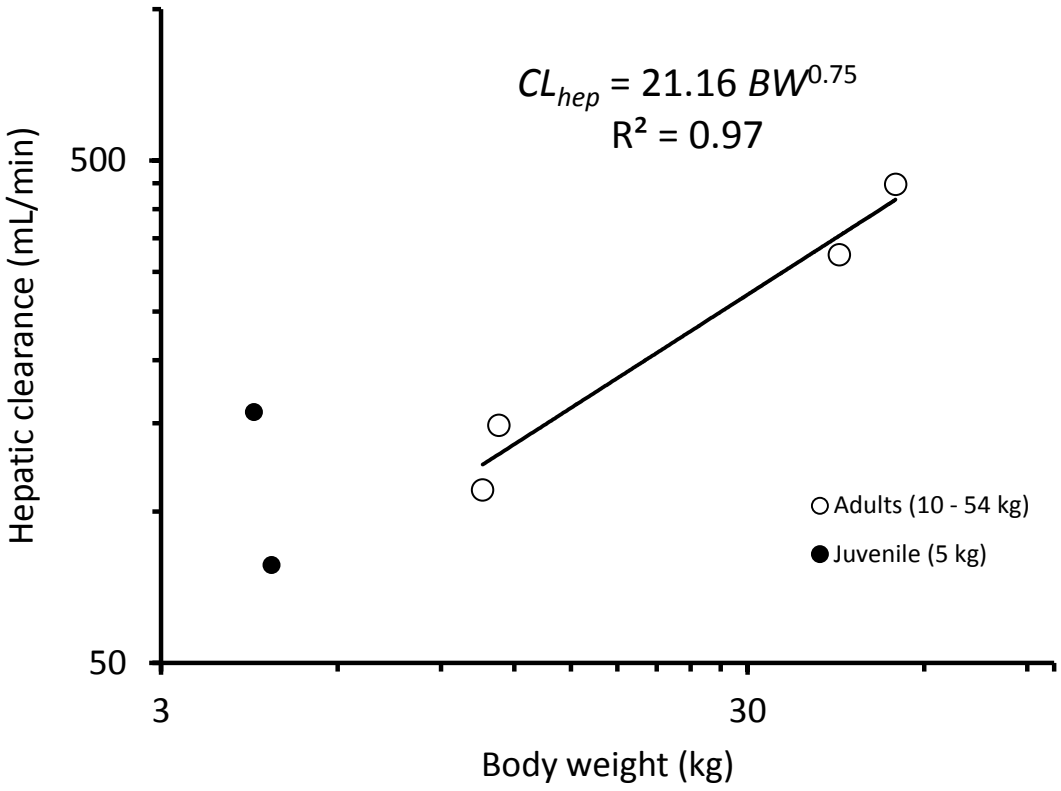

Figure 17. Scatter plot showing the allometric relationship between hepatic clearance of vinblastine determined in four adult male dogs (10 - 54 kg) and body weight (kg). With the increase in body weight, the hepatic clearance of vinblastine per unit body weight had decreased.

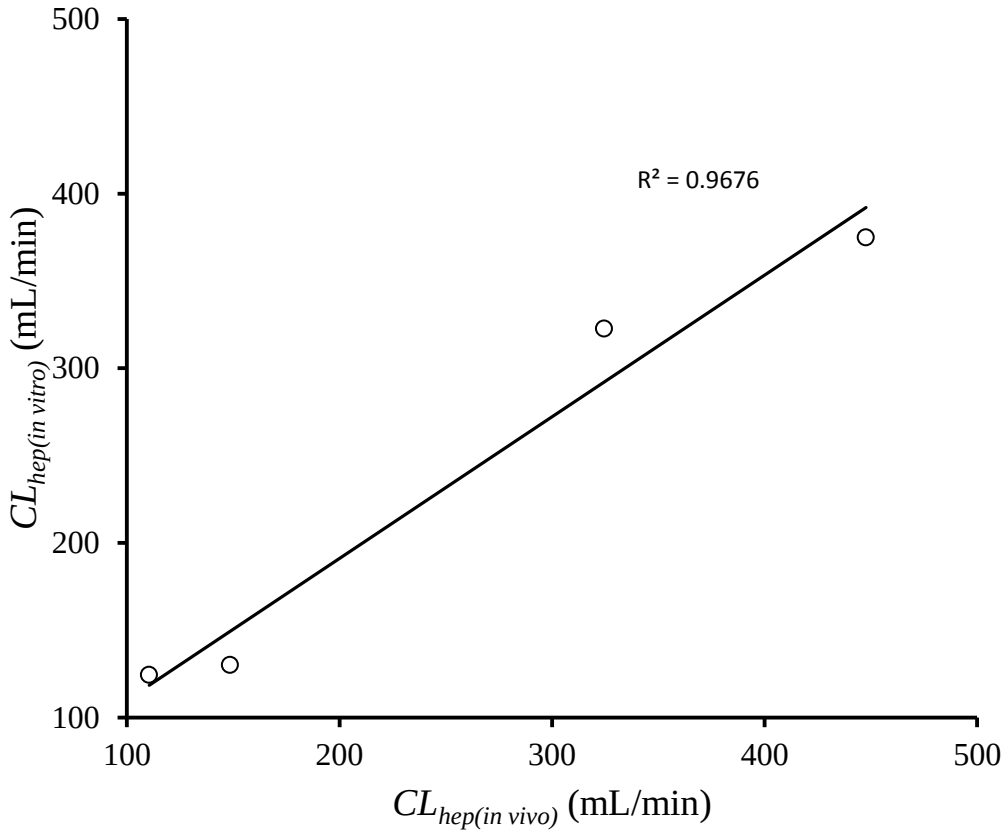

Figure 18. Correlation between hepatic clearances of vinblastine determined *in vivo* in four adult male intact dogs (10 – 54 kg) and *in vitro* hepatic clearance of vinblastine determined by the allometric equation of parallel tube model (figure 14). An R^2 value of 0.97 indicates good predictive ability of the *in vitro* method to predict the hepatic clearance of vinblastine in dogs.

CHAPTER V

SIMULTANEOUS QUANTIFICATION OF VINBLASTINE AND DESACETYLVINBLASTINE CONCENTRATIONS IN CANINE PLASMA AND URINE SAMPLES USING LC/APCI-MS/MS

Abstract

A highly sensitive and specific liquid chromatography-atmospheric pressure chemical ionization-mass spectrometry (LC/APCI-MS/MS) method has been developed and validated for simultaneous quantification of vinblastine and its metabolite, desacetylvinblastine, in canine plasma and urine samples. Plasma and urine samples were processed by a solid phase extraction procedure. The optimal chromatographic behavior of these analytes was achieved on pentafluorophenyl (PFP) propyl analytical column (5 μm, 50 x 2.1 mm) under isocratic elution of 0.75 mL/min with a mobile phase of 5 mM ammonium acetate and methanol. The samples were analyzed in positive ion, multiple reaction monitoring mode. The calibration curves were linear over 0.125 - 2 ng/mL (lower calibration curve); 2 - 100 ng/mL (higher calibration curve) and 0.125 - 5 ng/mL for vinblastine and desacetylvinblastine in plasma, and over 1 - 2000 ng/mL and 0.5 - 100 ng/mL for vinblastine and desacetylvinblastine in urine samples, respectively. The limits of quantitation of vinblastine and desacetylvinblastine were 0.125 ng/mL in both matrices. The intra- and inter-day accuracy was above 89% and precision below 8.6% for both analytes in both matrices. The developed method was successfully applied to ongoing *in vivo* vinblastine pharmacokinetic studies in dogs.

Keywords: vinblastine, desacetylvinblastine, vinorelbine, dog, LC/MS/MS, analysis

Introduction

Vinblastine (vincaleucobastine; VLB) is a vinca alkaloid isolated from dicotyledonous Madagascar periwinkle plant, *Catharanthus roseus* (family: Apocyanaceae). Vinblastine was the first vinca alkaloid isolated and has been used for the treatment of soft tissue tumors both in human and veterinary medicine as a single agent or in combination with other anticancer drugs. 4-O-desacetylvinblastine (DVLB) is a human metabolite of vinblastine that is itself considered to be a potent and active anticancer xenobiotic (Owellen et al., 1977) . Vinca alkaloids work by

binding to beta-tubulin and preventing the formation of microtubules during mitosis, thereby arresting cell division (Gan and Kavallaris, 2008; Kavallaris et al., 2008; Cheng et al., 2009). Vinca alkaloids were also shown to inhibit angiogenesis (Pasquier and Kavallaris, 2008). In order to increase the therapeutic utility or decrease the potential for toxic side effects, semi-synthetic vinca alkaloids, such as vinflunine, vindesine sulfate and vinorelbine (VRB) were developed. Although all of these vinca alkaloids share common features in structure and affinity to microtubules, there is variability in their therapeutic efficiency, therapeutic indications, and toxicities (Damen et al., 2009). Currently, toxicity adjusted dosing is the most accepted method of dose adjustment for vinblastine administration in dogs (Rassnick et al., 2008; Welle et al., 2008). A variety of methods, including radioimmunoassay and high performance liquid chromatography (HPLC) coupled with ultraviolet (UV), fluorescence, or electrochemical detection have been used to quantify vinblastine concentrations in biological matrices (van Tellingen et al., 1991; van Tellingen et al., 1993; Gupta et al., 2005; Puozzo et al., 2007). A reversed phase - HPLC/fluorescence method was successfully developed in this laboratory for the analysis of *vinca* alkaloids with a maximal sensitivity of 1 ng/mL. Incurred sample analysis indicated the need of even higher sensitive method below 1 ng/mL. To the best of authors' knowledge, there are no published reports on highly sensitive and specific analytical methods to quantify the concentrations of vinblastine and desacetylvinblastine in the biological matrices of dog. The literature indicated successful liquid chromatography tandem mass spectrometry (LC/MS/MS) methods below this level (Ramirez et al., 1997), so this laboratory began pursuing an LC/MS/MS method based on a previously published method to measure vinorelbine (Niwa and Kawashiro). In LC/MS/MS, monitoring precursor drug mass and product ion fragment mass gives high specificity in the quantitation of a drug. Sensitivity of the LC/MS/MS is also higher than other analytical methods. The use of LC/MS/MS is becoming more prevalent in drug metabolism and *in vitro* screening of new chemical entities (NCEs) in drug development process because of its high sensitivity and specificity (Hsieh, 2008).

In this paper, a highly sensitive and specific liquid chromatography / atmospheric pressure chemical ionization – tandem mass spectrometry (LC-APCI-MS) analytical method was developed to simultaneously quantify vinblastine and desacetylvinblastine concentrations in canine plasma and urine samples. The developed method was successfully applied to the *in vivo* pharmacokinetic study of vinblastine in dogs.

Materials and methods

Chemicals and materials:

Vinblastine sulfate ($C_{46}H_{58}N_4O_9 \cdot H_2SO_{4)}$ solution (1 mg/mL) was purchased from APP Pharmaceuticals LLC, Schaumburg, IL, USA. Vinorelbine tartrate ($C_{45}H_{54}N_4O_8 \cdot 2C_4H_6O_6$) 10 mg/mL was purchased from Teva, North Wales, PA, USA. 4-O-desacetylvinblastine ($C_{44}H_{56}N_4O_8$) was purchased from Council of Europe, European Pharmacopeia, Strasbourg, Cedex, France. HPLC – grade ammonium acetate, methanol, and acetonitrile and silanized glassware were purchased from Fisher Scientific Company, New Jersey, NJ, USA. Oasis® HLB 1 mL solid phase extraction cartridges were purchased from Waters® Corporation, Milford, MA, USA.

Liquid chromatography/Mass spectrometry

A Schimadzu HPLC system (Shimadzu corporation, Kyoto, Japan) consisted of a system controller (CBM-20A), binary solvent delivery unit (LC-20AD), in-line degasser (DGU-20A5), an auto-sampler (SIL-20AC) with thermostatic injector set at 4 0C and a column oven set at 40 0C (CTO-20AC) with a Restek Allure Pentafluorophenyl (PFP) Propyl 5 μm 50 x 2.1 mm column (Restek, Bellefonte, PA), and guard cartridge (Restek 5 μm, Ultra Biphenyl, 10 x 2.1 mm) were used. An Applied Biosystems 4000 Q-Trap MS/MS system (Applied Biosystems, Foster City, CA) equipped with an atmospheric pressure chemical ionization source and a

NitroGen N300DR nitrogen generator was used (Peak Scientific Instruments Ltd, Paisley, United Kingdom). Analyst® 1.5 software for Windows® was used to acquire and analyze the data.

Mobile phase

The mobile phase consisted of 10% 5 mM ammonium acetate buffer, adjusted to a pH of 3.5 with glacial acetic acid, and 90% HPLC grade methanol. Separation was achieved by isocratic elution at a flow rate of 0.75 mL/min.

Preparation of stock solutions

All stock and working solutions of analytes were prepared under an externally vented fume hood per chemotherapy safe handling and administration standards (Hayes, 2005; Connor and McDiarmid, 2006; Eisenberg, 2009). Stock solutions and working solutions for all three analytes were prepared in methanol using silanized glassware as vinca alkaloids are known to adsorb onto glassware (Puozzo et al., 2007; Zorza et al., 2007). All stock solutions were stable at - 20 ^{0}C for up to 9 months. Depending on the necessity of sensitivity in each matrix, different ranges of calibrating concentrations for vinblastine and desacetylvinblastine were used. For vinblastine , a range of calibrators (6.25 to 5,000 ng/mL for plasma samples; 500 to 100,000 ng /mL for urine samples) were prepared. For desacetylvinblastine, 6.25 to 250 ng/mL for plasma samples and 25 to 5,000 ng/mL for urine samples were prepared. Vinorelbine was used as the internal standard; stock solution was prepared at the concentration of 100,000 ng/mL and working internal standard solution was prepared at the concentration of 500 ng/mL. All calibrators were stable for at least 3 months at 4 ^{0}C.

Sample preparation for plasma and urine

For calibrants and quality controls, 480 µL of blank plasma or urine were added to micro-centrifuge tubes. Ten micro liters of vinblastine and 10 µL of desacetylvinblastine calibrator solutions in methanol were added to achieve final concentrations of 0.125 - 100 ng/mL and 0.125 - 5 ng/mL for plasma samples; 1 – 2,000 ng/mL and 0.5 - 100 ng/mL for urine samples,

respectively. Incurred samples from dogs were thawed at room temperature and 500 µL of sample matrix were added to labeled micro centrifuge tubes. All samples were diluted with 500 µL water containing 10 µL of 500 ng/mL vinorelbine and vortex mixed. Oasis® HLB cartridges were preconditioned with 1 mL of methanol and 1 mL of water. Samples were loaded onto the column slowly, at a rate of approximately 1 – 2 drops per second. Cartridges were washed with 2 mL of water, and then dried at maximum airflow for 30 minutes. Samples were slowly eluted with 2 mL of methanol into labeled silanized glass tubes. The eluted samples were dried under nitrogen at 30 0C and were resuspended in 150 µL of buffer, containing 50% 5 mM ammonium acetate, 25% acetonitrile, and 25% methanol. For plasma samples, 100 µL of the redissolved sample was injected onto the system, whereas 20 µL were injected for urine samples. Silanized glassware was used wherever possible during sample preparation to avoid systemic under-estimation of analyte concentration and to increase sensitivity (Trim et al., 2008; Damen et al., 2009; Damen et al., 2010) .

Calibration curve

For the quantification of vinblastine and desacetylvinblastine concentrations in experimental samples, the ratio of peak area of vinblastine or desacetylvinblastine to the peak area of the internal standard, vinorelbine, was used. For vinblastine, two calibration curves were prepared in plasma samples to obtain acceptable linearity of calibration curves, whereas only one calibration curve was used for urine samples. For desacetylvinblastine, only one calibration curve was used in both matrices. At least 6 calibrators were included for each calibration curve. Different weighting schemes were used for each analyte; 1/x weighting was used for high and low vinblastine calibration curves. For desacetylvinblastine, no weighting was used for plasma curves, whereas $1/x^2$ weighting was used for urine calibration curves. The best weighting model was chosen based on the accuracy of calculated concentrations and coefficient of determination (R^2) value. The limit of quantitation was defined as accuracy and coefficient of variation within 20%

of nominal concentrations. Acceptability criteria for all runs included accuracy within 15% in at least four concentrations in the calibration curve above the LOQ and an R^2 of 0.99 or above.

Method validation

Matrix effects, recovery efficiency, and process efficiency were determined for validation of vinblastine and desacetylvinblastine in plasma and urine. Samples were prepared in triplicate at 5 ng/mL concentration for each analyte. Matrix effect (ME) was determined as the percentage of the ratio of peak areas of analytes fortified after extraction (B) to peak areas of analytes in resuspending buffer (no extraction) (A) (Matuszewski et al., 2003). Recovery efficiency (RE) was calculated as the percentage of peak areas of analytes fortified before extraction (C) to peak areas of analytes fortified after extraction (B). Process efficiency (PE) was determined as the percentage of peak areas of analytes fortified before extraction (C) to peak areas of analytes in resuspending buffer (no extraction) (A).

ME (%) = B/A x 100

RE (%) = C/B x 100

PE (%) = C/A x 100

In addition to the assessment of calibration curve performance, intraday and interday accuracy and precision values were calculated in five replicate samples for each analyte in plasma and urine. The precision was calculated as the relative standard deviation (RSD), or standard deviation divided by the mean concentration, and expressed as a percentage. Accuracy within 20% of the nominal concentration at the lower limit of quantitation (LLOQ) and 15% of the nominal concentration at all higher concentrations were set as the acceptable limits. Similarly, an RSD of 20% at the LLOQ and 15% at higher concentrations were set as the acceptable parameters.

Specificity

To assess the assay's ability to measure the concentrations of each analyte distinctly in the presence of other analytes, peak areas of each analyte were compared by injecting each analyte alone and in the presence of other analytes in resuspending buffer and after extraction in sample matrices. The selected reaction monitoring (SRM) traces of each ion for each analyte and blank plasma were compared.

Sensitivity

In addition to evaluation of the lowest concentration that met accuracy and precision criteria of 20% at the LLOQ, a multiple calibration curve method, deemed the statistical method, was used to estimate the limit of detection (LOD) and LLOQ using triplicate calibrants in the range of 0.1 to 10 ng/mL in plasma. After linear regression of the resulting concentration versus response curves, the y-intercept and slope of each best fit line were used to calculate the standard deviation (SD) of the y-intercepts and the mean of the slopes of calibration curves. The LOD was calculated as (3.3 * SD of the y-intercepts) / (mean of the slopes of calibration curves). The LOQ was calculated as (10 * SD of the y-intercepts) / mean of the slopes of calibration curves (Armbruster et al., 1994).

Freeze-thaw stability

Freeze-thaw stability of plasma samples stored at – 80 ^{0}C was evaluated by fortifying blank samples with vinblastine at 10 ng/mL and 50 ng/mL and desacetylvinblastine at 0.5 and 2 ng/mL, in triplicate. One batch of fortified plasma samples were frozen and thawed twice while the other batch of fortified plasma samples were thawed only once before sample processing.

Application to *in vivo* vinblastine pharmacokinetic study in dogs

The novel highly sensitive analytical method was successfully applied to quantify the concentrations of vinblastine and desacetylvinblastine in plasma and urine samples of four adult and two juvenile dogs (4 – 54 kg) that received an intravenous bolus dose of 0.075 mg/kg vinblastine sulfate. Plasma and urine samples were collected at pre, 2 min, 5, 10, 15, 20, 30, 45

min, 1 hr, 2, 3, 4, 5, 6, 9, 12, and 24 hrs post drug administration; pre sample, 1 hr, 3, 7, 12, 24, 32, 48, 56, and 72 hr, respectively following vinblastine sulfate administration, respectively. The data was analyzed on WinNonlin® 5.2 pharmacokinetic software (Pharsight Corp., Mountain View, CA) to analyze the pharmacokinetic parameters.

Results and discussion

Sample pretreatment optimization

Different sample pretreatment procedures were investigated to optimize sample recovery and chromatography. Published liquid -liquid extraction procedures were investigated using different solvents such as: a mixture of hexane and ethyl acetate, chloroform and isopropanol, and ether (Ramirez et al., 1997). Liquid-liquid extraction was unsuccessful due to poor recovery of analytes, base line noise, formation of by-products, appearance of degradation products, or column obstruction. Protein precipitation with acetonitrile was also attempted, but recoveries of the analytes were very poor (Zorza et al., 2007). Poor recovery of vinca alkaloids might be due to high protein binding (Steele et al., 1983). In order to overcome different complications encountered in the aforementioned methods, solid phase extraction was examined using HLB and MCX cartridges. The solid-phase extraction (SPE) protocol using Oasis® HLB cartridges provided the highest analyte recovery. To the authors' knowledge, the use of HLB columns in extraction of vinblastine and desacetylvinblastine has not been previously published. However, among the vinca alkaloids, the use of HLB columns has been reported in metabolism studies of vinorelbine in several matrices (de Graeve et al., 2008). The HLB SPE cartridges were selected for investigation in the present study because their polymeric reversed phase materials give wide versatility for use with a variety of polar and non-polar drugs and can be allowed to dry completely (Farre et al., 2007).

Chromatographic optimization

Different mobile phase compositions were explored to optimize the separation of analytes. Good separation and chromatography were achieved using isocratic elution with 10% 5 mM ammonium acetate (pH: 3.5) and 90% methanol at a flow rate of 0.75 mL/min. No carryover of analytes in successive injected samples was observed. The absence of carryover was confirmed by injection of resuspending buffer after injection of the highest calibrant.

Instrument settings and optimization

Direct infusion of analytes was used to determine the optimal instrument parameters, such as nebulizing gas (gas1): 40; turbo ion spray (TIS, gas2): 20; temperature: 400 ^{0}C; collision energy (CE): 49 eV; collision cell exit potential (CXP): 8 V. Optimization of these parameters was important in removing or decreasing interferences in combination with chromatographic separation. Ion path for MS/MS detection of compounds was tuned by infusion of a mixture of all three analytes into the tandem mass spectrometry. For vinca alkaloids, electron spray ionization (ESI) is the most often used method of ionization. But ESI gave low sensitivity, poor resolution, and more baseline noise with ESI(Damen et al., 2010). In order to overcome these problems, atmospheric pressure chemical ionization (APCI) with positive mode ionization was used and gave satisfactory sensitivity. Few publications have described the use of APCI for the quantification of vincristine and vinblastine (Read and Black, 1999). In APCI, ionization occurs in the gas phase, unlike ESI, where ionization occurs in the liquid phase. General advantages of APCI include high ionization efficiency, low susceptibility to chemical interferences, and also, APCI is considered to be more robust method of ionization than ESI (Read and Black, 1999; Politi et al., 2006). Multiple reaction monitoring (MRM) was used as this is the superior method compared to single ion monitoring (SIM) (Damen et al., 2010). A typical fragment ion is selected in MRM while a single molecular ion is selected in SIM. Methods using MRM had reported higher sensitivity than SIM mode (Damen et al., 2010).

Specificity

Specificity was verified by looking at the identification (ID) ratios of qualifier ions for each analyte (table 1). ID ratios within ± 20% of mean of ID ratios were considered as an acceptable limit. For quantitation of analytes, major ions were chosen, such as 811.5/355.1 for vinblastine, 769.4/355.1 for desacetylvinblastine, and 779.4/658.2 for vinorelbine. The major fragment of vinblastine was 811.5 whereas previously reported major fragments for vinblastine were 751 and 793 (Zhou et al., 2005; Trim et al., 2008).

Calibration curve

In order to obtain linear calibration curves within acceptable limits for vinblastine, two calibration curves were prepared in plasma. A wide range of vinblastine calibrants were included (0.125 ng/mL to 100 ng/mL) in plasma to quantify the expected concentrations of vinblastine in both adult and juvenile dogs. A similar method of quantitation of vinblastine in human plasma using LC/APCI-MS was previously described (Ramirez et al., 1997). However, the LOQ and range of calibration curves reported in this paper were lower and wider than the previous work. The concentrations of desacetylvinblastine in the incurred samples were within a small range and required only one calibration curve. The accuracy of both vinblastine and desacetylvinblastine in all calibration curves were above 80% at the limit of quantitation and above 85% at higher concentrations. At least, six calibrators were retained for each calibration curve and calibrators having back calculated values more than 15% were removed from the curves.

Method validation

Matrix effects, recovery efficiency, and processing efficiency were calculated for each analyte in both matrices (Matuszewski et al., 2003). Recoveries of both vinblastine and desacetylvinblastine were lower in plasma as compared to urine (Table 2). This could be attributed to binding of both analytes to plasma proteins or to ion suppression (Steele et al., 1983; Matuszewski et al., 2003; Peters et al., 2007; Damen et al., 2008).

The intraday and interday precision of vinblastine and desacetylvinblastine in both matrices were within 8.6% (table 3 and 4). This low value indicates the repeatability of the developed method. The lowest value of the intraday and interday accuracy of both analytes in both matrices was 89% indicating good accuracy of the developed method. For both analytes, the coefficient of determination was greater than 0.99 in all validation experiments and in incurred sample analysis.

Vinblastine and 4-O-deacetylvinblastine freeze-thaw stability in plasma samples processed after single thawing and double thawing were within acceptable limits (table 5).

Sensitivity

The sensitivity of the novel method was tested by both statistical and empirical approaches (figures 6 and 7). The sensitivity of the method based on the empirical approach was higher than that predicted by the statistical approach. The LLOQ of vinblastine and desacetylvinblastine were 0.125 ng/mL and 0.125 ng/mL with the empirical approach, but were 0.45 ng/mL and 0.21 ng/mL with the statistical approach, respectively. Although the statistical method is useful for initial predictions of LOD and LLOQ values, the empirical method is able to more concretely define the LLOQ that meets the predetermined acceptance criteria for these values (Armbruster et al., 1994).

Application to *in vivo* vinblastine pharmacokinetic study in dogs

The vinblastine concentrations determined *in vivo* in dogs ranged from 0.8 to 51.1 ng/mL and 0.45 to 884 ng/mL in plasma and urine samples, respectively. The desacetylvinblastine concentrations were ranged from 0.22 to 1.03 ng/mL and 0.25 to 30.2 ng/mL in plasma and urine samples. Figure 8 represents a typical pharmacokinetic profile of vinblastine sulfate in dogs. As seen in figure 8, the time course disposition of plasma concentrations of vinblastine in dogs was described. The concentrations of vinblastine and desacetylvinblastine were above LLOQ until 24 hr plasma samples and 72 hr urine samples. The data from *in vivo* vinblastine pharmacokinetic

study was applied to the on-going studies to develop novel dosing equations in dogs to calculate the doses of anticancer drugs more accurately.

Conclusions

A highly sensitive, specific, and reliable analytical method to quantify the concentrations of vinblastine and its metabolite, desacetylvinblastine, in canine plasma and urine samples using liquid chromatography – atmospheric pressure chemical ionization – mass spectrometry was developed and validated. This newly described assay is highly reproducible. The high sensitivity of the method would be particularly useful in determining the concentrations of vinblastine and its metabolite, desacetylvinblastine in small sized dogs and to study the pharmacokinetics of vinblastine and desacetylvinblastine in dogs. The analytical method developed could be useful in the toxicity adjusted dosing of vinblastine in dogs.

References

Armbruster DA, Tillman MD and Hubbs LM (1994) Limit of detection (LQD)/limit of quantitation (LOQ): comparison of the empirical and the statistical methods exemplified with GC-MS assays of abused drugs. *Clin Chem* **40:**1233-1238.

Cheng T, Si D and Liu C (2009) Rapid and sensitive LC-MS method for pharmacokinetic study of vinorelbine in rats. *Biomed Chromatogr* **23:**909-911.

Connor TH and McDiarmid MA (2006) Preventing occupational exposures to antineoplastic drugs in health care settings. *CA Cancer J Clin* **56:**354-365.

Damen CW, Lagas JS, Rosing H, Schellens JH and Beijnen JH (2009) The bioanalysis of vinorelbine and 4-O-deacetylvinorelbine in human and mouse plasma using high-performance liquid chromatography coupled with heated electrospray ionization tandem mass-spectrometry. *Biomed Chromatogr* **23:**1316-1325.

Damen CW, Rosing H, Schellens JH and Beijnen JH (2010) High-performance liquid chromatography coupled with mass spectrometry for the quantitative analysis of vinca-alkaloids in biological matrices: a concise survey from the literature. *Biomed Chromatogr* **24:**83-90.

Damen CW, Rosing H, Tibben MM, van Maanen MJ, Lagas JS, Schinkel AH, Schellens JH and Beijnen JH (2008) A sensitive assay for the quantitative analysis of vinorelbine in mouse and human EDTA plasma by high-performance liquid chromatography coupled with electrospray tandem mass spectrometry. *J Chromatogr B Analyt Technol Biomed Life Sci* **868:**102-109.

de Graeve J, van Heugen JC, Zorza G, Fahy J and Puozzo C (2008) Metabolism pathway of vinorelbine (Navelbine) in human: characterisation of the metabolites by HPLC-MS/MS. *J Pharm Biomed Anal* **47:**47-58.

Eisenberg S (2009) Safe handling and administration of antineoplastic chemotherapy. *J Infus Nurs* **32:**23-32.

Farre M, Petrovic M and Barcelo D (2007) Recently developed GC/MS and LC/MS methods for determining NSAIDs in water samples. *Anal Bioanal Chem* **387:**1203-1214.

Gan PP and Kavallaris M (2008) Tubulin-targeted drug action: functional significance of class ii and class IVb beta-tubulin in vinca alkaloid sensitivity. *Cancer Res* **68:**9817-9824.

Gupta MM, Singh DV, Tripathi AK, Pandey R, Verma RK, Singh S, Shasany AK and Khanuja SP (2005) Simultaneous determination of vincristine, vinblastine, catharanthine, and vindoline in leaves of catharanthus roseus by high-performance liquid chromatography. *J Chromatogr Sci* **43:**450-453.

Hayes A (2005) Safe use of anticancer chemotherapy in small animal practice. *In Practice* **27:**118 - 127.

Hsieh Y (2008) HPLC-MS/MS in drug metabolism and pharmacokinetic screening. *Expert Opin Drug Metab Toxicol* **4:**93-101.

Kavallaris M, Annereau JP and Barret JM (2008) Potential mechanisms of resistance to microtubule inhibitors. *Semin Oncol* **35:**S22-27.

Matuszewski BK, Constanzer ML and Chavez-Eng CM (2003) Strategies for the assessment of matrix effect in quantitative bioanalytical methods based on HPLC-MS/MS. *Anal Chem* **75:**3019-3030.

Niwa M and Kawashiro T Sensitive measurement of vinorelbine in dog plasma by liquid chromatography-electrospray ionization tandem mass spectrometry utilizing transitions from double-charged precursor ions. *Biomed Chromatogr* **25:**517-523.

Owellen RJ, Hartke CA and Hains FO (1977) Pharmacokinetics and metabolism of vinblastine in humans. *Cancer Res* **37:**2597-2602.

Pasquier E and Kavallaris M (2008) Microtubules: a dynamic target in cancer therapy. *IUBMB Life* **60:**165-170.

Peters FT, Drummer OH and Musshoff F (2007) Validation of new methods. *Forensic Sci Int* **165:**216-224.

Politi L, Groppi A and Polettini A (2006) Ionisation, ion separation, and ion detection in LC-MS. In A. Polettini (Ed.), Applications of LC-MS in Toxicology (2nd ed.): Pharmaceutical Press.

Puozzo C, Ung HL and Zorza G (2007) A high performance liquid chromatography method for vinorelbine and 4-O-deacetyl vinorelbine: a decade of routine analysis in human blood. *J Pharm Biomed Anal* **44:**144-149.

Ramirez J, Ogan K and Ratain MJ (1997) Determination of vinca alkaloids in human plasma by liquid chromatography/atmospheric pressure chemical ionization mass spectrometry. *Cancer Chemother Pharmacol* **39:**286-290.

Rassnick KM, Bailey DB, Flory AB, Balkman CE, Kiselow MA, Intile JL and Autio K (2008) Efficacy of vinblastine for treatment of canine mast cell tumors. *J Vet Intern Med* **22:**1390-1396.

Read RW and Black RM (1999) Rapid screening procedures for the hydrolysis products of chemical warfare agents using positive and negative ion liquid chromatography-mass spectrometry with atmospheric pressure chemical ionisation. *J Chromatogr A* **862:**169-177.

Steele WH, King DJ, Barber HE, Hawksworth GM, Dawson AA and Petrie JC (1983) The protein binding of vinblastine in the serum of normal subjects and patients with Hodgkin's disease. *Eur J Clin Pharmacol* **24:**683-687.

Trim PJ, Henson CM, Avery JL, McEwen A, Snel MF, Claude E, Marshall PS, West A, Princivalle AP and Clench MR (2008) Matrix-assisted laser desorption/ionization-ion mobility separation-mass spectrometry imaging of vinblastine in whole body tissue sections. *Anal Chem* **80:**8628-8634.

van Tellingen O, Beijnen JH, Baurain R, ten Bokkel Huinink WW, van der Woude HR and Nooyen WJ (1991) High-performance liquid chromatographic determination of vinblastine, 4-O-deacetylvinblastine and the potential metabolite 4-O-deacetylvinblastine-3-oic acid in biological fluids. *J Chromatogr* **553:**47-53.

van Tellingen O, Beijnen JH, Nooijen WJ and Bult A (1993) Tissue disposition, excretion and metabolism of vinblastine in mice as determined by high-performance liquid chromatography. *Cancer Chemother Pharmacol* **32:**286-292.

Welle MM, Bley CR, Howard J and Rufenacht S (2008) Canine mast cell tumours: a review of the pathogenesis, clinical features, pathology and treatment. *Vet Dermatol* **19:**321-339.

Zhou H, Tai Y, Sun C and Pan Y (2005) Rapid identification of vinca alkaloids by direct-injection electrospray ionisation tandem mass spectrometry and confirmation by high-performance liquid chromatography-mass spectrometry. *Phytochem Anal* **16:**328-333.

Zorza G, Van Heugen JC, De Graeve J and Puozzo C (2007) Development of a sensitive liquid chromatography method coupled with a tandem mass spectrometric detection for the clinical analysis of vinflunine and 4-O-deacetyl vinflunine in blood, urine and faeces. *J Chromatogr B Analyt Technol Biomed Life Sci* **853:**294-302.

Q1 (parent ion)	VLB (811.5 m/z)	DVLB (769.4 m/z)	VRB (779.4 m/z)
Q3 (daughter ion)	144.1	124.2	122.2
	224.1	144.1	457.2
	355.1	355.1	658.2

Table 1. Parent ion (Q1) and product ion (Q3) masses for VLB, DVLB, and VRB

	Plasma			Urine		
	VLB	DVLB	VRB	VLB	DVLB	VRB
Matrix effects	65.7	76.5	78.0	100.7	106.6	110.5
Recovery efficiency	65.3	72.0	68.7	103.6	108.5	84.6
Processing efficiency	42.9	55.1	53.6	104.4	115.7	93.5

Table 2. Mean percentages of matrix effects, recovery efficiency, and process efficiency of extraction of plasma and urine samples fortified with vinblastine, desacetylvinblastine, and vinorelbine in triplicate ; fortified at the concentrations of 5 ng/mL vinblastine and desacetylvinblastine, and 10 ng/mL vinorelbine. The matrix effects, recovery efficiency, and processing of efficiency of all three analytes were lower in plasma samples compared to urine samples.

Analyte	Intraday precision and accuracy							
	Plasma (n=5)				Urine (n=3)			
	Nominal conc. (ng/mL)	Observed conc. (mean ± SD) (ng/mL)	RSD %	Accuracy %	Nominal conc. (ng/mL)	Observed conc. (mean ± SD) (ng/mL)	RSD %	Accuracy %
VLB	0.5	0.51 ± 0.03	5.7	98.4	25	25.47 ± 0.9	3.5	98.1
	2	2.19 ± 0.07	3.4	90.3	250	251 ± 5.29	2.1	99.6
	10	11.04 ± 0.53	4. 9	89.6	1500	1523 ± 64.3	4.2	98.4
	50	52.6 ± 3.31	6.3	94.8				
DVLB	0.5	0.46 ± 0.02	3.6	92.7	5	4.92 ± 0.25	5.0	98.5
	2	1.85 ± 0.16	8.6	92.2	25	26.8 ± 1.44	5.4	96.1

Table 3. Intraday accuracy and precision of analytes in plasma and urine were presented as mean ± standard deviation. The intraday accuracy and precision of both analytes in both matrices were within acceptable limits.

Analyte	Interday precision and accuracy							
	Plasma (n=5)				Urine (n=3)			
	Nominal conc. (ng/mL)	Observed conc. (mean ± SD) (ng/mL)	RSD %	Accuracy %	Nominal conc. (ng/mL)	Observed conc. (mean ± SD) (ng/mL)	RSD %	Accuracy %
VLB	0.5	0.4 ± 0.02	5.1	92.8	25	25.37 ± 1.12	4.4	96.3
	2	1.84 ± 0.11	5.5	89.2	250	250.8 ± 12.5	5.0	97.5
	10	9.9 ± 0.74	7.6	93.4	1500	1588.9 ± 95	6	94.1
	50	50.1 ± 4.5	8.4	95.3				
DVLB	0.5	0.45 ± 0.02	4.7	89.6	5	4.9 ± 0.27	5.6	97.2
	2	1.86 ± 0.13	7.0	92.8	25	25.4 ± 2.0	8.1	96.1

Table 4. The values of interday accuracy and precision of analytes in plasma and urine in seven runs over a period of nine months and 3 runs over a period of two moths, respectively were presented as mean ± standard deviation. The values of interday accuracy and precision of both analytes in both matrices were within acceptable limits.

	Freeze – thaw stability testing						
		Single thaw (n=3)			Double thaw (n=3)		
Analyte	Nominal conc. (ng/mL)	Mean ± SD	RSD%	Accuracy%	Mean ± SD	RSD%	Accuracy%
VLB	10	8.61 ± 0.19	2.2	86.1	9.94 ± 0.19	1.9	99.4
	50	53.9 ± 1.04	1.9	92.2	46.8 ± 1.31	2.8	93.6
DVLB	0.5	0.56 ± 0.001	1.77	88.4	0.56 ± 0.004	0.6	87.8
	2	1.89 ± 0.20	10.7	94.3	1.74 ± 0.10	5.7	86.8

Table 5. Freeze – thaw stability of plasma samples fortified with vinblastine and 4-O-desacetylvinblastine was tested by storing the samples at -80 ^{0}C in triplicate. One batch of samples were thawed once and another batch were thawed twice, and then samples were processed together to test the freeze-thaw stability. The analytes were stable for up to two freeze-thaw cycles.

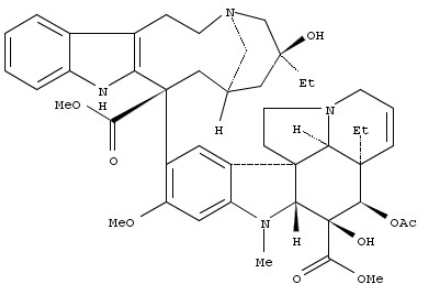

Vinblastine (811)

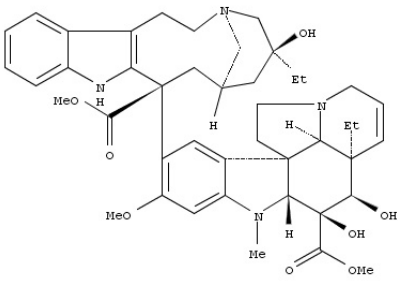

Desacetylvinblastine (769)

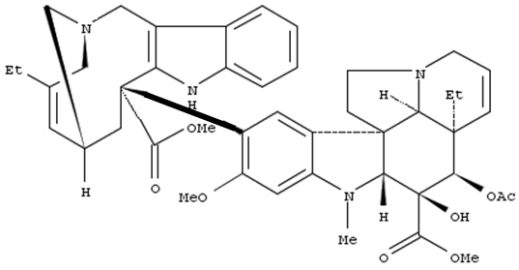

Vinorelbine (779)

Figure 1. Chemical structures of vinblastine, desacetylvinblastine, and vinorelbine

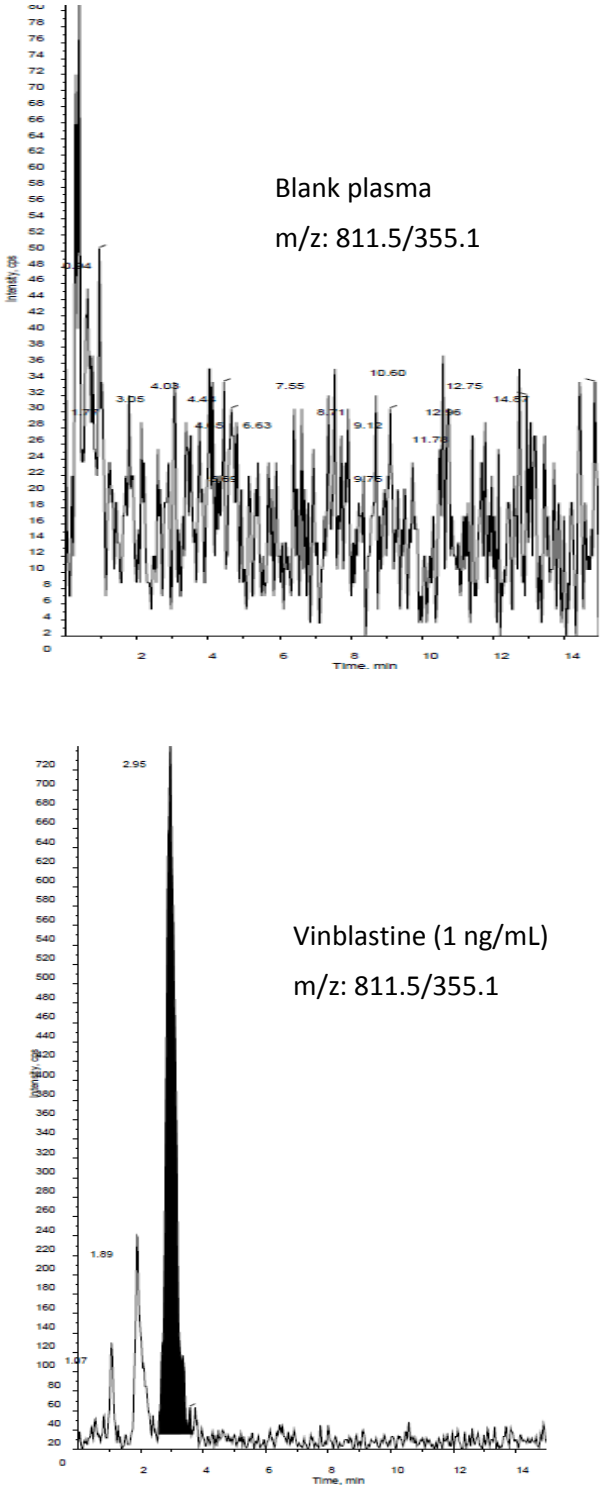

Figure 2. Representative SRM traces of blank plasma (m/z 811.5/355.1) and vinblastine (m/z 811.5/355.1) showing the specificity of vinblastine identification in plasma samples.

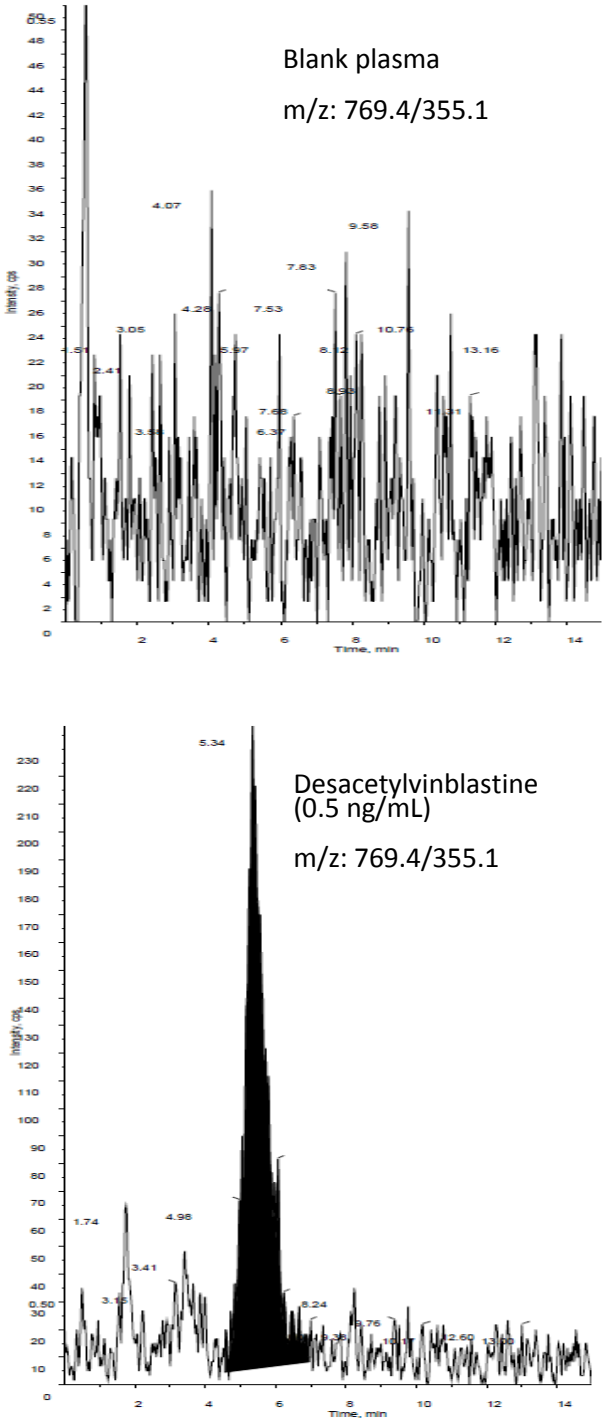

Figure 3. Representative SRM traces of blank plasma (m/z 769.4/355.1) and desacetylvinblastine (m/z 769.1/355.1) showing the specificity of desacetylvinblastine identification in plasma samples.

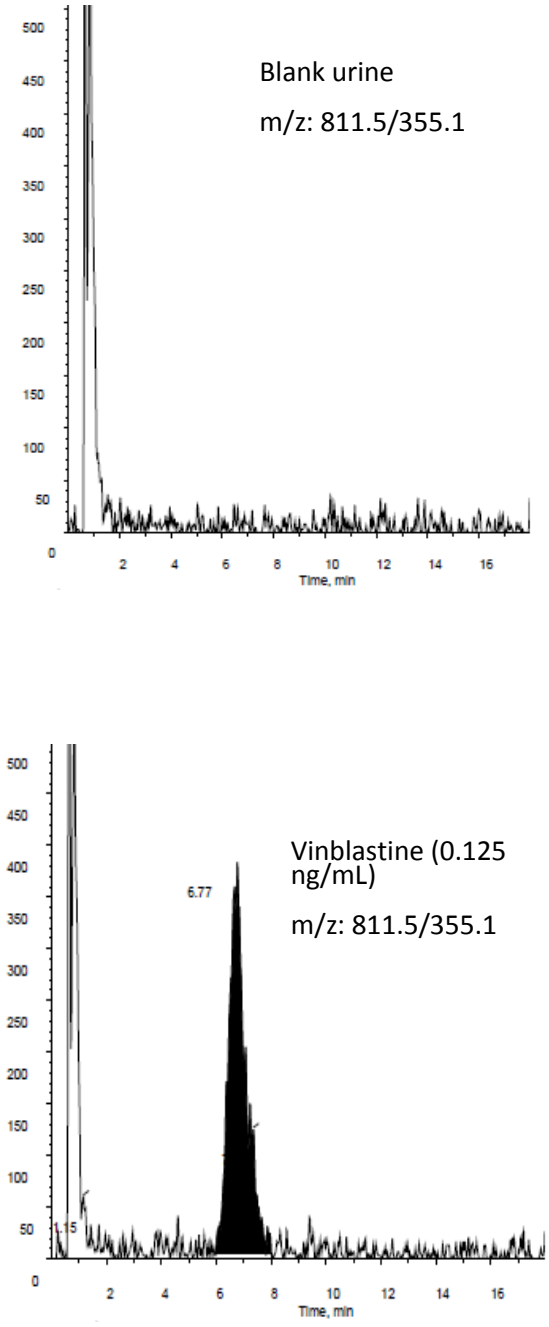

Figure 4. Representative SRM traces of blank urine (m/z 811.5/355.1) and urine fortified with vinblastine (m/z 811.5/355.1) showing the specificity of vinblastine identification in urine samples.

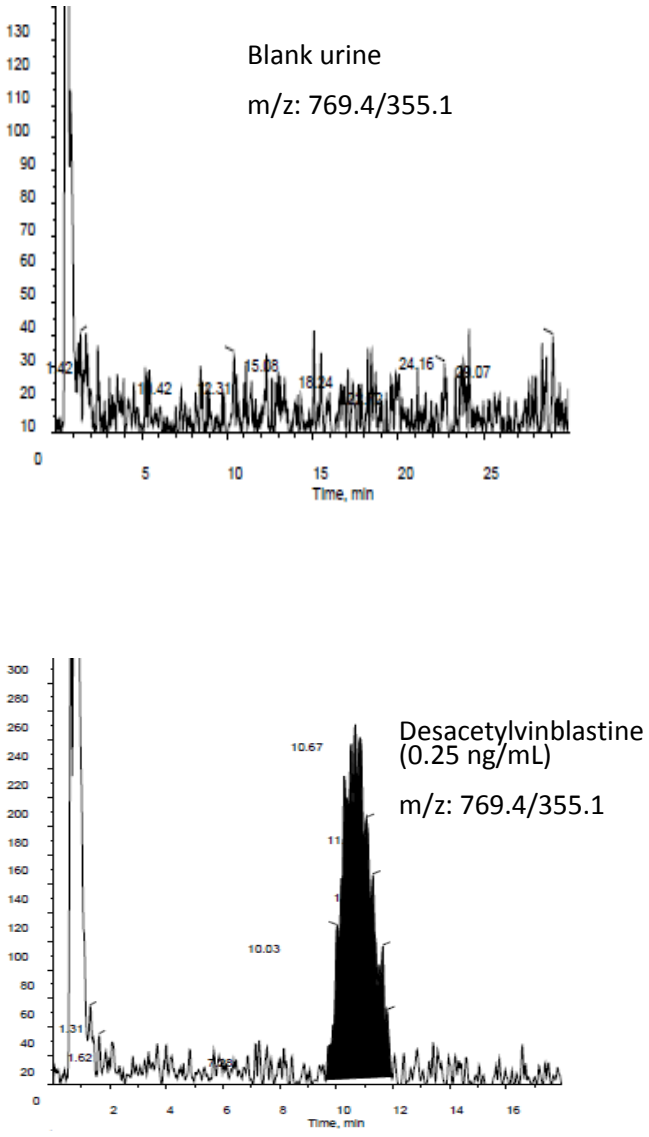

Figure 5. Representative SRM traces of blank urine (m/z 769.4/355.1) and desacetylvinblastine extracted from urine fortified with desacetylvinblastine (m/z 769.4/355.1) showing the specificity of desacetylvinblastine identification in urine samples.

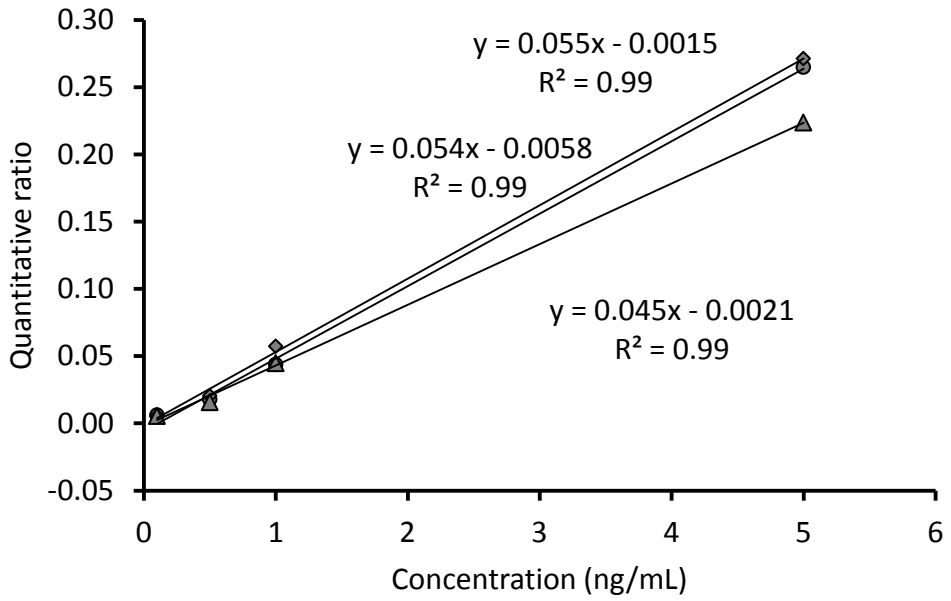

Figure 6. Calibration curves of vinblastine in plasma, in triplicate, to determine the sensitivity of the method using the statistical approach. Quantitative ratio was calculated as ratio of peak area of analyte to peak area of internal standard.

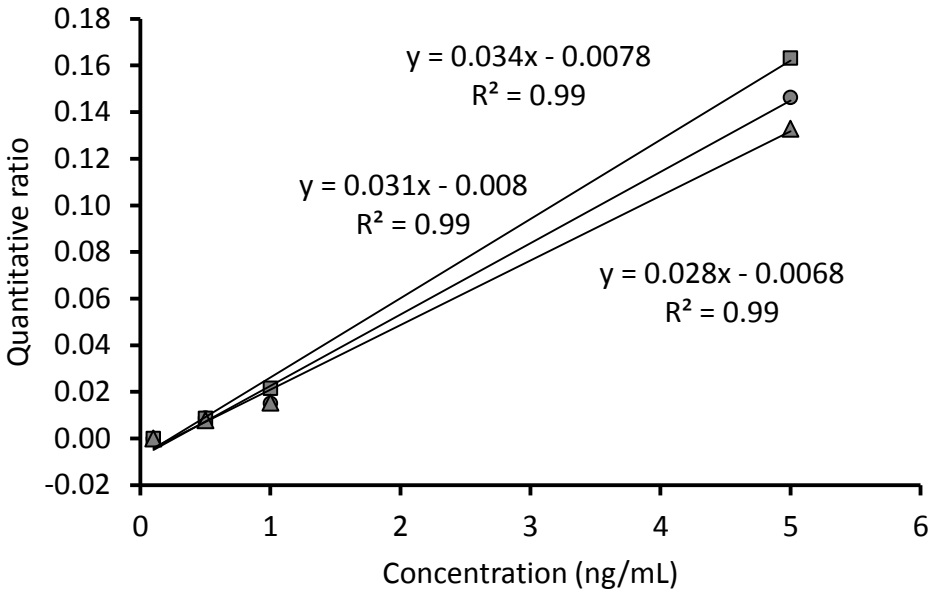

Figure 7. Calibration curves of desacetylvinblastine in plasma samples in triplicate to determine the sensitivity of the method using the statistical approach.

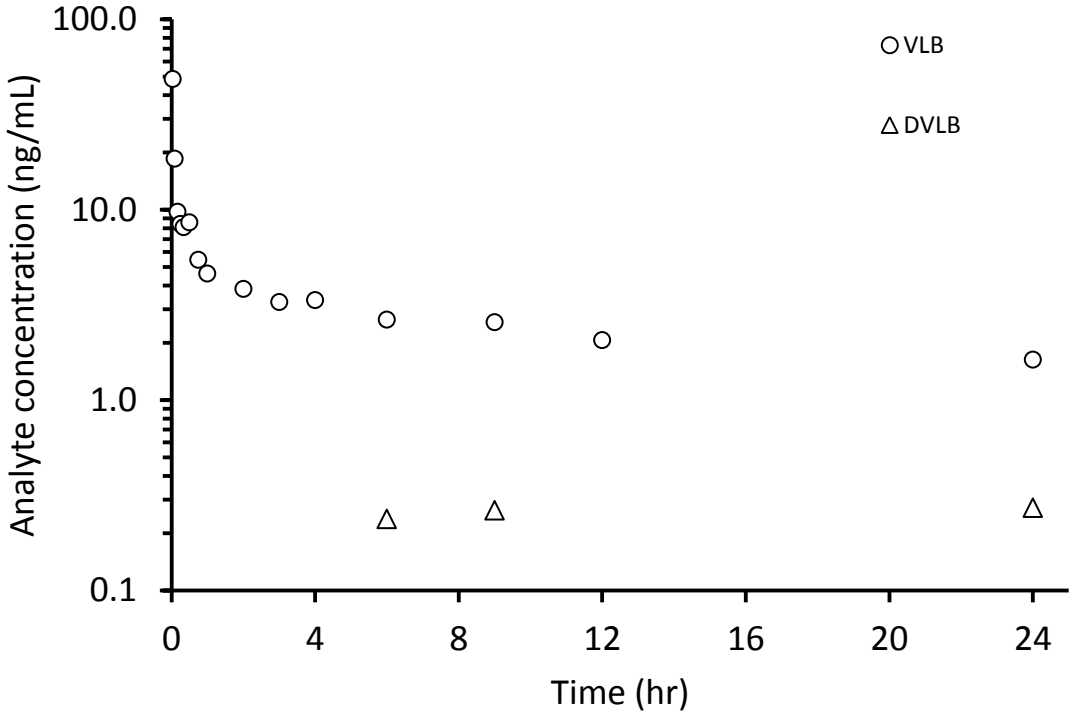

Figure 8. A representative time course disposition of vinblastine in a dog (10 kg body weight), that received an intravenous bolus dose of 0.075 mg/kg vinblastine sulfate.

CHAPTER VI

SUMMARY AND CONCLUSIONS

Anticancer drugs are characterized by a narrow therapeutic index and wide variability in therapeutic outcome and toxicity. Inappropriate dosing of anticancer drugs contributes to therapeutic failure, suboptimal outcomes, multi-drug resistance, and toxicity. Therefore, the doses of anticancer drugs should be calculated as accurate as possible from the initiation of treatment. Currently, the doses of most anticancer drugs are calculated as a direct proportion of body surface area (BSA) (Pinkel, 1958). As there is wide variation in the adult body weights of dogs, ranging from a 1 kg Chihuahua to a 100 kg St. Bernard, dogs represent the ideal species to examine the effect of intraspecific allometry on drug disposition. As with most drugs, the efficacy of anticancer agents correlates best with total drug exposure. Mathematically, drug exposure is calculated as the area under the plasma concentration versus time curve (AUC) (Moore and Erlichman, 1987; van den Bongard et al., 2000; Hempel and Boos, 2007). Total body clearance is the important pharmacokinetic parameter that affects drug exposure. Therefore, if the allometric factors influencing drug clearance are better understood, the dose required to produce a desired drug exposure can be accurately calculated. Physiologically based pharmacokinetic (PBPK) models are increasingly popular to predict absorption, distribution, metabolism, and excretion of a drug or a chemical compound. To predict the disposition of a drug using these PBPK models, accurate estimates of organ weights, blood flow through the organs, and estimates of pharmacokinetic parameters are needed. However, current estimates of organ weights, physiological parameters, and pharmacokinetic parameters are primarily available for standard-sized, laboratory beagle dogs that don't adequately predict these values over a wide range of canine breeds. With this background, we hypothesized that the concomitant consideration of body weight, gender, and ontogeny on organ physiology and drug handling will accurately predict the clearance of drugs. The objectives of this study were to determine the clearance of anticancer drugs by considering anatomical, physiological, and pharmacokinetic parameters, to develop allometric equations for estimating organ weights, physiological parameters, and drug disposition for a wide range of body weights in dogs for PBPK modeling, and, ultimately, to optimize drug

exposure of anticancer drugs among disparate canine patients. In order to test our hypothesis, two model anticancer drugs, cisplatin and vinblastine, were selected as agents that are primarily dependent upon renal and hepatic clearance, respectively.

Allometric scaling of renal clearance of cisplatin in dogs

Cisplatin is a platinum containing alkylating agent that acts by establishing cross links between and within purine bases of DNA, thereby arresting DNA replication (Legendre et al., 2000). Cisplatin is indicated for the treatment of variety of solid tumors in both veterinary and human medicine (Barabas et al., 2008; Fouladi et al., 2008; McDuffie et al., 2010). Cisplatin is primarily excreted through the kidneys and therefore will serve as a model anticancer drug for renally cleared anticancer drugs. Nephrotoxicity is the dose limiting toxicity of cisplatin. Carboplatin is a sister analogue of cisplatin with reduced nephrotoxicity (Hanigan et al., 2009). The doses of carboplatin were successfully normalized among human patients as a function of creatinine clearance and AUC using the formula: Dose = AUC (GFR + 25) (Calvert et al., 1989). Unfortunately, renal functional markers, such as glomerular filtration rate (GFR), did not correlate well with the clearance of cisplatin in several previous human studies (Peng et al., 1997; de Jongh et al., 2001). The poor standardization of cisplatin drug exposure in previous studies, combined with its primarily renal route of elimination, make the prediction of cisplatin disposition a worthwhile goal of improved drug dosing algorithms. To that end, studies were undertaken to investigate the allometric factors that underlie cisplatin clearance.

Liver, kidney, and heart weights were collected from a total of 383 dogs, including 146 juvenile and 237 adult dogs, from nearby urban animal shelters and from the Oklahoma Animal Disease Diagnostic Laboratory (OADDL), Stillwater, OK. Data collected from animal shelters was used as the training data set to develop allometric equations. The data collected from

OADDL was used as the validation data set to test the newly developed equations. In addition, the newly developed allometric equations were compared to the standard method of organ weight prediction, which uses a fixed proportion of body weight (Steward et al., 1975). Based on *a priori* inclusion criteria, a total of 167 dogs (juveniles and adults) were retained in the training data for kidney weights. Body weight and ontogeny significantly influenced kidney weights, whereas gender did not. The newly developed allometric equation for kidney weight was: *Kidney wt. (g)* = $9.35 \cdot BW^{0.79} \cdot 10^{0.095 \cdot ontogeny}$; R^2 = 0.93, *sy.x* = 0.088 (where a*dult*=0, *juvenile*=1). The newly developed allometric equations were compared against the standard method, where estimates are a fixed proportion of body weights (1.13% for juveniles and 0.4% for adults). The residual plots and sum of absolute residuals for predicted kidney weights demonstrated that the newly developed allometric equations better predicted organ weights than did the fixed proportion approach.

In vivo physiological and pharmacokinetic studies were conducted in ten intact male dogs (4 – 54 kg), including two juvenile dogs (8 – 12 week old, 4 – 5 kg). Inulin and para-aminohippuric acid were used as markers for the determination of glomerular filtration rate (GFR) and effective renal plasma flow (ERPF) (Earle and Berliner, 1946; Mann and Kinter, 1993). Cisplatin was administered as a constant rate infusion for 20 minutes at the dose rate of 1 mg/kg body weight. Concentrations of platinum in plasma ultra-filtrate and urine samples were quantified by inductively coupled plasma mass spectrometry (ICP-MS). The data were analyzed compartmentally using the WinNonlin® pharmacokinetic software program. Renal physiological parameters, total body clearance, and renal clearance of cisplatin were $\log_{10}$ transformed and regressed against $\log_{10}$ body weights. In contrast to previous findings in humans, the clearance of cisplatin was well correlated with glomerular filtration, with an allometric exponent similar to $3/4^{th}$ power of standard allometry (Peng et al., 1997; de Jongh et al., 2001). The exponents of effective renal plasma flow and effective renal blood flow were similar to the 2/3 power of

*intra*specific allometry. These findings demonstrated that the initial doses of cisplatin correlate well with GFR in dogs. The lack of correlation between GFR in previous studies may instead stem from alteration of cisplatin kinetics with subsequent doses of cisplatin or species-specific differences (Aleksunes et al., 2008).

The allometric relationship between kidney weights, renal physiological parameters, cisplatin renal and total clearance and body weight suggests a common underlying basis for the allometry of kidney form and function. Furthermore, the initial dose of cisplatin followed standard allometry and correlated well with GFR in dogs. Pharmacokinetic studies with multiple doses of cisplatin in dogs would be needed to determine whether the clearance of cisplatin continues to correlate well with GFR with successive doses, or if subsequent doses affect its own clearance.

Allometry of Hepatic Metabolism of Vinblastine in Dogs

Mast cell tumors are one of the most common cutaneous tumors in all breeds and ages of dogs. Vinblastine and prednisone regimens are commonly used to treat mast cell tumors. However, while dogs tolerate these regimens well, their efficacy is less than 50% of treated dogs. The inverse relationship between efficacy and toxicity of anticancer agents suggests that dogs may be under-dosed by the currently used doses of vinblastine. Vinblastine is primarily metabolized by the liver and excreted through bile(de Lannoy et al., 1994). In order to understand the factors influencing the total body clearance of vinblastine, different aspects of anatomical, *in vivo* drug handling, and *in vitro* drug metabolism of vinblastine were studied in dogs.

Based on *a priori* inclusion criteria, data was retained for 235 dogs (80 juveniles and 155 adults) for multiple linear regressions of body weight, ontogeny, and gender against liver weights. Body weight and ontogeny significantly influenced liver weights, whereas gender did not. Liver weight depended on body weight and ontogeny with the following allometric equation: *Liver wt*

(g) = $49.8 \cdot BW^{0.90} \cdot 10^{0.105 \cdot ontogeny}$, $R^2 = 0.93$, *sy.x = 0.094* (where adult=0, juvenile=1). The newly developed allometric equation was compared to the commonly used fixed proportion approach, where liver weight is estimated as 3.5% of body weight (Steward et al., 1975). The newly developed allometric equation relating body weight and ontogeny to liver weight was tested in the validation data set by inspection of residual plots, and the sum of absolute residuals. Both residual plots and the sum of absolute residuals demonstrated that the allometric equation more accurately predicted liver weight as compared to the fixed proportion of body weight approach.

An *in vivo* pharmacokinetic study of vinblastine disposition was performed in four adult intact male dogs (10 – 54 kg). Vinblastine was administered as a bolus dose at the rate of 0.075 mg/kg body weight. The concentrations of vinblastine and its metabolite desacetylvinblastine in plasma and urine samples were quantified using a newly developed liquid chromatography/tandem mass spectrometry analytical method. The data were analyzed compartmentally using the WinNonlin® pharmacokinetic software program. The total and hepatic clearance of vinblastine were $\log_{10}$ transformed and regressed against $\log_{10}$ (10) body weight. Total and hepatic clearances of vinblastine depended on body weight as: $CL_{total} = 21.6\ BW^{0.78}$, $R^2 = 0.97$ and $CL_{hep} = 21.2\ BW^{0.75}$, $R^2 = 0.97$, respectively.

Concurrent with the collection of organ weights, liver samples were collected from twenty three adult dogs (2.3 – 54 kg). Hepatic microsomes were purified by homogenization followed by differential centrifugation using a previously published standard protocol (Schneider, 1948). The concentrations of microsomal protein in microsomes were quantified using the Bradford protein assay (Bradford, 1976). The density of cytochrome P450 enzymes in the microsomal samples was quantified using the ascorbate reduced dithionate difference spectra (Matsubara et al., 1976). The intrinsic clearance of vinblastine was quantified with the substrate depletion approach, by incubating 0.025 – 61.65 μM of vinblastine in microsomal samples (Jones

and Houston, 2004; Nath and Atkins, 2006). The concentrations of vinblastine were quantified using reversed phase high performance liquid chromatography. The data were analyzed by WinNonlin® pharmacokinetic software program to obtain the values of the theoretical maximum rate of reaction (V_{max}) and Michaelis constant (K_m). The *in vitro* intrinsic clearance of vinblastine was calculated as the ratio of V_{max} to K_m. The *in vitro* intrinsic clearance of vinblastine was scaled to the whole animal *in vivo* intrinsic clearance of vinblastine using a scaling factor of 55 mg of microsomal protein per gram of liver (Smith et al., 2008). The *in vivo* intrinsic clearance of vinblastine was combined with physiological parameters, such as fraction of unbound drug and hepatic blood flow, to predict the hepatic clearance of vinblastine using several predictive models: the well stirred, parallel tube, and dispersion models (Pang and Rowland, 1977; Houston and Carlile, 1997). The hepatic clearance of vinblastine determined *in vitro* was compared to the *in vivo* hepatic clearance of vinblastine. For the first time, the allometric dependence of the density of cytochrome P450 enzymes on body weight was shown in dogs, confirming the allometric dependence of cellular metabolism on body size (Porter, 2001). The *in vitro* drug metabolism studies predicted hepatic clearance of vinblastine within 10 % of the measured *in vivo* values of hepatic clearance. Such *in vitro/in vivo* correlations could increase the utility of intraspecific allometric equations and decrease the number of live animal studies involved in drug development phases.

In conclusion, the allometric equations developed for organ weights, physiological parameters, and the clearance of model anticancer drugs could be utilized in predictive pharmacokinetic models. Such models require the accurate input of key anatomical, physiological, and pharmacokinetic parameters to accurately standardize drug exposure in a disparate population of dogs.

References

Aleksunes LM, Augustine LM, Scheffer GL, Cherrington NJ and Manautou JE (2008) Renal xenobiotic transporters are differentially expressed in mice following cisplatin treatment. *Toxicology* **250:**82-88.

Barabas K, Milner R, Lurie D and Adin C (2008) Cisplatin: a review of toxicities and therapeutic applications. *Vet Comp Oncol* **6:**1-18.

Bradford MM (1976) A rapid and sensitive method for the quantitation of microgram quantities of protein utilizing the principle of protein-dye binding. *Anal Biochem* **72:**248-254.

Calvert AH, Newell DR, Gumbrell LA, O'Reilly S, Burnell M, Boxall FE, Siddik ZH, Judson IR, Gore ME and Wiltshaw E (1989) Carboplatin dosage: prospective evaluation of a simple formula based on renal function. *J Clin Oncol* **7:**1748-1756.

de Jongh FE, Verweij J, Loos WJ, de Wit R, de Jonge MJ, Planting AS, Nooter K, Stoter G and Sparreboom A (2001) Body-surface area-based dosing does not increase accuracy of predicting cisplatin exposure. *J Clin Oncol* **19:**3733-3739.

de Lannoy IA, Mandin RS and Silverman M (1994) Renal secretion of vinblastine, vincristine and colchicine in vivo. *J Pharmacol Exp Ther* **268:**388-395.

Earle DP, Jr. and Berliner RW (1946) A simplified clinical procedure for measurement of glomerular filtration rate and renal plasma flow. *Proc Soc Exp Biol Med* **62:**262-264.

Fouladi M, Chintagumpala M, Ashley D, Kellie S, Gururangan S, Hassall T, Gronewold L, Stewart CF, Wallace D, Broniscer A, Hale GA, Kasow KA, Merchant TE, Morris B, Krasin M, Kun LE, Boyett JM and Gajjar A (2008) Amifostine protects against cisplatin-induced ototoxicity in children with average-risk medulloblastoma. *J Clin Oncol* **26:**3749-3755.

Hanigan MH, Townsend DM and Cooper AJ (2009) Metabolism of cisplatin to a nephrotoxin. *Toxicology* **257:**174-175; author reply 176-177.

Hempel G and Boos J (2007) Flat-fixed dosing versus body surface area based dosing of anticancer drugs: there is a difference. *Oncologist* **12:**924-926.

Houston JB and Carlile DJ (1997) Prediction of hepatic clearance from microsomes, hepatocytes, and liver slices. *Drug Metab Rev* **29:**891-922.

Jones HM and Houston JB (2004) Substrate depletion approach for determining in vitro metabolic clearance: time dependencies in hepatocyte and microsomal incubations. *Drug Metab Dispos* **32:**973-982.

Jordan MA and Wilson L (2004) Microtubules as a target for anticancer drugs. *Nat Rev Cancer* **4:**253-265.

Legendre F, Bas V, Kozelka J and Chottard JC (2000) A complete kinetic study of GG versus AG plantination suggests that the doubly aquated derivatives of cisplatin are the actual DNA binding species. *Chemistry* **6:**2002-2010.

Mann WA and Kinter LB (1993) Characterization of the renal handling of p-aminohippurate (PAH) in the beagle dog (Canis familiaris). *Gen Pharmacol* **24:**367-372.

Matsubara T, Koike M, Touchi A, Tochino Y and Sugeno K (1976) Quantitative determination of cytochrome P-450 in rat liver homogenate. *Anal Biochem* **75:**596-603.

McDuffie JE, Sablad M, Ma J and Snook S (2010) Urinary parameters predictive of cisplatin-induced acute renal injury in dogs. *Cytokine* **52:**156-162.

Moore MJ and Erlichman C (1987) Therapeutic drug monitoring in oncology. Problems and potential in antineoplastic therapy. *Clin Pharmacokinet* **13:**205-227.

Nath A and Atkins WM (2006) A theoretical validation of the substrate depletion approach to determining kinetic parameters. *Drug Metab Dispos* **34:**1433-1435.

Pang KS and Rowland M (1977) Hepatic clearance of drugs. I. Theoretical considerations of a "well-stirred" model and a "parallel tube" model. Influence of hepatic blood flow, plasma and blood cell binding, and the hepatocellular enzymatic activity on hepatic drug clearance. *J Pharmacokinet Biopharm* **5:**625-653.

Pasquier E and Kavallaris M (2008) Microtubules: a dynamic target in cancer therapy. *IUBMB Life* **60:**165-170.

Peng B, English MW, Boddy AV, Price L, Wyllie R, Pearson AD, Tilby MJ and Newell DR (1997) Cisplatin pharmacokinetics in children with cancer. *Eur J Cancer* **33:**1823-1828.

Pinkel D (1958) The Use of Body Surface Area as a Criterion of Drug Dosage in Cancer Chemotherapy. *Cancer Research* **18:**853-856.

Porter RK (2001) Allometry of mammalian cellular oxygen consumption. *Cell Mol Life Sci* **58:**815-822.

Schneider WC (1948) Intracellular distribution of enzymes; the oxidation of octanoic acid by rat liver fractions. *J Biol Chem* **176:**259-266.

Smith R, Jones RD, Ballard PG and Griffiths HH (2008) Determination of microsome and hepatocyte scaling factors for in vitro/in vivo extrapolation in the rat and dog. *Xenobiotica* **38:**1386-1398.

Steward A, Allott PR and Mapleson WW (1975) Organ weights in the dog. *Res Vet Sci* **19:**341-342.

van den Bongard HJ, Mathot RA, Beijnen JH and Schellens JH (2000) Pharmacokinetically guided administration of chemotherapeutic agents. *Clin Pharmacokinet* **39:**345-367.

VITA

Satyanarayana Achanta

Candidate for the Degree of

Doctor of Philosophy

Thesis: PHARMACOKINETIC SCALING OF ANTICANCER DRUGS IN DOGS

Major Field: Veterinary Biomedical Sciences (Pharmacology)

Biographical:

Personal data:
Born in Coringa, East Godavari District, Andhra Pradesh, India. Son of Mr. Govinda Raju Achanta and Mrs. Mani Achanta

Education:
Completed the requirements for the Doctor of Philosophy in Veterinary Biomedical Sciences at Oklahoma State University, Stillwater, Oklahoma, USA in July, 2012.

Completed the requirements for the Bachelor of Veterinary Sciences and Animal Husbandry at Acharya NG Ranga Agricultural University, Hyderabad, Andhra Pradesh, India in November, 2005.

Experience:
12/2008 - 7/2012: Graduate Teaching Assistant, Veterinary Comparative Anatomy (VMED 7243), Center for Veterinary Health Sciences, Oklahoma State University, Stillwater, OK
8/2007 - 7/2012: Graduate Teaching Assistant, Veterinary Histology (VMED 7123), Center for Veterinary Health Sciences, Oklahoma State University, Stillwater, OK
6/2006 - 7/2007: Veterinary Assistant Surgeon, Department of Animal Husbandry, Andhra Pradesh, India
12/2005 - 5/2006: Associate Veterinarian, Vet 'n' Pet Clinic, Hyderabad, India
5/2005 - 7/2005: Intern, Veterinary Polyclinic, Gudiwada, Andhra Pradesh, India

Professional Memberships:
American Association for Advancement of Sciences (AAAS), American Academy of Veterinary Pharmacology and Therapeutics (AAVPT), Veterinary Cancer Society (VCS), Veterinary Council of India (VCI), Phi Zeta Honorary Society of Veterinary Medicine

Name: Satyanarayana Achanta Date of Degree: July, 2012

Institution: Oklahoma State University Location: Stillwater, Oklahoma

Title of Study: PHARMACOKINETIC SCALING OF ANTICANCER DRUGS IN DOGS

Pages in Study: 190 Candidate for the Degree of Doctor of Philosophy

Major Field: Veterinary Biomedical Sciences (Pharmacology)

Scope and Method of Study: Anticancer drugs are characterized by a narrow therapeutic index and wide inter-individual variability in therapeutic outcome, disposition, and toxicity. The accurate calculation and administration of anticancer drugs from the initiation of treatment is necessary to attain a good therapeutic outcome. Currently, the doses of anticancer drugs are calculated based on the body surface area approach, which requires prior dose escalation studies to establish the maximum tolerated dose. In addition, several studies have questioned the ability of standard dosing methods to adequately normalize drug exposure for several anticancer drugs. As with most drugs, the efficacy of anticancer drugs correlates best with total drug exposure, or the area under the plasma concentration versus time curve. If the clearance of a drug is accurately known, then the dose required to produce a desired total drug exposure can be calculated accordingly. Therefore, it is important to understand the factors that influence the clearance of a drug. Physiological based pharmacokinetic (PBPK) modeling can predict absorption, distribution, metabolism, and excretion of a drug by consideration of anatomical, physiological, and pharmacokinetic parameters. We hypothesized that the concomitant consideration of the effects of body weight and ontogeny on organ physiology and drug handling will accurately predict the clearance of several model anticancer drugs. In order to test our hypothesis, organ and body weights were collected from 383 dogs, *in vivo* physiological and pharmacokinetic studies of vinblastine and cisplatin disposition were conducted in ten intact male dogs (4 - 54 kg), and *in vitro* drug metabolism studies of vinblastine were conducted. The overall objective of this project was to determine the clearance of model anticancer drugs in order to optimize the drug exposure of anticancer drugs among disparate canine patients.

Findings and Conclusions: Heart, liver, and kidney weights were allometrically related to body weight. The newly developed allometric equations better predicted organ weights than did the established, fixed proportion of body weight approach. In contrast to previous studies, the clearance of cisplatin correlated well with glomerular filtration rate (GFR), suggesting that initial doses of cisplatin were directly related to GFR in healthy dogs. A highly sensitive liquid chromatography/tandem mass spectrometry analytical method was developed to quantify the concentrations of vinblastine and its putative metabolite, desacetylvinblastine, in plasma and urine samples of dogs. The predicted *in vitro* hepatic clearance of vinblastine was within 10% of measured *in vivo* values. The use of *in vitro/in vivo* correlations of drugs may reduce the number of live animal studies needed for dose calculations of novel anticancer drugs. Further, the newly developed allometric equations of organ weights, physiological, and pharmacokinetic parameters can be used as data for input into PBPK models.

ADVISER'S APPROVAL: Dr. Lara K. Maxwell